UNIVERSITY OF
KWAZULU-NATAL

INYUVESI
YAKWAZULU-NATALI

VOLTAGE CONTROL AND STABILITY ANALYSIS IN A MULTI-MACHINE POWER SYSTEM WITH INCREASING PENETRATION OF INTERMITTENT RENEWABLE ENERGY GENERATION

by

Kabulo Loji

Submitted in fulfilment of the requirement for the degree

MASTER OF SCIENCE: ELECTRICAL ENGINEERING

COLLEGE OF AGRICULTURE, ENGINEERING AND SCIENCE

UNIVERSITY OF KWAZULU-NATAL

2020

Supervisor: Dr. Rémy TIAKO

DECLARATION 1 - PLAGIARISM

I, **Kabulo Loji**, declare that:

1. The research reported in this thesis, except where otherwise indicated, is my original research.

2. This thesis has not been submitted for any degree or examination at any other university.

3. This thesis does not contain other persons' data, pictures, graphs or other information, unless specifically acknowledged as being sourced from other persons.

4. This thesis does not contain other persons' writing, unless specifically acknowledged as being sourced from other researchers. Where other written sources have been quoted, then:
   a. Their words have been re-written but the general information attributed to them has been referenced
   b. Where their exact words have been used, then their writing has been placed in italics and inside quotation marks, and referenced.

5. This thesis does not contain text, graphics or tables copied and pasted from the Internet, unless specifically acknowledged, and the source being detailed in the thesis and in the References sections.

Signed: ..... 

Date …12/Jan /2021……

Kabulo Loji.

As the candidate's supervisor, I agree to the submission of this thesis.

Signed: ..... 

Date…… Dr. R Tiako

DECLARATION 2 - PUBLICATIONS

The following publications emanated from this research investigation and form part and/or include research presented in this thesis. This includes publications in preparation, submitted, in press and published, giving details of the contribution of each author:

[1] **K. Loji**, I. E. Davidson, and R. Tiako, "Voltage Profile and Power Losses Analysis on a Modified IEEE 9-Bus System with PV Penetration at the Distribution Ends," presented at the Southern African Universities Power Engineering Conference/Robotics and Mechatronics/Pattern Recognition Association of South Africa (SAUPEC/RobMech/PRASA) Bloemfontein, South Africa, January 2019.

[2] G. Sharma and **K. Loji**, "Critical Aspects of AGC Emerging from Optimal Control to Machine Learning Techniques," *Indonesian Journal of Electrical Engineering and Informatics (IJEEI),* vol. 7, no. 1, pp. 101-114, March 2019

[3] G. Sharma, **K. Loji**, and M. Kabeya, "Application of Diverse FACTS in AGC of Multi-Area Interconnected Energy Systems," Indonesian Journal of Electrical Engineering and Informatics (IJEEI), vol. 7, no. 1, pp. 101-115, March 2019.

[4] N. Loji, **K. Loji**, R. Tiako, I.E. Davidson and T. Akindeji, "Loadability Assessment of a Photovoltaic Penetrated Grid to Offset Intermittency and Reduce Total Power Losses using Battery Energy Storage System". Accepted for (SAUPEC/RobMech/PRASA) North West Univeristy, South Africa, January 2021.

Signed, Durban 12/Jan/2021

Kabulo Loji

ACKNOWLEDGEMENTS

Over some years, I have had the opportunity to become indebted to many people in the world, in the Electrical Power Engineering Department, as well as in other places. Thanks to all for the enjoyable time I have spent with you while producing this dissertation. However, there are some people to whom am especially grateful.

My late Father, Elie Kabulo Loji, and my Mother, Jeanne Kasongo Kabuya, for deciding to bring me to life and supporting me with sacrifices under hard life conditions.

I value and thank my supervisor Dr. Rémy Tiako, for his willingness to carry out the burden of guiding me during this journey. It was an honour to have you as my supervisor.

Special thanks to my colleagues: Dr. Gulshan Sharma for his selfless commitment in assisting me to understand the hidden meanders of the research world, Clarence Leoanaka for his encouragements and advice in assuring me always that everything is possible, and Milton Estrice for always motivating me and anticipating a successful academic future by kindly calling me *Dr. Loji*. Please do draw joy from this milestone, this work is also yours.

To my friend, colleague from VUT and brother Shariff Khaiye, who never stopped reminding me that I gave it all to DUT and forgot to focus on my own development. Without your insistence, an achievement of this degree was very uncertain and hypothetical.

Last but certainly not least, I would like to thank my family, the meaning of my life and the justification of all sacrifices endured, Nomhle my wife, Jeanne Kasongo and Umba Muyampe my daughters and, Elie Kabulo and Mutamba Simphiwe my boys.

ABSTRACT

Among multiple distributed generation (DG) supply means, photovoltaic (PV) and wind technologies are the most important and widely used renewable energy sources (RES) throughout the world. However, solar intermittency and the stochastic nature of radiation on one hand and grid integration-related issues on the other are fundamental concerns in the development and smooth deployment of solar energy contribution to conventional power systems networks. In addition, given that they modify both the structure and the operation of the distribution networks, RES increase uncertainty in power system operations, thus affecting power systems variables such as the voltage profiles and direction of network power flows. It is also largely established that a high penetration of DGs at the distribution end is associated amongst others, with voltage rises at PV buses that may lead to the violation of grid codes, if not adequately mitigated. There is a need to investigate both the effect and the impact of increasing penetration of these intermittent RES on, particularly, voltage and frequency stability power systems and the utilization thereof of such sources to improve voltage stability margins and predict voltage stability conditions. This research work investigated voltage control and stability conditions at Solar PV buses through various case studies and scenarios simulated using the Power Factory® tool, both in static and dynamic analysis modes.

A modified standard IEEE 9-Bus Sub-transmission system was used to assess the voltage profile, system loadability and system stability. The comparison and discussion of the results obtained from the integration of the Solar PV and FACTS devices under various scenarios revealed that their respective impacts and abilities to improve voltage stability differ. The results confirmed that under any operating conditions, reactive power control remains the most effective method to control voltage stability and power transfer capability, especially in the context where an increasing penetration of renewable and inertia-less generating sources is planned. The results further revealed that there is a specific location and a specific siting architecture for a given size of PV that produces the best results for voltage stability, as well as improved system stability and loadability conditions for a given load distribution profile in a particular network. Lastly, the results demonstrated the effectiveness of the use of a Battery Energy Storage System (BESS) in achieving voltage control and regulation in distribution networks highly penetrated by PV generation, subsequently enabling greater RE penetration.

TABLE OF CONTENTS

LIST OF FIGURES

LIST OF TABLES

CHAPTER 1: INTRODUCTION AND OBJECTIVES

Introduction

This introductory chapter presents an overview of the research. It includes the background to the study and presents its the justification. The problem statement, the aims, key questions, limitations and delimitations, the methodology of the study, as well as the scope of this research work are also presented.

1.1 Research background and justification

The earliest grids were direct current-based and then, power plants only supplied electricity to consumers close to the generating plants [1]. The balance of power generated and consumed was somewhat achieved using batteries that were directly connected to the DC grid. Far ahead, AC technological evolutions allowed not only the transportation of power over longer distances but also the potential increase in generation units' output capacity [1]. For many years, electric systems, as shown in Figures 1-1 and 1-2, were specifically designed and constructed to transport electrical energy from production centres to load consumption centres situated several kilometres away.

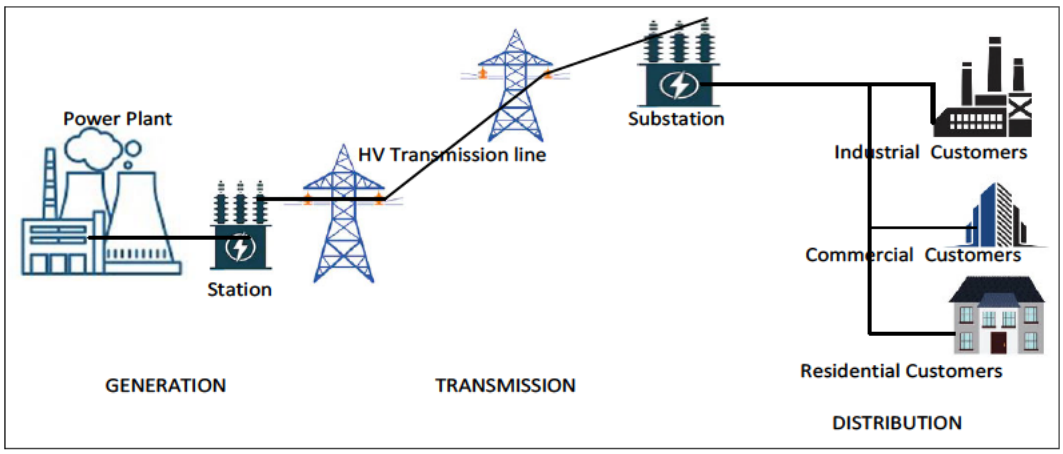

Figure 1-1: Traditional electric network configuration

The concept of power flow was then unidirectional, understood as transiting from bulk generating stations, currently constituted of a greater percentage of coal-fired stations, hydraulic or nuclear sources, toward medium and low-voltage customers [2, 3] to load distribution centres essentially made of domestic, industrial and business centres [4]. The demand/supply balance was achieved by monitoring instantaneous variation of large loads[1].

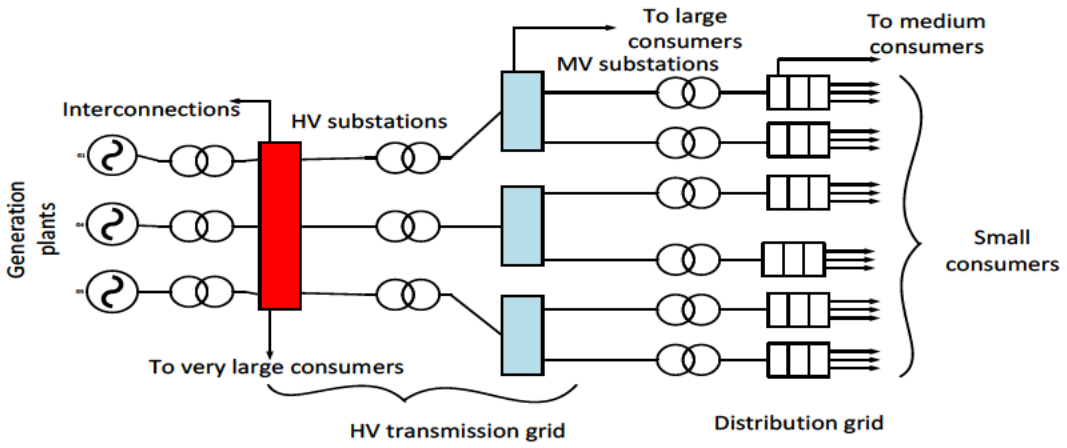

Figure 1-2: Power system configuration and structure

In today's power grid, generation units, transmission lines and loads are connected in power system networks that are becoming more and more complex, as illustrated in Figure 1-3, and this complexity is persistently increasing due to of the growing number of interconnections and the development of novel technologies [5-7]. These new technologies are mainly constituted of small-scale and decentralised renewable energy technologies, of which solar and wind together currently hold the major share [1].Accompanying these small scale generation units, local storage has also resurfaced.

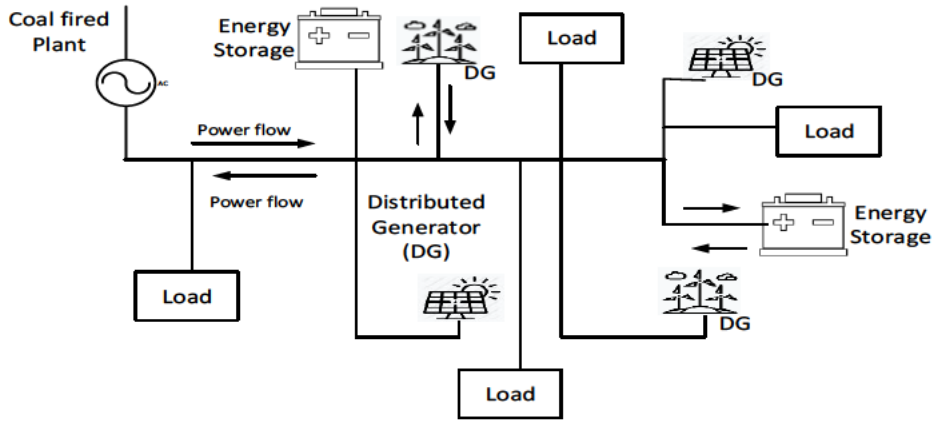

Figure 1-3: Electric system topology with DGs and storage systems

As it can be seen in Figure 1-4, findings from The Renewable 2019 Global Status Report [8] confirm an increasing growth of the renewable energy share led especially by solar and wind energy [9]. Furthermore, from the report published by Bloomberg NEF, it is projected as presented in Figure 1-5 that in the next 30 years, more than a half of the energy worldwide will be produced from wind and solar energy sources [10].

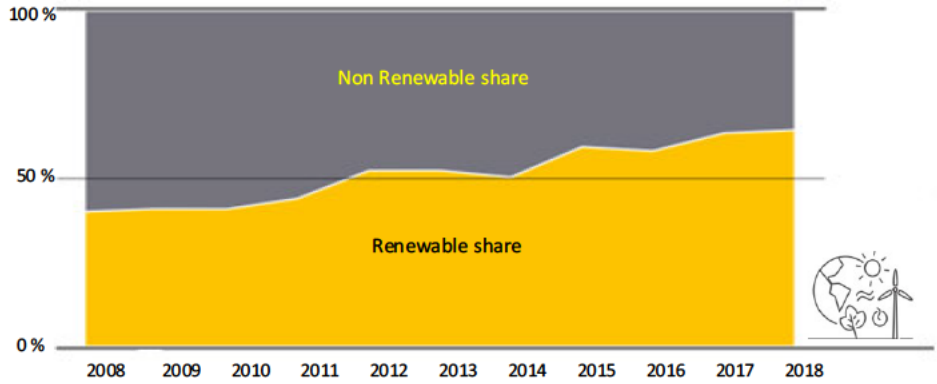

Figure 1-4: Share of renewable energy in net annual additions of power generation capacity [8]

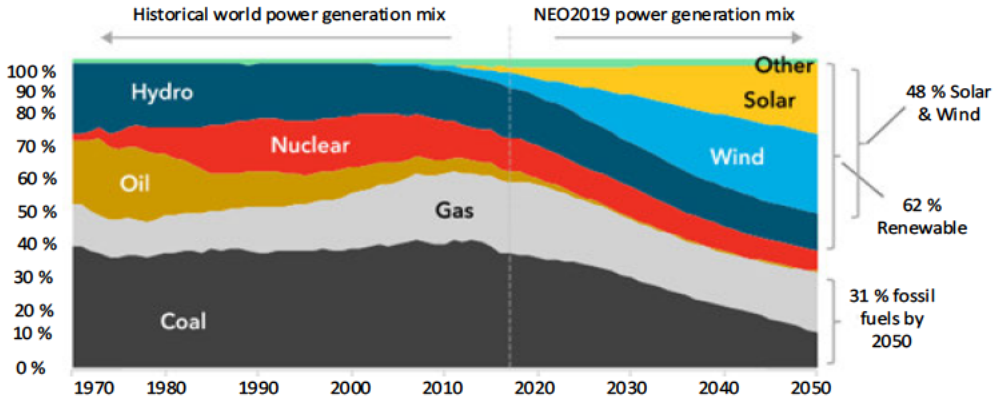

Figure 1-5: Projected power generation mix by year 2050 [10]

With this increasing integration of renewable energy being of an intermittent and unpredictable nature, the energy flow is in some cases reversed and energy may flow from the customer into the transmission system [2],with negligible or reduced reactive power contribution [11, 12].

Interest in the significant renewable energy sources (RES) grid integration has indeed developed mostly because of the exponentially increasing demand for power delivery, a more secure energy future and energy policies adopted by governments in an effort to reduce CO_2 and greenhouse gas emissions [13-18] by at least 60 % by 2050 [19]. Other reasons for the increasingly widespread use of DGs at loads ends are the minimisation of infrastructures' financial burden related to equipment upgrade and loss reduction [5] by reducing the overall technical burden on the primary generation units [13]. In fact, DG plants do not require lengthier installation times, subsequently permitting reasonable investment risk [20-22] besides reducing voltage dips and acting as primary backup during utility outages [5].

While it is expected that the RES share keeps on increasing [8-10] for the reasons mentioned above, subsequent rising concerns on the impact caused by the penetration of RES onto the

utility grid is equally expected. The impact of the integration of DGs of an intermittent nature is actually not negligible as it affects the network power quality, operation and control especially with regard to voltage and frequency stability. Additionally, due to the stochastic characteristic of DGs in general and solar irradiation in particular, the reliability performance of a PV penetrated power system may be quite dissimilar from the conventional centralised architecture one [23]. The power system (PS) will in fact encounter numerous variabilities, fundamentally the planning and the operation of the electric system, both technically and economically [24].

1.2 Problem statement

The requirement of supplying reliable and quality power to customers is a key characteristic to well operated and stable grids. Voltage and rotor angle stability are equally important to prevent collapse of parts or the PS network, with all imaginable consequences The increased number of intermittent and not dispatchable RES in multi-machine PS bring new challenges and concerns on voltage and frequency as well as on switchgear fault ratings. When planning to integrate solar PV generation resources into existing system grids, these should enable connection without violating statutory technical limits or standards. Attention must therefore be given to the installation capacity and the location of PV as the severity of the impacts will depend on the siting and the sizing. There is therefore a need to investigate both the effects and impact of the sizing and location of increasing the penetration of RES on voltage and frequency stability, as well as the utilisation of such sources to improve voltage stability and loadability margins.

1.3 Aims and objectives

1.3.1 Aims

This research study aims to improve the voltage stability of power systems that have increasing penetration of DG in the broad perspective of achieving power system stability. In other words, to investigate the effects of PV-based units increasing penetration and location on voltage stability and power losses.

1.3.2 Objectives

The main research objective is to study the system stability of a power system, with a particular focus on DG penetration impacts. It proposes to analyse the power systems voltage behaviour

and characteristics and assess system loadability and power losses under the increasing influence of RES, namely PV systems, as well as to suggest probable ways of mitigating any violations. The impact of PV units on static voltage and dynamic transient stability of an unbalanced PS is studied by considering the following factors:

(i) Load increase;
(ii) High PV penetration levels;
(iii) Stability conditions after disturbance

The sub-objectives of the study are to:

- Review the general Voltage-VAR problems with FACTS and increased DG integration;
- Analyse the effects of DG units on voltage stability, system stability, system loadability and power losses;
- Investigate the effect of DG siting and sizing and identify the PV share that a system can handle before current regulations are violated ($V_{profile} = f$ (DG Sizing);
- Explore Voltage stability improvement techniques in utility grids with solar plants integration and compare levels of improvement;
- Study the relationship between voltage stability and change of location in the context of increased penetration of DG under various scenarios;
- Optimally locate and size the DGs;
- Stress incrementally the network and evaluate the impact of grid-connected PV systems closer to voltage instability;
- Investigate the effectiveness of the incorporation of battery energy storage systems and
- Discuss the results and propose recommendations.

1.4 Key research question

In light of the above research aims and objectives, the research questions that this study attempts to answer are:

1. To what extent does increasing the penetration of RES at the distribution ends effects voltage stability?
2. In addition to their primary function of providing much needed extra power to respond to the increasing power demand, can DGs be used to effectively perform

FACTS functions to enhance controllability, voltage support and stability, and thus increase power systems' loading margins?

3. Which measures can be taken to ensure that in the context of DGs integration, voltage remains controlled and undisturbed at key buses under normal conditions and under disturbances?
4. What PV energy optimum share and best location can a particular system handle before stability limits and violations of standard codes can be reached?
5. Can BESS perform a supportive function in mitigating the impact of the increased grid penetration of DG?

1.5 Limitations and delimitations

1.5.1 Limitations

The research is completed on virtual networks using simulation tools as it is almost impossible to conduct this kind of research on live power systems.

1.5.2 Delimitations

The following delimitations are to be considered:

1. This study work is bounded to voltage behaviour and power losses of the PS when subjected to increased penetration of DGs of an intermittent nature, with special attention to sizing/capacity and siting/location.
2. The study will only focus on the effect of the load increase as the cause for voltage instability and possibly voltage collapse. The other causes: generators and static VAR systems (SVS) reaching their reactive power limits, tap changing transformers' action or contingencies such as line tripping or generator outages will not be considered.
3. Although other types of DGs are briefly reviewed through the literature, only the Solar PV type is considered for the purpose of this study.
4. The impact on system frequency is also discussed and reviewed in the literature, but will not be considered in the simulation section.
5. The impact on frequency, harmonics and flicker, impact on the protection system and protection philosophy and economic impact do not form part of this work.
6. The study is limited to the use of *DigSILENT® PowerFactory* as the research tool.

1.6 Research methodology and design

An extensive literature survey is carried out on the following contributing topics:

- Traditional electric systems and the challenges of power systems stability;
- Renewable Energy Resources and the challenges of increased penetration;
- Current electric systems, Distributed generation and voltage stability issues; and
- PS voltage control in the context of RES integration.

Systems test were then mathematically designed and/or modelled, followed by simulations performed under various case studies and scenarios using *DigSILENT® Power Factory®* considering static and dynamic analysis and the results are presented and discussed.

1.7 Research publications

Some of the results of these dissertation and some other related collaborative investigations have been presented at a local conference and published in accredited journals [15, 25, 26].

1.8 Organisation of the dissertation

The dissertation consists of 8 chapters as outlined below:

Chapter One provides an introductory overview of the research. It includes particularly the background to and justification for the study, the problem statement, the key questions, limitations and delimitations of the study, the methodology, as well as the scope of the work.

Chapter Two presents the literature review, with a focus on the context of the research and the relationship between previous studies and theories. It also highlights current information on the research area as well as other people working in the same area, with the aim of spotting gaps and major seminal works that have been thus far completed. The main Methodologies and research techniques of other researchers are also presented in order to establish similarities and differences with the main topic.

Chapter Three discusses the historical development of distributed generators, with particular emphasis on increasing penetration and voltage stability issues. Existing techniques to mitigate the impacts of DGs penetration are also reviewed under this chapter.

Chapter Four reviews methods and technologies are used to achieve voltage control in active distribution networks. A section is dedicated to traditional means of controlling voltage, while the rest of the sections deal with the impacts associated with DG integration.

Chapter Five covers discussions on system network modelling and the justification of the choice of system elements and components that are used in the study. The simulation tool, the parameter settings, the techniques applied and the design methodologies used are also presented and described in detail in this chapter.

Chapter Six presents case studies and scenarios used in this research work and the corresponding simulations conducted on the network models presented in Chapter 5.

Chapter Seven The results of the case studies conducted are presented and discussed in this chapter using a comparative analysis approach.

Chapter Eight provides the conclusions of the research work and the recommendations drawn from the study. Details of pertinent issues and interest for future work are also presented in this concluding chapter.

1.9 Summary

This chapter introduced the context of the research and provided an overview of the organisation of the dissertation as well as the scope of the work.

CHAPTER 2: LITERATURE REVIEW

Introduction

This chapter addresses, amongst other matters, the context for the research and the relationship between previous studies and theories. It also highlights existing information on the field of study as well other people who have researched in the area in order to identify the gaps in the literature and highlight major seminal works that have been done thus far. The main methodologies and research techniques by other researchers are also presented in an attempt to establish similarities and differences with the subject under research.

2.1 Background on stability issues

2.1.1 Historical review on traditional power systems

Structures, descriptions and the operation of traditional power systems, also referred to as centralised systems, have for years been the subject of extensive literature from various authors. Points of generation of electric power are indeed situated several kilometres away from points of consumption, hence for economic reasons and a secure supply of electrical power, long distance bulk power transfer is essential [27]

Until the 1990s, the electric power industry was inclined to have a vertical integration approach to generation and transmission, justified most by economic reasons, rather than the improvement of the overall efficiency of the system [28]. The need to unbundle these vertically integrated utilities for more decentralised systems and the benefits and challenges of such a shift will be discussed in later sections.

In an exhaustive historical review of stability problems, Kundur [6] reports that power systems stability was first recognized as an important problem only about a century ago, in 1920. First laboratory tests on miniature systems were reported in 1924 and a year later, the first field tests on a practical system were conducted. It was then noticed that for economic reasons, systems were operated close to their steady-state stability limits and instability occurred much more frequently following short-circuits and other disturbances, rather than during steady-state [6]. Methods of stability analysis and models used then were dictated and limited by the development in the art of computation combined with the Stability Theory of Dynamic Systems. Slide rules and mechanical calculators with graphical techniques such as equal-area criterion

and circle diagrams were adequate for the analysis of simple systems that could be effectively treated as two-machine systems [6].

As power systems began to grow, it was found to be economically attractive to interconnect independent generation units, transmission lines and loads to form networks. One of the paramount benefits of network interconnection is increased reliability [27, 29-32], meaning mutual support between generation from different areas, thereby suggesting that a number of interconnected systems can sustain contingencies that an standalone system could not. However, the expansion of PS in larger sized networks led to the complexity of stability problems as systems could no longer be treated as two-machine systems [6]. In 1930, the network analyser, also known as the AC calculating board, was developed and permitted a power flow analysis of multi-machine systems. However, motion and swing equations still had to be solved by hand using step-by-step numerical integration suited for the solution of algebraic equations rather than differential equations [6]. The stability study of power systems was focused on the network rather than on the synchronous machines, which were viewed as simple voltage sources behind fixed reactance and loads were considered as constant impedance. In the 1950s, electronic analogue computers and thereafter digital computers were developed and used to analyse problems requiring detailed modelling of the synchronous machine, excitation system and speed governor. The progress mentioned above, was followed by the development of digital computer programs for PS analysis, bringing improvement over network analyser methods in both the size of the network to be simulated and the modelling of equipment dynamic characteristics [6].

2.1.2 Power systems dynamics

In reference [33], Tabatabaei Aghbolaghi, Bizon and Blaabjerg note that in amalgamated and interconnected PS, a number of various electromagnetic field manifestations occur and effect, at any time/location, parameters such as currents, voltages, frequency or power quality (PQ), compelling users to be interested in the preservation of PQ. Power systems dynamics can be categorised into four groups depending on their physical character and their involved phenomenon time frame. [28]. These four groups of power systems dynamics are defined as: wave, electromagnetic, electromechanical and thermodynamic phenomena. Table 2-1 below shows the dynamic phenomena time-frame ranging from fastest to slowest. Furthermore, careful inspection of Table 2-1 reveals that the classification of power systems dynamics with respect to time-frame is closely related to where the dynamics occur within the system.

Table 2-1: Power system dynamics and time-frames

Phenomenon	Waves	Electromagnetic	Electromechanical	Thermodynamic
Description	Lightning strikes or switching operations	Electromagnetic dynamics taking place in machine windings following disturbance, operation of protection systems or interaction between the electrical machines and the network.	Electromechanical dynamics due to oscillation of rotating masses of generators and motors following disturbance, operation of protection systems or voltage and prime mover control	Thermodynamic changes resulting from boiler control action in steam power plants as the demand of automatic generation control are implemented
Time-frame	From microseconds (µs) to milliseconds	From milliseconds (ms) to a second	From seconds (s) to several seconds	From several seconds (s) to few hours

Authors in [28] established that the fastest phenomena occur from the electrical RLC circuits of the transmission network, through the generator armature windings to the field and damper winding, then along the generator rotor to the turbine until finally the boiler is reached. They conclude that the relationship between the phenomenon and where it occurs within the system has important consequences for the modelling of the system elements, particularly with respect to the level of accuracy required in the models used to represent these elements. Mihalič, Povh and Zunko in [34] state further that although they are more or less connected to each other, stability problems are often divided into various categories and there are specific methods normally applied to study specific stability categories.

The phenomena mentioned and described above are key to understanding the fundamentals of stability issues in power systems networks and subsequently the analysis and search for mitigation solutions for suitable PS planning and safe operation.

Anderson and Fouad [35] note that primitively, stability was viewed as a concern of a PS operating under stable load conditions and this steady state is disturbed, causing the re-adjustment of the synchronous machine (SM) rotor and power-angle correlation [6] of the synchronous machines of the system. Adjustment to new operating conditions is referred to as 'the transient period' and the system behaviour is referred to as 'dynamic system performance'. The main criterion was then that the SM maintain synchronism at the end of the transient period, in other words, the system can settle down to a new or original steady state after the transients

disappear [32]. However, this criterion of maintaining/loosing synchronism shall not be considered as sufficient. Kundur, in [6], evidenced that instability might happen with no synchronism loss. This is supported, for instance, by examples of a system consisting of a synchronous generator feeding an induction motor load, whereby the system can become unstable because of the collapse of load voltage. Another example is of loads covering an extensive area supplied by a large system. To provide further clarity on the phenomenon, Kundur as referred to by Grigsby in [36] states that stability is a condition of equilibrium between opposing forces, and instability will occur when a disturbance leads to a sustained imbalance between these opposing forces.

2.2 Definition of stability

The performance evaluation of a PS depends on its capability to supply quality power on demand while maintaining voltage and frequency within prescribed limits. Stability problems are considered, besides power flow and fault analysis, to be one of the major studies of power systems [37].

In 2004, a CIGRE-IEEE task force composed of prominent PS specialists led by Kundur provided a more comprehensive and inclusive definition for power system stability. Indeed, the task team defined power system stability as "the ability of an electric power system, for a given initial operating condition, to regain a state of operating equilibrium after being subjected to a physical disturbance, with most system variables bounded so that practically the entire system remains intact" [38]. Grigsby in reference [39] refers to PS stability as the aptitude to recover a counterbalance condition post occurrence of a disturbance in the system.

As power systems are non-linear, their stability depends on both the initial conditions and the size of the disturbance [28]. With regard to the size of the disturbance, power systems may experience small disturbances or large disturbances. Small disturbances are normal fluctuations of short amplitude, such as load variations leading to mild oscillations often not requiring any dumping, and large disturbances often caused by faults on transmission lines; the loss of one or more generating units; or the insertion or loss of a huge load, developing into big oscillations usually requiring control actions [37, 40].

Stability analysis is categorised into steady state stability also referred to as "dynamic stability", and transient stability. The former depends on operation conditions only while the latter is effected by both PS operation and disturbances [41-43].

Understanding stability is closely linked to the understanding of steady-state stability (SSS) and steady-state stability limit (SSSL). SSS is defined as the stability of the system under conditions of gradual or relatively slow changes in load [44]. SSS is associated with SSSL, with reference to maximum power transferrable through the PS with no alteration of stability condition, but with a possible loss of synchronism at loads or disturbances below the steady state limit if they are suddenly applied or removed [45].

In [46], Savulescu suggests that searching the stability limit from the perspective of "distance to instability" and "case worsening" brings promising results, especially because SSSL is quantifiable. This approach will be used in Study Case 2 of this research work.

2.3 Forms of power systems instability

The stable operation of a PS results from the balance between energy input and electrical energy consumed by a continuously changing load. If the input to the generator does not rapidly balance the electrical load, the system speed and the voltage will deviate from normal to violate grid codes[47]. This condition may be exacerbated by adverse conditions such as loss of transmission line or generator, fault, and/or application/disconnection of large blocks of load.

Kundur et al. in [38] suggest that a PS is essentially a localised single problem,. Nevertheless, because of the high magnitude and intricacy of stability problems, it helps to analyse specific problems using an appropriate degree of system details and analytical techniques. This leads to the need for the classification of the phenomena into categories. The following considerations have been proposed for the classification by Kundur [6]:

- The physical nature of the resulting mode of instability as indicated by the main variable in which instability can be observed;
- The size of the disturbance considered, which influences the method of calculation and prediction of stability;
- The devices, processes and time span that must be taken into consideration in order to assess stability; and
- The most appropriate method of calculation and prediction of stability.

Figure 2.1 shows that a PS can be divided into the following categories and sub-categories [28, 38]:

1) Rotor (short term): Small signal and Transient stability.
2) Frequency: Short and Long-term
3) Voltage: Small and large disturbance (Short/Long term.)

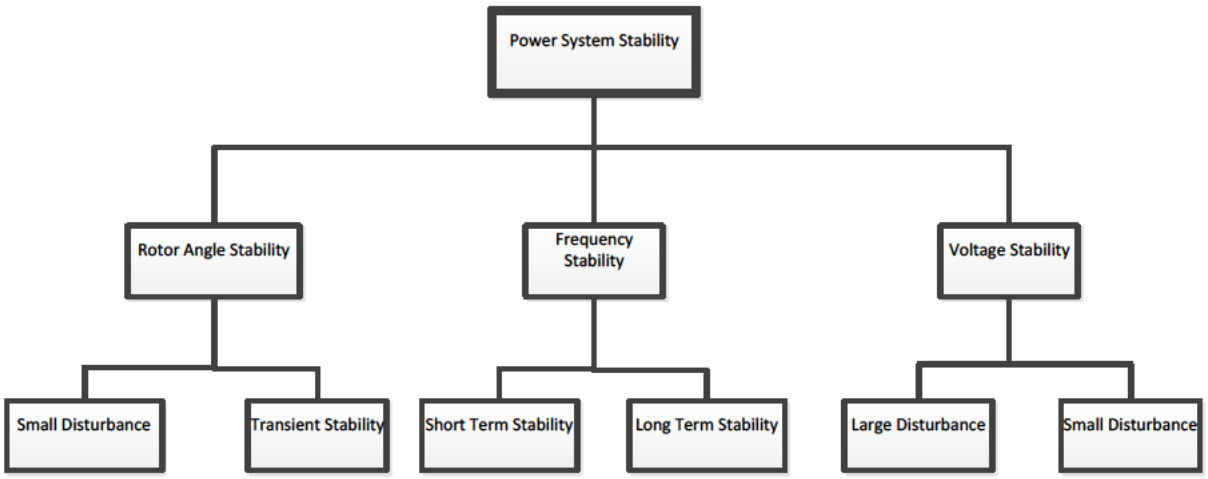

Figure 2-1: Classification of power system stability [38]

These forms of instability are succinctly described and discussed below with a special and fairly large focus on voltage stability. It is judicious to note that although the three categories are concerned with different aspects of the stability problem, in terms of analysis and simulations, they are in fact extensions of one another without clearly defined boundaries. When working on solutions to stability problems of one category, these should not be achieved at the expense of another, thus some degree of overlap in the phenomena being analysed is desirable.

2.3.1 Rotor angle stability

2.3.1.1 Definition and description of the phenomenon

Rotor angle stability, also often referred to as generator stability, is the ability of interconnected synchronous machines of a power system to remain in synchronism under normal operating conditions or after being subjected to a disturbance [6, 38]. Pure rotor angle stability is concerned with a radial feed from a remote generator to a large system, as shown in Figure 2-2.

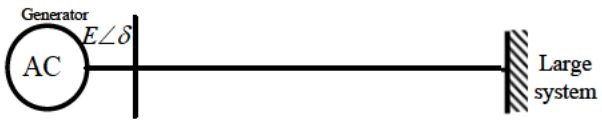

Figure 2-2: Angle stability: radial feed from remote generator to a large system

Gupta in [45] suggests that the term *stability* means *maintenance of synchronism* and these two terms may be used one at the place of the other. This form of stability is related to the manner in which SM power outputs fluctuate depending of their rotors' oscillation [6, 48]. The voltages and currents' frequency must be equal while their rotor mechanical speed must be synchronized to this frequency [6]. Power systems dynamics are hence said to be intently associated to the mechanical and electrical dynamic state variables of all interconnected SMs [49]. Increasing angular swings of some of the machines may cause instability which leads to a likely loss of synchronism [38, 50].

Rotor angle stability phenomena depend on both the initial operating state of the system and the severity of the disturbance and it is characterised in terms of small-signal or small-disturbance stability and transient stability [6].

In order to never lose synchronism, the electrical power system should be designed and operate to withstand various types of contingencies [6, 51-53].

2.3.1.2 Impact of distributed generation (DG) on rotor angle stability

With relation to distributed generation, rotor angle stability studies have been previously conducted both for transmission and distribution systems [54-57]. Authors in [57] studied the impact of DG technology on transient stability, comparing inverter-based and rotating-based types and they found a strong dependency between transient stability and technology employed. Reza et al. in reference [56] investigated the dependency of the rotor transient stability of a transmission power system to high DG penetration levels. They examined transient stability using scenarios of faults in all possible branches and concluded that the penetration level of the DG units affects power flow and hence the transient stability of the network [50]. Ameur et al. [55] performed a stability analysis on an extra high voltage (EHV) network using critical fault clearing time (CFCT) and found that the transmission power system stability was not affected.

2.3.2 Frequency stability

2.3.2.1 Definition and description of the phenomenon

The frequency of a PS is of utmost importance because the satisfactory operation of a PS requires constant frequency. Frequency variations result in a mismatch between generation and load. At any instant, the load demand is catered by the generator and/or by the within system stored energy. [19]. If suddenly the load changes increasingly, the rotational inertia will initially

provide the extra energy needed, consequently decreasing the generator's speed, thus proportionally decreasing the frequency.[19]. The control of frequency is therefore said to be closely linked to the system's active power control and balance. Frequency, or system's electrical speed is therefore firmly dependent on the speed of rotation of the turbo-generator's shaft, which is also referred to as the mechanical speed of the machine [19]. Indeed, the rotational energy, also termed as inertial stored energy in the turbo-generator due to the substantial mass and high rotational speed, is directly dependent on the moment of inertia and the square of frequency [6, 19]. Equation (2-1) shows the relationship between the three quantities:

$$E_{Rot} = \frac{1}{2} M^{\circ}.(2\pi f)^2 \tag{2-1}$$

where, E_{Rot} is the rotational energy, M° is the moment of inertia and f is the frequency.

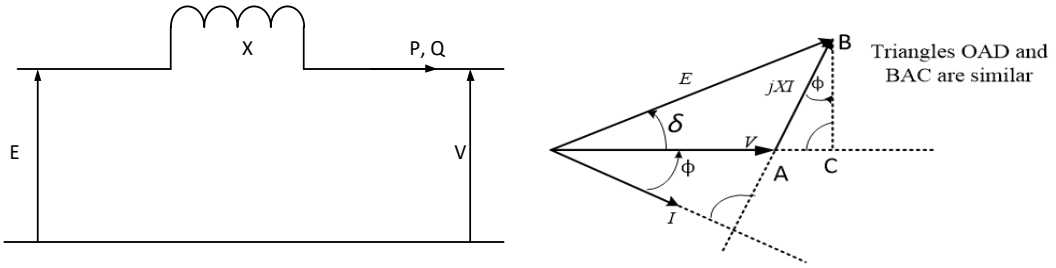

Figure 2-3 Equivalent diagram of a simplified model of network element and phasor diagram [28]

On the other hand, since a PS network is simply represented by its main elements, it is modelled as a two-port 4-terminal RLC network (two-port) as shown in Figure 2-3 and from which Machowski et al. [28] extracted the expression of the power leaving the network as follows:

$$P = \frac{EV}{X} \sin\delta \tag{2-2}$$

where, E and V are the phases of the voltage at the generator bus and at the load bus respectively, δ is the angle between their phasors and X is the series line inductance.

Equation (2-2) shows that the real power P depends on the product of phase voltages and the sine of the angle δ. Since node voltages must be kept within a small percentage of their nominal values, small variations of V and E cannot sensibly influence the value of real power, in which large changes are functions of changes in the sine of the angle δ [28]. Moreover, because this

angle is also strongly connected to the system frequency *f*, the frequency will in return be strongly dependent on active power *P*.

From the phasor diagram in Figure 2.2, knowing that $Q = VI\sin\delta$ and $Cos\delta = \sqrt{1-\sin^2\delta}$,it is established that:

$$Q = \sqrt{\left(\frac{EV}{X}\right)^2 - P^2} - \frac{V^2}{X} \qquad (2\text{-}3)$$

It is convenient to note that this fundamental relationship *Q(V)* corresponds to an inverted parabola where small changes in *V* cause large changes in reactive power ,prompting that voltage control strongly influences reactive power flow and vice-versa [28]. The relationship in Equation (2-3) will be referred to for voltage stability analysis using V-Q curves and reactive power reserve.

With regard to the impact of frequency on traditional power systems, Kundur warns that a significant frequency decrease beyond limits, could induce high magnetizing currents in induction motors and other PS elements.[6]. Each country regulates and defines acceptable limits for a power system's frequency response. Countries worldwide suggest two levels of operation, namely: the operational limit (± 0,2 Hz) and the statutory limit (± 0,5 Hz).

2.3.2.2 Impact of DG penetration on frequency stability

With respect to Distribution Generation, a number of researchers have been working on frequency stability and frequency response issues pertaining to the impact of increasing the penetration of RES into power system grids. It is widely established and accepted that a high penetration of non-synchronous generating means, with non-rotating masses meaning no stored inertial energy, causes a reduction of the total system inertia [25, 26, 58-67]. While it is obvious that PV systems have non-rotating masses, Daly et al. in ref. [60] note that wind turbines, although having rotating masses, are often not synchronously connected to the grid as their connection is mostly achieved through power electronic devices.

The reduction of system inertia due to an increased share of inertia-less resources has mainly two frequency stability implications:

(1) Faster Rate of Change of Frequency (RoCoF) resulting in possible tripping of grid components, especially embedded renewable generation, conventional generation pole slipping and cascade tripping and

(2) Higher frequency deviations (nadirs/zeniths) or the time to maximum frequency deviation, potentially leading to unintended load-shedding and in worst cases, system collapse [59, 60, 62].

In other words, the higher the penetration of RES, the lower the system frequency and the higher the RoCoF, the shorter the time-frame to reach minimum frequency.

2.3.2.3 Mitigation of frequency instability

The primary speed control function for frequency deviation mitigation is provided by speed governors supplemented by a central control [6].

For the last six decades, research efforts conducted by many authors have proposed automatic generation control (AGC) as an important technique to maintain constant frequency with the load demand [25, 26, 68-71] and many studies have developed various control strategies to design AGC controllers. Ibraheem et al. in [72] note, however, that AGC solutions have not been practically implemented due particularly to system operational constraints associated with power plants having thermal generations because of the non-availability of required storage energy capacity other than the synchronous machine inertia. Methods to overcome these include, but are not limited to, incorporating flexible alternating current transmission systems (FACTS) devices, BESS and other energy storage systems [26, 58]. Other frequency control strategies are based on the use of fast-acting energy storage devices or fast acting reserves (FAR).

Loji and Sharma in [25] critically reviewed various aspects of AGC in order to determine their role in the modern electrical system as well as to maintain the frequency standards to nominal value, besides maintaining the power interchange between the interconnected control areas in order to distribute value and cost-effective power. Indeed, Miller and Malinowski in [47] note that when equipped with computational capabilities, Automatic Generation Control schemes can provide efficient support to interconnected systems operation.

In case of severe disturbances such as all generating units loss or loss of an important load, Berger and Iniewski in [2] suggest measures similar to those identified and proposed by CIGRE in ref. [73] and they include:

- Disconnection of selected loads or load-shedding;

- Emergency HVDC power transfer control, also referred to as fast re-scheduling of an active power section;
- Disconnection of generation;

2.3.3 Voltage stability

Voltage stability has emerged as the main limiting factor for loading and for the power transfer capability of power systems [74]. At any point in time, a power system's operating condition should be stable, meeting various operational criteria and remaining secure in the event of any credible contingency. Voltage stability is the ability of a power system to maintain steady state acceptable voltages at all buses in the system, both under normal operating conditions and after being subjected to a disturbance [6, 38, 40, 75]. Pure voltage stability is concerned with a large system feeding a load at the end of a radial configuration like presented in Figure 2-4. Also referred to as load stability, voltage stability is predominantly associated with load stability and may be interpreted as the deficiency of any PS to transfer an infinite quantity of P to its loads [6, 49, 76] [6, 49, 76, 77]. Voltage stability in this case is considered to be the maximum Megawatts (MW) capacity that the system is able to transfer to a load bus prior to voltage collapse [43, 49, 78].

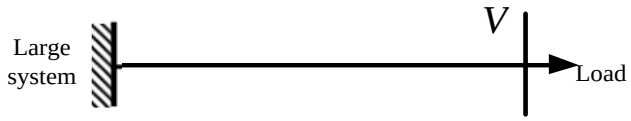

Figure 2-4: Voltage stability: radial feed from a large system to a load

Voltage instability/collapse is caused by PS inability to meet system MVAR demand [38, 76, 79] in the presence of inductive loads or a disproportionate absorption of Q by the system itself, meaning high Q losses to keep desired voltages [75, 80, 81].

2.4 Voltage instability and voltage collapse

2.4.1 In a centralised traditional power system structure

A PS enters into voltage instability state when, following a disturbance, voltage progressively and uncontrollably decays. [75]. For the last fifty years, voltage instability phenomena have been considered as one of the key causes of power insecurity as ascertained by post research on so many supply loss incidents and events [82, 83].

Voltage instability problems pose complex challenges to many planners and operators because of, amongst other reasons, the following [81]:

- Unlike in angular/frequency stability problems that are normally limited to those of power plants, any bus in the system from bulk transmission to distribution is a potential candidate for voltage instability;
- Voltage instability can occur in the midst of an otherwise perfectly healthy system; and
- An in-depth analysis of voltage instability may require data and information not normally available to the system planner, including over-excitation limiter characteristics, the nature and magnitude of the loads, OLTCs, location of power compensation devices, etc.

2.4.2 Voltage collapse

2.4.2.1 Definition

According to the IEEE, voltage collapse is defined as the process by which post-disturbance equilibrium voltage falls to a low, unacceptable value as a result of an avalanche of events accompanying voltage instability [6, 75, 84] subsequently leading to a loss of voltage in a significant part of the system [76, 77]. Typically, voltage instability is initially a local phenomenon involving a PS load area. However, it can spread into a larger area and ultimately cascade to blackout and if appropriate measures are not taken in reasonable time, conditions will deteriorate progressively with a widespread impact. Under normal circumstances, PS are operated often closer to voltage stability limits at relatively steady levels, resulting in a higher probability of voltage instability or collapse [6, 74, 85].

System control engineers are faced with the challenge of recognizing conditions which might lead to voltage collapse and how to avoid the risk of it occurring whilst not unduly compromising the objective of dispatching generation in an economic order [85].

2.4.2.2 Voltage stability indices (VSIs)

Saadati and Mirzaei in [86] note that in order to prevent voltage collapse, there is a desperate need to identify the methods that can be used to predict the occurrence of this phenomenon. Voltage Stability Indices (VSIs), also called voltage proximity/prediction indices, are used as tools to identify system's weakest areas, critical lines and power stability margins [86].

With regard to voltage stability prevention, various aspects of VSIs have been researched by several authors. Lee and Han in [87] suggest the Thévenin equivalent (TE) impedance estimation, which has the advantage of being simple. Indeed current and voltage data from local phasor measurement units (PMU) lead to the determination of the TE impedance of the remaining systems and when the measured load is equal to Z_{THE} ,meaning the maximum power delivered point, voltage instability occurs. By translating the load observation and Z_{THE} to the system margin, monitoring of voltage stability can be achieved.

2.4.3 Classification of voltage stability

Voltage instability incidents may also be clustered according to their duration or time span. With regard to that, the authors in [6, 49, 84] identify short-term and long-term voltage stability dynamics, also simply called short-term and long-term dynamic stability. Automatic voltage regulators (AVR), excitation systems, turbine and governor's dynamics [82],. Long-term voltage stability problems are due to large disturbances between generators and load occurring in heavily loaded systems where the electrical distance between the load and generator is large [40] and depend thus on the detailed topology of the power system [82]. Taylor in [84] provides in Figure 2-5 components and controls that may affect the voltage stability of a power system, along with their time-frame of operation.

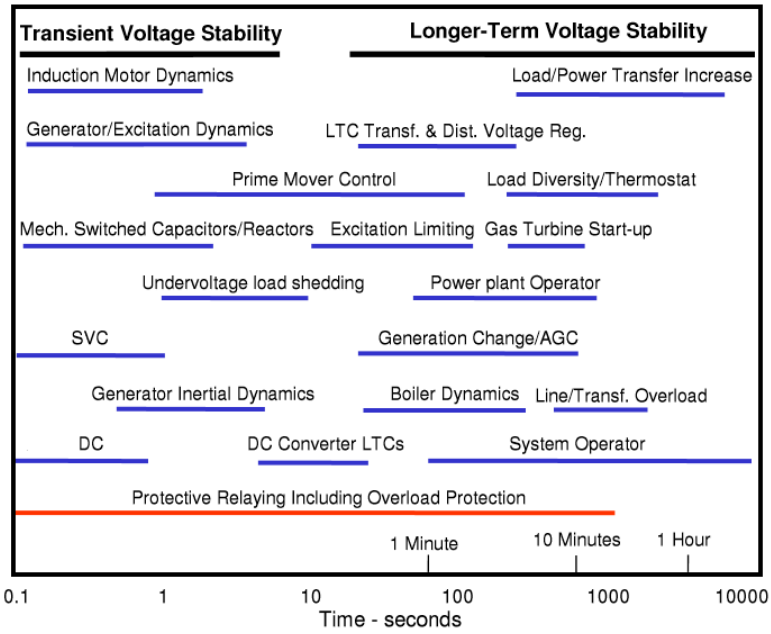

Figure 2-5: Transient and long-term voltage stability causes and time frames [88]

2.5 Voltage stability assessment/simulation

In simulation approaches, as well as in real power system networks, voltage assessment requires a power monitoring tool to control the PS because of hourly changes caused by various situations that occur in the system [89]. Koessler in [81] suggests that the best way to start a voltage stability investigation is with a conventional power flow with a constant power load model and reactive power limits on generators. Lo et al. in [90] note that researchers have applied different analysis methods, with a debate on whether voltage stability is a static or a dynamic phenomenon. The authors in [75] and [79] suggest that voltage stability can be studied either on static (slow time-frame) or dynamic (long time-frame) considerations. According to Taylor, dynamic simulation is essential for short-term voltage stability (as for angle stability) assuming dynamic models for motor loads, generators and SVCs, but can also be valuable for long-term stability, with the purpose of performing coordination controls and greater accuracy and insight of the problem [88]. A number of researchers noted that although stability studies in general require PS dynamic model, static approaches are widely used for the assessment of voltage stability [74, 90, 91] as they are less complex and require low computational times to carry out a system stability analysis [92]. Static approaches are adequate whilst analysing due to the fact that the system dynamics influencing voltage stability are usually slow [93-95], and the dynamical behaviour may be closely approximated by a series of snapshots matching the system condition at various time-frames along the time domain trajectory [95].

2.5.1 Variation of V on P-Q plane

Considering a simple two-bus system as show in Figure 2-6. and Equations (2-2) and (2-3),

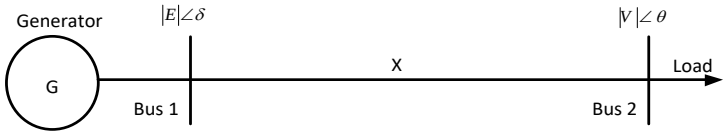

Figure 2-6: Two-bus test system

given by $P=\frac{EV}{X}\sin\delta$ and $Q=\sqrt{\left(\frac{EV}{X}\right)^2-P^2}-\frac{V^2}{X}$ respectively, as developed and deduced from section 2.3.2.1. above, and after normalization, the relationship $v=f(p,q)$ is expressed by Equation (2-4) as follows:

$$v^4+v^2(2q-1)+(p^2+q^2)=0 \tag{2-4}$$

where $p = v\sin\delta$ and $q = -v^2 + v\cos\delta$ assuming that $v = V/E$, $p = P.X/E^2$ and $q = Q.X/E^2$

The set of possible solutions of *v* from Equation (2-4) are:

$$v = \sqrt{\frac{1}{2} - q \pm \sqrt{\frac{1}{4} - p^2 - q}} \tag{2-5}$$

The subsequent plot of the voltage in the $p-q-v$ plane is depicted in Figure 2-7 in which a close scrutiny allows to note that for each point in the plan (p,q), there are two voltage solutions: (1) For high voltage or stable solution and (2) For low voltage or unstable solution.

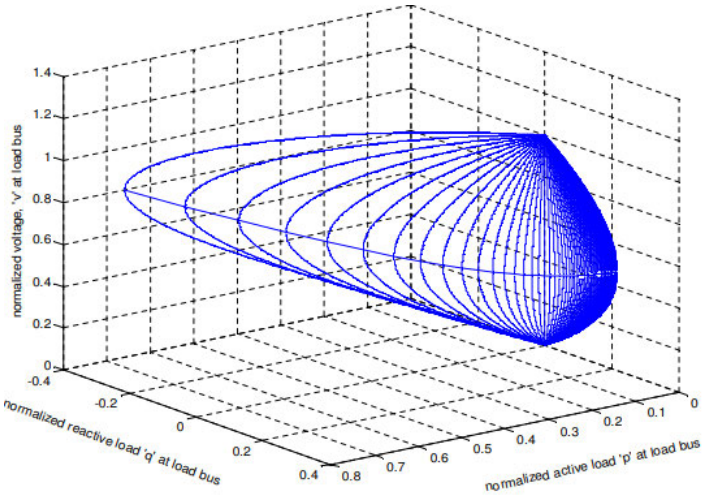

Figure 2-7: Voltage plot on the P-Q-V plane for a 2-bus test system [96]

There are several analytical methods available for voltage stability margins estimation and for voltage collapse points prediction [86].

P-V and Q-V curves, also called nose curves [76], have been used to analyse the voltage stability of a PS [40]. Having studies comparatively various methods and techniques, Persai and Thakur in [79] found and suggest P-V and Q-V curves methods as effective tools for stability analysis.

Given that this research also uses the P-V curves for the determination of loadability conditions in some simulated cases, section 2.5.2.1 is dedicated to a deeper focus on this method.

2.5.2 Voltage stability analysis

The complexity of voltage stability assessment is that the voltage profile comprising all bus voltages shall result from the combined effect of the whole network topology, load-generation

pattern and reactive power compensation on the system behaviour and on the voltage margin [74]. In the search for solutions, a performing approach would be the one capable to clearly reveal the effect of all system characteristics and events on the voltage stability margin, which remains a real challenge. In reference [74], fast and easy calculations from a synchronously measured voltage profile without any need of system modelling and simulation and without any dependency on network size is one of the attractive features for a suitable approach, as suggested by Aghamohammadi et al. [40].

Kumar et al., amongst others, suggest that the voltage stability analysis for a system involves the examination of two aspects: Proximity to voltage instability and Mechanism of voltage instability[77].

The literature provides several methods to carry out a voltage stability analysis. Conventional methods may be broadly classified into the following categories [79, 82]: (1) P-V curve methods, (2) the V-Q curve method and Q reserve, (3) the Singularity of power flow Jacobian matrix at the point of voltage collapse and (4) the Continuation of power flow method.

P-V and V-Q curve power flow programs have been often, both used for the planning and operation of PS [97] and the following sections provide more detail on the methods.

2.5.2.1 P-V curve method

P-V curve method provide the available MWs margin to instability point. The curves describe the voltage path against the consumers' power demand [82, 83, 98] and they allow the operator to effectively identify the loadability margin. The method relies on the accuracy of data to build up the curves[83]. This method can be used to analyse radial systems, large meshed networks, transmission interfaces or interconnections and consist essentially of monitoring the voltage at the critical bus, $V_{critical\_bus}$, against the changes in real power in a radial system. In mesh networks the real power P can be the total active load in the load area and V the voltage at the critical or representative bus [82, 83].Considering the two-bus system given in Figure 2.3, equation 2-4 gives real solutions of v^2 as $(1-4q-4p^2)\geq 0$. If it is assumed at a constant power factor, meaning $\frac{q}{p}=\cos\theta=k$, the inequality can be expressed as $p\leq\frac{1}{2}((1+k^2)^{\frac{1}{2}}-k)$,which determines the maximum value of the active power and can allow computing of the active power margin for a load with a suitable constant power factor. For different values of power factors, normalized values of load active power are show in Figure 2-8 (a). It is evidenced that for different power

factors, from lagging to leading power factor values, the knee point shifts toward higher values of real power and higher voltages, suggesting the improvement of voltage stability [77].

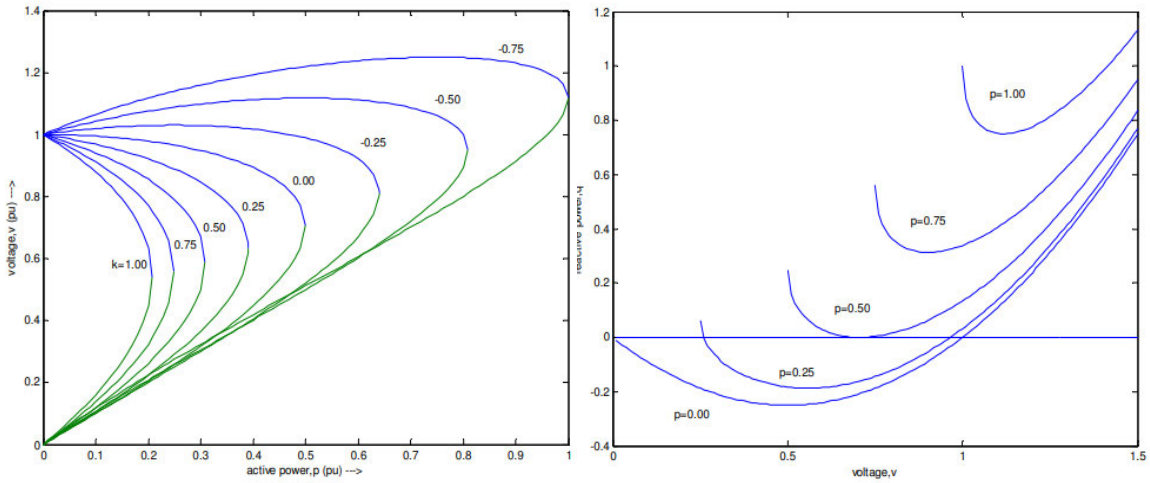

(a) Normalised P-V curves (b) Normalised V-Q curves

Figure 2-8: P-V and V-Q curves for a 2-bus test system

Notwithstanding the above considerations, Thanekar et al. in [83] warn that a major mathematical error may arise in this method when the load flow simulation close to maximum power limits are diverging. P-V curves analysis is used in this research work to assess system stability conditions of a PV penetrated network and to determine the limit of the system loadability, as well as the critical voltage collapse point.

2.5.2.2 V-Q curve method and Q reserve

This method is used to investigate voltage instability problems during the post-transient period and does not require to be represented as a two-bus equivalent, unlike the P-V curve method [38, 84, 96]. Chawdhury and Taylor in [97] indicate that the V-Q method was developed for stressed cases close to maximum power transfer where the power flow program was converging with difficulties. Convergence was then achieved by fixing the voltage at a critical or a test bus and this voltage is plotted against reactive power at that particular bus, with the voltage magnitude scheduled as an independent variable and the reactive power injection as a dependent variable [97]. For a given condition of operation at each bus of the system, an increase of V at bus occurs, while Q injection at the same bus varies [99]. However, Chakrabarti found that V-Q curves, similar to P-V curves, are also possible where reactive power at one or many buses are independent variables, and voltages at many other buses are dependent variables.). As justified by Equation (2.3). Chakrabarti in [82] notes that the voltage security of a bus is closely related to the available reactive power reserve, which can be found from the V-Q curve of the

bus under consideration. The reactive power margin is the MVAR distance between the operating point and the nose point, or the point where capacitor characteristics at the bus are tangent to the V-Q curve [84]. The analysis can be done for a power flow base or an outage case with a series of voltage magnitudes scheduled at a selected important bus that is changed to a fictitious PV bus and this analysis can be applied to more than one bus [97].

Equations of V-Q curves for constant power loads can be derived from the normalization equation $q = -v^2 + v\cos\delta$. From this equation, a range of values of voltage and different active power levels and normalized V-Q curves can be plotted as shown in Figure 2-8 (b). The curves are of two different types: (1) reactive "*demand*" curves and (2) reactive "*supply*" curves. The former curves show the reactive injections at a bus or a group of buses necessary to sustain a certain voltage and the latter set of curves indicates the MVARs produced by shunt compensation as a function of bus voltages [81]. The critical point or nose point of the characteristics corresponds to the voltage where $\frac{dQ}{dV} = 0$. If the minimum point of the V-Q curve is above the horizontal axis, then there is deficiency of reactive power- in other words, additional reactive power sources are needed to prevent voltage collapse [82].

Chawdhury and Talylor in [97] suggest the following non-exhaustive list of advantages when compared to the P-V Curve method:

(3) The V-Q method is fast if case studies are automated and this method has no convergence problem, even on the "unstable" left side of the curve;
(4) The reactive power compensation requirements are approximately provided by the compensation characteristics, meaning that the compensating devices output can be superimposed on the V-Q system characteristic; and
(5) The stiffness of the bus can be qualitatively evaluated from the slop of the right portion of the V-Q curve. The greater the slop, the stiffer the bus and therefore the more vulnerable to voltage collapse it is [82].

The disadvantages of the V-Q method include:

(1) The method is artificial, involving stress at a single bus for local area evaluation [6];
(2) The allowable power loading or interface flow is not directly given and V-Q curves may be required per contingency case and per power level considered;

(3) V-Q curves indicate local (bus) compensation needs for a given operating condition rather than global optimal compensation needs; and,

(4) Similar to other power flow-based methods, generator and load models are generally used in place of more real load, and the time-dependent aspects of control actions are not represented.

2.5.2.3 Singularity of power flow Jacobian matrix at the point of voltage collapse

One of the most popular methods for voltage stability analysis based on the singularity of power flow Jacobian matrix at the point of voltage collapse is the modal analysis of the Jacobian matrix [6, 38, 100].

This method uses the first Lyapunov theory based on the behaviour of the linearized system around the vicinity of its equilibrium point by examining the eigenvalues of the state matrix.

The power system linearized model can be represented by: $\Delta\dot{x} = A\Delta x + B\Delta u$,where matrix A is a square (*n* x *n*) matrix defined as state matrix and B is the control matrix. Matrix A describes the dynamic behaviour of the system with no-control action applied to it and matrix B accounts for the dynamic behaviour response to control actions [37].

The left and right eigenvectors of the state matrix A of the system can be calculated using the following equations: $Ax = \lambda x$ and $yA = \lambda y$ where $\lambda =$ eigenvalue of A, x (n x 1) = $X = [x_1, x_2, x_3, ...x_n]$ is the right eigenvector or modal matrix and y (1 x n) = $Y = [y_1^T, y_2^T, y_3^T, ..., y_n^T]$ is the left eigenvector, which both have $\det(A - \lambda I) = 0$ as the characteristic equation.

Power flow equations can be written in matrix form as:

$$\begin{bmatrix} \Delta P \\ \Delta Q \end{bmatrix} = \begin{bmatrix} J_{p\delta} & J_{pV} \\ J_{q\delta} & J_{qV} \end{bmatrix} \cdot \begin{bmatrix} \Delta\delta \\ \Delta V \end{bmatrix} \tag{2.6}$$

where ΔP and ΔQ are the changes in the real and reactive powers respectively and, $\Delta\delta$ and ΔV are the deviations in bus voltage angles and voltage magnitude respectively.

To calculate V-Q sensitivities, the changes in real power can be assumed to be zero, meaning $\Delta P = 0$ thus equation (2.6) becoming: $\begin{bmatrix} 0 \\ \Delta Q \end{bmatrix} = \begin{bmatrix} J_{p\delta} & J_{pV} \\ J_{q\delta} & J_{qV} \end{bmatrix} \cdot \begin{bmatrix} \Delta\delta \\ \Delta V \end{bmatrix}$.

Processing and equating leads to

$$J_{p\delta}.\Delta\delta + J_{pV}\Delta V = 0 \text{ or, } .\Delta\delta = -J_{p\delta}{}^{-1} J_{pV}\Delta V \tag{2.7}$$

and

$$\Delta Q = J_{q\delta}.\Delta\delta + J_{qV}\Delta V \tag{2.8}$$

Substituting $\Delta\delta$ (2.7) into (2.8) and assuming $J_R = J_{qV} - J_{q\delta}.J_{p\delta}^{-1}.J_{pV}$ leads to $\Delta Q = J_R.\Delta V$ or

$$\Delta V = J_R^{-1}.\Delta Q \tag{2.9}$$

or,

$$.\Delta\delta = -J_{p\delta}{}^{-1} J_{pV}\Delta V \tag{2.10}$$

$$\Lambda^{-1} = \begin{bmatrix} \lambda_1^{-1} & ... & ... & ... & 0 \\ 0 & \lambda_2^{-1} & ... & ... & 0 \\ 0 & 0 & \lambda_3^{-1} & ... & 0 \\ 0 & 0 & 0 & \lambda_{n-1}^{-1} & 0 \\ 0 & 0 & 0 & ... & \lambda_n^{-1} \end{bmatrix} \tag{2.11}$$

Pai et al. in [101] warn that the singularity of the Jacobian matrix is necessary but not sufficient to indicate voltage instability.

The modal indexes involve Eigen values where the smallest serve as the index to judge the stability of the system. Voltage stability applications with PMU have been addressed by several references. [102] that propose WAMS and a wide area voltage index (WAVI).

2.5.2.4 Continuation power flow (CPF)

The CPF method has been widely applied. Chakrabarti in [82] indicates that it is numerically difficult to obtain a power flow solution near the voltage collapse point since the Jacobian matrix becomes singular and to this deficiency, CPF is used for mitigation and as a solution that can be obtained near or at the voltage collapse point [6, 82, 96]. In [103], Krishna and Manohar explain that the CPF method is used to find successive load flow solutions according to a load scenario by predicting and correcting steps based on a known base solution. A tangent predictor is used to estimate the next solution for a specified pattern of enhancement load. Then the corrector steps determine the exact solution by using the Newton-Raphson technique employed in a conventional power flow [103]. It uses a gradual loading factor. Depending on the system load condition and on their analytical definition, some indexes grow or extinguish when no control actions are applied during system loading increment.

2.5.2.5 Other methods of voltage stability analysis

In [83], the authors studied the voltage stability phenomenon and reviewed the application of the phasor measurement unit (PMU) which is a model composed of a traditional state estimator, a concentrator and a control centre. State estimation is a method of estimating voltage magnitude and angles at all the buses of a power system from available measurements obtained through suitable means, and these measurements are processed through the state estimation algorithm to obtain all the voltage magnitudes and angles at all the buses. Most power systems analysis software, including *DigSILENT™ PowerFactory™*, have the state estimation algorithm embedded in them with the possibility to enable the functionality of voltage stability analysis via the quasi-simulation tool.

State estimation depends on the accuracy of measurement. The higher the accuracy of the measurement, the higher the accuracy of state estimation.

With regard to contingency analysis, the authors in reference [104] proposed a model approach for power quality and voltage instability that consists of a two-block technique, meaning filter out the dangerous contingency and assess it for severity based upon the performance index.

2.5.3 DG penetrated grids and voltage stability

Mahmud and Zahedi in [105] analysed the direct impacts of the increased accommodation of renewable DGs on the distribution network operation and evaluated the current research status of voltage control strategies and approaches involving their pros and cons. FACTS and so many other traditional methods have been commonly used as voltage variation mitigation strategies in DG penetrated grids. Oni et al. in [106] comparatively studied the impact of the HVDC scheme on AC systems' short-term voltage stability and found that HVDC compared to FACTs devices help in enhancing voltage stability and help, for instance, to improve critical clearing /isolating times for disturbances on the system better than FACTs. Using the rapidly growing capability in computer and communication technologies, Berger and Iniewski in [2] point to the necessity of introducing smoother schemes that will be used in a wide-area emergency control and protection system. This emergency system, accompanied by powerful and synchronised actions, has to be activated when the power system has entered into transition towards instability after surviving the initial disturbance and having systems dynamics triggered [2]. Table 2-3, summarises wide-area monitoring and control strategies with reference to voltage stability [2].

Table 2-2: Considered Real-Time Wide-Area Monitoring and Control Strategies for Voltage Stability [2]

Function	Uni-bidirectional	Maximum Delay	Sample Rate	Reference
VOLTAGE STABILITY				
Local voltage stability monitoring	Unidirectional	10-30 s	0.5-5 s	
Wide-area voltage stability monitoring	Unidirectional	0.5-5 s	0.5-5 s	
Wide-area voltage stability control	Bidirectional	0.5-5 s	0.5-5 s	
Wide-area FACTS and HVDC control	Bidirectional	30 s to 2 mins	30 s to 2 mins	
Cascading failure control	Bidirectional	0.5-5 s	0.5-5 s	

2.6 Voltage control

Section 4.10 specifically addresses voltage control in relation with the context of this research work.

Some of the control actions used as counter-measures against voltage collapse is as follows: • Switching of shunt capacitors • Blocking of tap-changing transformers • Re-dispatch of generation • Re-scheduling of generator and pilot bus voltages • Secondary voltage regulation • Load-shedding.

2.7 Summary

This chapter primarily reviewed the most relevant research on the historical development of traditional power systems with respect to power system stability issues. The review included power systems dynamics and power systems instability phenomena. Secondly, rotor angle stability and frequency stability were discussed, with a particular focus on how they are effected by inertia-less means of generating power, such as distributed generation. Lastly, in a fairly more elaborated account, voltage stability, voltage instability assessment and subsequent mitigation techniques were presented and discussed. With regard to DG penetration, it was noted that the distribution network became an active system with power flows and voltages determined both by the generation as well as the loads.

CHAPTER 3: DISTRIBUTED GENERATION

Introduction

Due to increases in electricity demand and environmental policies compelling the world to reduce its CO_2 footprint, renewable energy sources (RES) have massively and rapidly developed. RES are often intermittent and geographically dispersed, but their integration into the grid is fundamentally similar to that of any other fossil fuel-powered generator and it is based on the same principles [19]. However, the integration of DG units into the grid, mainly via power electronic mediums, increases uncertainty in power system operations as they modify both the structure and the operation of the distribution network, with a particular impact on voltage stability margins.

This chapter discusses the historical development of distributed generation technologies, with a particular focus on PV and Wind technologies. Focus will be further directed at the increasing penetration of PV into the distribution end and their impact on power system voltage stability. Existing techniques to mitigate various impacts of DGs grid penetration are also reviewed under this chapter.

3.1 Definition of distributed generation

3.1.1 Definition

Bhadoria et al.[107] note that in literature, definitions for distributed generation are not consistent and a large number of terms and definitions are proposed. Ackermann et al. in [108] recommend that due to large variations in the proposed definitions, there was rather a need to use issues pertaining to distributed generation in order to define it more precisely. Those issues, resulting from an agreement amongst different authors and organisations, are as follows: purpose, location, rating, power delivery area, technology, environmental impact, mode of operation, ownership and penetration into the grid [108]. Figure 3-1 shows the criteria used to classify DG. The purpose of DG is to provide active electric power. This means that DG does not need to be able to provide reactive power. It is accepted that the rating of the DG, the power delivery area, the technology, the environmental impact, the mode of operation, the ownership and the penetration into the grid are not relevant to this definition. In view of all these considerations, distributed generation can be defined as a relatively small power generation

source, compared to the central generating plants [107], that is directly connected to the distribution networks and is close to the loads being served[108, 109].

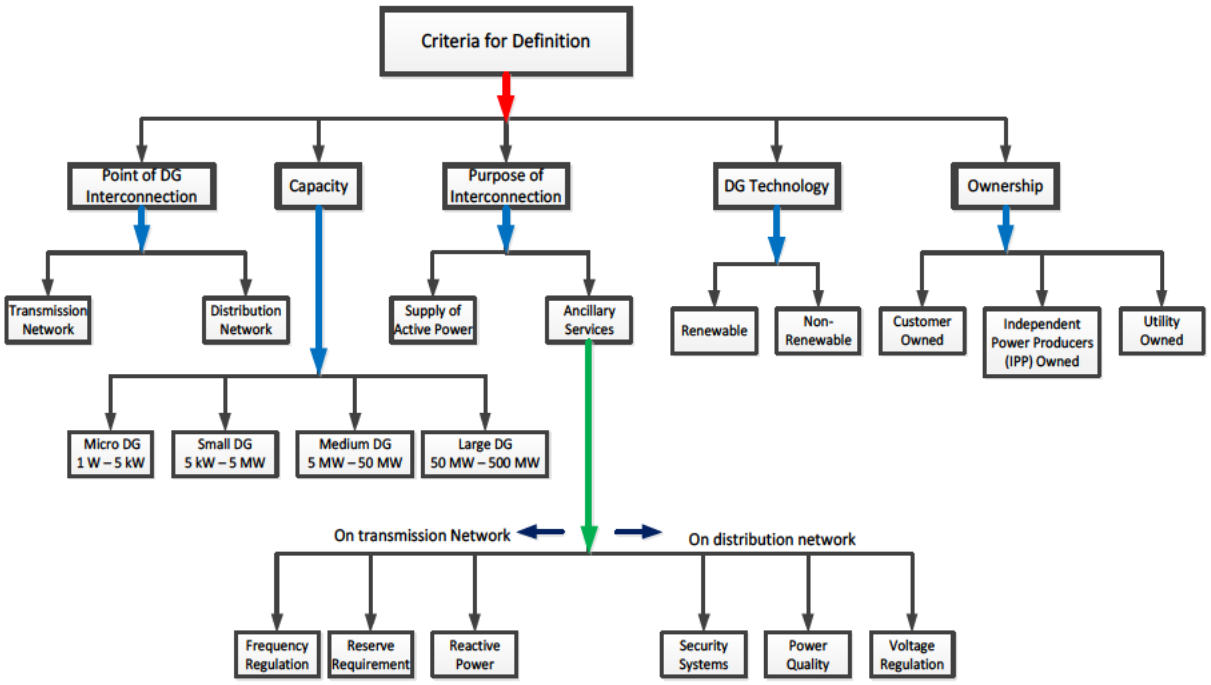

Figure 3-1: Criteria for classification of DG[110]

With regard to various terminologies employed to name distribution generation, embedded generation, dispersed generation, distributed energy resources (DER) and decentralised generation have also been used in the context of DG. The term 'dispersed generation' in particular is usually referring to any distributed power generation, regardless of the technology and whether it is connected to the grid or is a standalone system.

3.1.2 Positive and negative impacts of DG on power systems

The introduction of DG to the distribution end has significant positive or negative impacts on power and voltage conditions throughout the system. Positive impacts are generally called 'system support benefits' and they include reduced loss, improved system reliability, backup or emergency power, voltage support and improved power quality, transmission and capacity release, deferments of new or upgraded transmission and distribution infrastructure, lowering costs of expansion of HV lines and low emission of air pollutants, meaning that it is environmentally friendly [111-116].

With regard to power system voltage issues, although from the definition provided above, DG does not need to provide reactive power, Kennedy in [117] amongst others notes that in fact

DG can provide improved reactive power, system voltage control and also reduce system losses. In section 3.2.2 below, a classification of DG in relation to real and reactive power delivery is provided.

3.2 Types of DG sources

3.2.1 Based on dispatchability and non-dispatchability

DG sources used in distribution systems can be classified into two main categories: dispatchable and non-dispatchable energy sources. Dispatchability is the ability of a power plant to be turned ON quickly to a desired level output [118]. Figure 3-2 below shows the classification of distributed generation sources based on the dispatchability or non-dispatchability of the source. Dispatchable sources can be controlled by operation and they include Micro turbines (*Natural gas turbine*), Reciprocating Internal combustion engines (*Diesel engine and Gas engine*), combustion engines (*Gas turbine*), Electro-mechanical energy sources (*Fuel cells*) and storage energy sources (*Batteries, Flywheels, Superconducting Magnetic Energy Storage and Super capacitors*) and some renewable energy (Bio-mass, Geo-thermal and Ocean Thermal Energy Conversion).

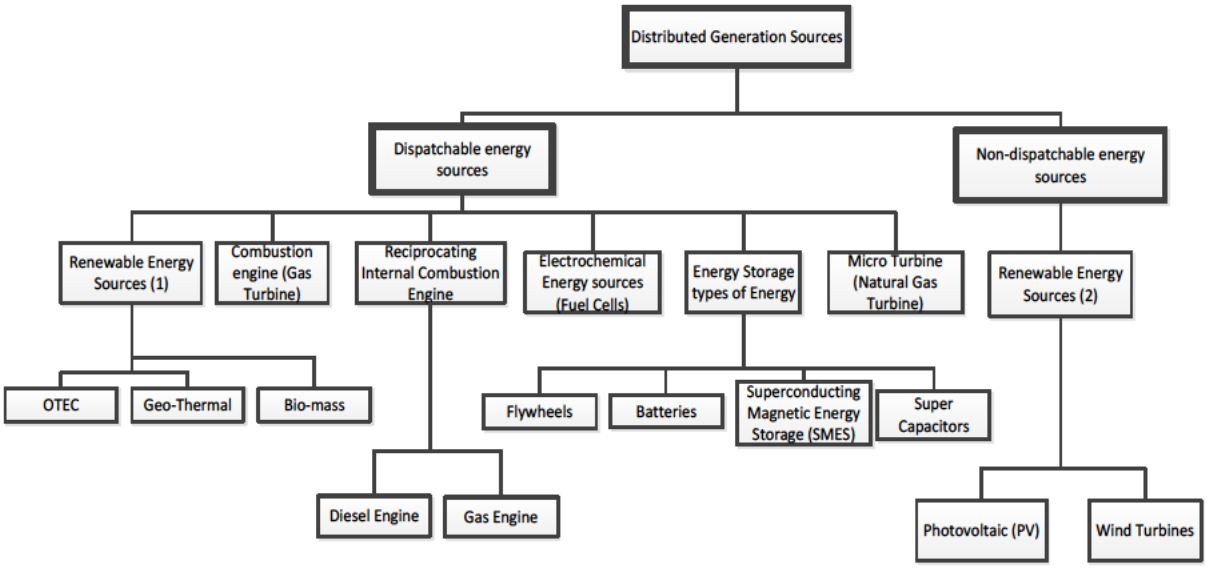

Figure 3-2: Classification of distributed generation sources

Non-dispatchable sources cannot be controlled by operation as they originate and depend on natural factors such as sun irradiation and wind that are not easy to domesticate and/or to bring under control. Non-dispatchable energy sources are essentially renewable energy sources, namely photovoltaic and wind turbines.

Besides being non-dispatchable, PV and wind energy resources are intermittent and of a stochastic nature, meaning that they occur at irregular intervals and have a random distribution or pattern over a period of time. They may be analysed statistically, but would not be predicted precisely. PV and wind resources cannot meet the continual load demand 24-hours a day, 365 days a year. Energy storage is therefore a desired feature to incorporate with renewable power systems. To achieve the cost and performance requirements, Bello in [111] suggests that during the planning stage, a balance is made between the average generating capacity of the PV, the battery storage capacity and the average load demand.

3.2.2 Based on real and reactive power delivery

The concept of distribution generation can be extended to the planning of their installation into grids and the subsequent requirements for their real and reactive power contribution to the power system network. In that regard, Sing and Sharma in [119] suggest that based on P and Q provision and delivery, DGs are classified into four categories as follows:

(i) **DG1 or T1**: provide only P power supported at unity power factor to the system. For example, PV cell, Solar systems, biogas, etc.

(ii) **DG2 or T2**: deliver P and Q power supported to system and operating at 0,80 – 0,99 leading power factors. For example, wind, tidal, wave, geo-thermal, etc.

(iii) **DG3 or T3**: deliver only Q supported for the system and operating at unity power factor. For example, synchronous condenser, inductor and capacitor banks; and

(iv) **DG4 or T4**: delivers Q to the system and absorbs P from the system and operating at 0,80 – 0.99 lagging power factor. For example, Doubly-Fed Induction generator (DFIG) wind turbine.

3.3 Solar technologies

3.3.1 Introduction to PV systems

PV is a solar energy technology that uses the unique properties of semiconductors to directly convert solar radiation into electricity [120]. Messenger and Ventre in [121] associate photovoltaic systems with photovoltaic cells. Zweibel and Dunlop recall and mention that the PV effect was discovered long before the solar cell [120, 122] by the French scientist Alexandre-Edmund Becquerel in 1839. However, solar cells came to light only around the 1950s and their subsequent development for energy conversion on a large scale became of

interest in the mid-1970s, surely triggered by the energy crisis of the time [122, 123]. For quite a relatively long period, Dunlop notes that space applications such as satellite were the first practical use of PV technology [120]. Sunlight is the fuel of solar cells, which are made from semiconductors and have much in common with other solid-state electronic devices such as diodes, transistors and integrated circuits [123].

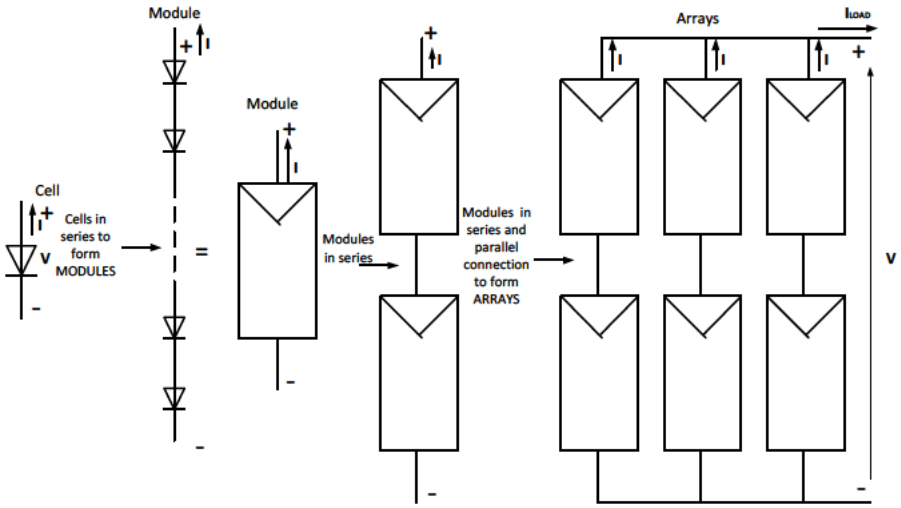

Figure 3-3: PV configuration, cells, modules and arrays[121]

A single cell produces less than 2 watts at approximately 0,5 V and to produce enough power for high power applications, cells are connected in a series-parallel configuration and then configured in modules and modules in arrays, as shown in Figure 3-3. Module power may reach 300 watts, while arrays power can range up to some kilowatts [22, 121, 122].

Conversion technologies are active and passive solar designs based on the optimal design of the buildings that capture the sun's energy in order to reduce the need for artificial light and heating [124, 125]. Due of the unpredictability of sun illumination, energy storage mechanism systems may be combined with PV for a fairly constant supply. The most common storage mechanism consists of rechargeable batteries with a charge controller into the system to prevent the batteries from overcharging or over discharging conditions. In addition to providing energy storage, batteries also provide transient suppression, system voltage regulation and serve as an available source of current beyond the PV arrays' capabilities [121]. The PV system delivers power directly to DC loads. For AC loads, an inverter coupled to the system will be needed. A PV system may be connected to a utility grid or may be a standalone system. Interconnection to the grid is achieved via suitable interfacing circuitry to allow the PV system to deliver the

excess of energy to the grid and/or to use the grid as back-up system in case of insufficient PV generation, as well as to disconnect it from the grid in the event of grid failure [121].

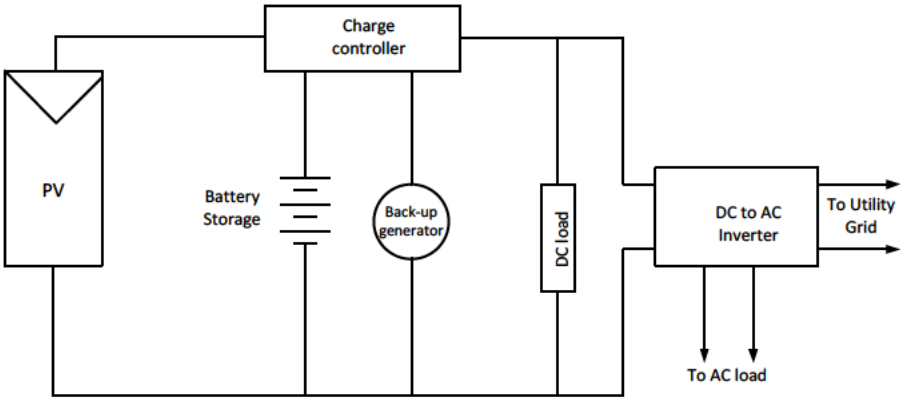

Figure 3-4: PV system with battery storage and back-up generator, charge controller, DC load inverter with connection to grid and to AC load

Photovoltaic cells are P-N junction type semi-conductor devices that have a large area which can be exposed to sunlight [22]. When the cell receives the illumination, the silicon crystalline absorbs photons from sunlight and releases them as electron-hole pairs by their interaction with the atoms. The electric field created by the cell junction causes photon-generated electron-hole pairs to separate, with electrons drifting into the N-region and holes drifting into P-region [121]

The simplified equivalent electrical circuit of a crystalline PV module is shown in Figure 3-5 below:

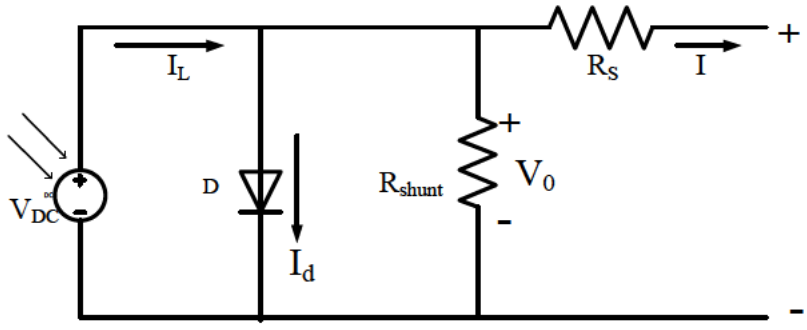

Figure 3-5: Equivalent circuit of the crystalline silicon PV module [126]

The output current I of the PV module is expressed in Equation (3-1) below:

$$I = I_L - I_d - \frac{V_0}{R_{shunt}} \tag{3-1}$$

where, I is the module's current, I_L is the photo current, I_d is the diode cell current, V_0 is open circuit voltage and R_{shunt} is the shunt resistance.

In Equation 3-1, the diode current I_d is given by Equation (3-2):

$$I_d = I_0[e^{\frac{qV_0}{nkT}} - 1] \tag{3-2}$$

where, I_0 is the reverse saturation of the diode, V_0 is open circuit voltage, , $q = 1{,}6x10^{-19}C$ is the charge of an electron, $k = 1{,}38x10^{-23}J/K$ is the Boltzmann constant , T is the cell temperature in Kelvin [K] and n is a factor whose value comprises between 1 and 2.

3.3.2 Terminal properties of the PV cell: I –V characteristic

Electrical performance of the cell is specified by the I-V curve, which represents all I-V operating points and is dependent on solar irradiation level and cell device temperature. The intensity of the solar radiation (insolation) that hits the cell controls the current I, while the voltage is reduced by the increases in the temperature of the solar cell [127]. The characteristic gives a detailed description of the ability to convert solar energy as well as the efficiency of the cell, the module or the array [121, 127]. The I-V characteristic is ideally represented by Equation (3-3), also known as Shockley's equation for a diode in terms of the output current I [121-123] and resulting from the combination of equations (3-1) and (3-2), assuming $n = 1$ in the later equation,

$$I = I_L - I_0(e^{\frac{qV_0}{kT}} - 1) \tag{3-3}$$

where I_L is the component of the cell current due to photons or light-generated current, I_0 is the reverse saturation of the diode, V_0 is the open circuit voltage, , $q = 1{,}6x10^{-19}C$ is the charge of an electron, $k = 1{,}38x10^{-23}J/K$ is the Boltzmann constant , T is the cell temperature in Kelvin [K].

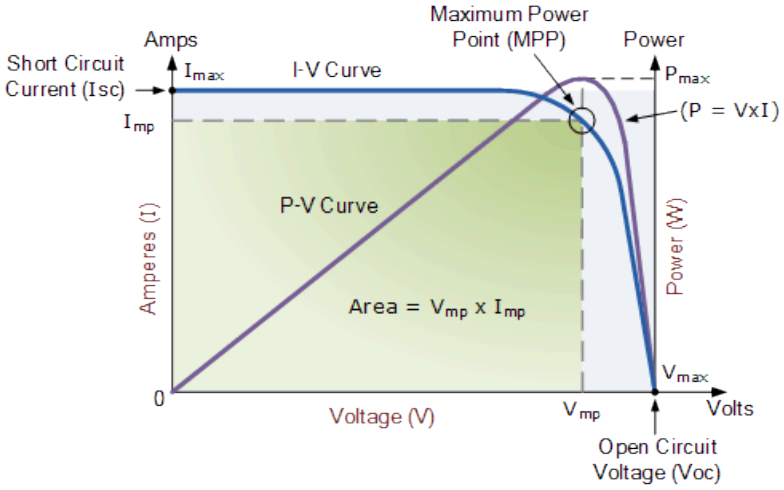

Figure 3-6: Solar-Cell I-V characteristic Curve [127]

With no load or sufficiently high resistive load connected to the cell, when the light shines on the cell, charges build up the electric field as they cannot leave the cell until the built-in field is unable to separate any newer free charges. This maximum build-up of separated charge is called open-circuit voltage (V_{OC}), which is the largest voltage the cell could generate and it is measured at no current flow from the cell [122]. By reducing the load resistance and allowing current to flow, the cell voltage drops a little as current (movement of charges) flows till a short circuit condition is made, in which case any solar photon entering the cell sends their electrons to the external circuit, thus no electric field is built, meaning a very low voltage cell with the maximum current that the cell can generate, also referred to as 'short circuit current' (I_{SC}). From the graph in Figure 3-6, it can be noted that at any operating point, the power provided by the cell is the product of its operating current and voltage. Under open circuit conditions, voltage is highest but with zero current, thus no power is provided by the cell. Similarly, under short circuit conditions, current is largest but with no voltage, thus no power. Between these two extremes, a compromise condition combining relatively highest current I_m and highest voltage V_m will result in maximum power $P_{\max}$ as presented in Equation (3-4), which basically will always be smaller than the actual product of V_{OC} times I_{SC}. The closeness with which maximum power approaches the product $V_{OC}.I_{SC}$ is termed fill factor (FF) and it is mathematically defined as the ratio of the power at maximum power condition to the product $V_{OC}.I_{SC}$. In a good cell, the fill factor is above 70 % [121-123].

$$P_{\max} = I_m.V_m = FF.I_{SC}.V_{OC} \tag{3-4}$$

It can be noted that since solar cell output voltage and current both depend on temperature, the actual output power will vary with changes in ambient temperature [127], with most PV cells being rated at 25°C. Additionally, PV array output varies depending on the type of cells used (thick crystal and having the highest performance and relatively expensive, polycrystalline, thin vapour films and laminate), the amount of light striking the cells, its angle of incidence and other ambient conditions [22].

3.3.3 Power factor

PV systems are usually designed to operate at unity power factor, meaning that they are only supplying active power to the utility as residential customers are only charged for active power withdrawn from the grid[128]. When there is a need for PV systems to operate at non-unity power factor, the IEEE recommended Practice for Utility Interface of PV systems [129] disposes that PV should operate at a power factor greater than 0,85 leading or lagging when their output is greater than 10 % of rating. However, specially designed systems that provide reactive compensation and voltage support may be operated outside of this range with utility approval.

3.3.4 Objectives of DG integration

The planning of the integration of DG into distribution networks considers the following objectives:

- Maximum of renewable DG penetration;
- Maximum of system reliability;
- Minimum investment and operational cost; and
- Reduction of system losses and improvement in voltage stability.

3.3.5 Merits and demerits of PV systems

PV systems are associated with many advantages, such as being environmentally friendly technology that causes no noise and no pollution, with potential economic savings as the fuel is free, readily available and does not have to be delivered, which is well-suited for portable and mobile applications [22, 120]. Further merits from an installation and usage standpoint are that PV systems are of a modular nature and the smallest-scale generation technology is available [22], making them flexible and easy to be expanded into larger arrays for increased capacity, and they also have almost no moving parts thus making them extremely reliable and

long-lasting with minimal maintenance [22, 120]. Other benefits include that PV systems offer energy independence as a supplemental PV system reduces the consumer's vulnerability to utility power outages and a stand-alone system eliminates it [120].

It is widely agreed that thus far, the demerits of PV systems are their high initial costs compared to prices for competing power-generating technologies and their need for electrical energy storage if 24-hour capability is required [22]. Figure 3-7 shows the variation of output power generated by PV arrays over 24 hours.

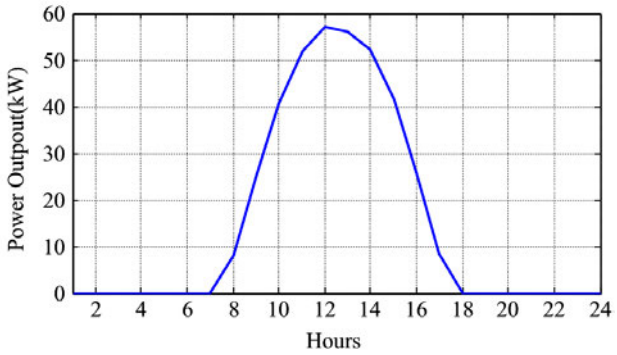

Figure 3-7: Variation of output power generated by PV arrays over 24 hours [110]

PV systems also require a relatively large array area to produce a significant amount of power. The availability of solar radiation resources at a particular location determines the feasibility of producing appreciable amounts of power [120].

3.4 Wind turbines (WT)

3.4.1 General

Despite the unpredictability and occasional violent storm, humanity has had cumulative experience with wind power for millennia. Its energy was harnessed for sail and other applications such as large mills and water pumps in many parts of the world [22].

Wind turbines convert wind kinetic energy into electric energy. Wind technologies have been expending over the years, mostly for its ecological nature. The primary energy is free, with a greatly reduced environmental impact. Synchronous and asynchronous or Induction Generators are used for wind turbines and they can be configured and connected to the grid in many different ways [109, 130] :

1. Fixed speed WT with direct grid-connected Induction Generator (IG),
2. Variable speed WT with variable rotor IG directly connected to the grid,

3. Variable speed WT with direct grid-connected doubly-fed induction generator (DFIG) and DC/AC rotor converter,
4. Synchronous machine and full scale AC/DC/AC converter.

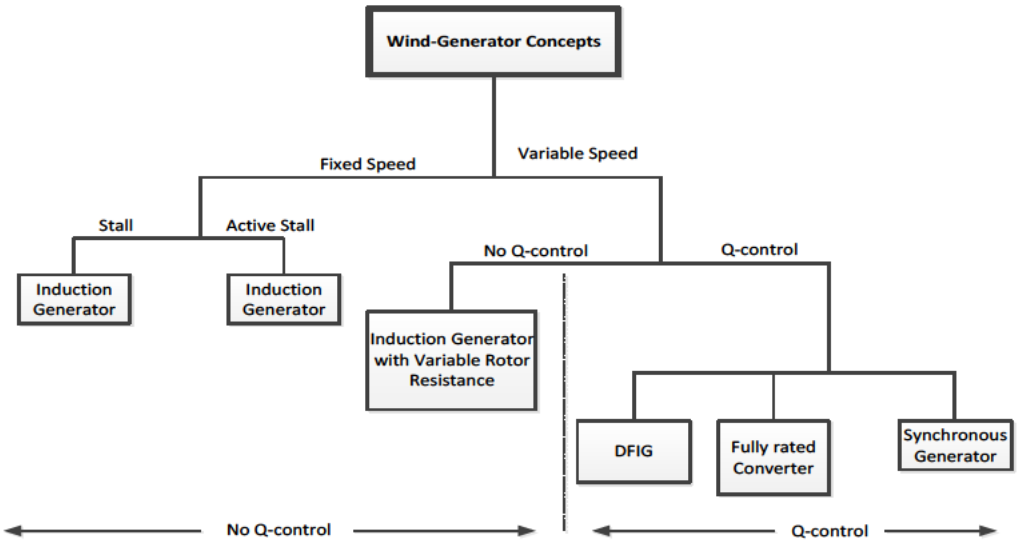

Figure 3-8: Wind generator concept [110]

A schematic of the wind-generator concepts is depicted in Figure 3-8. The rating of a single unit of wind turbine ranges from 200 W to just below 10 MW and presently, the biggest commercially available wind turbine is the V164-9,5 MW [131].

3.4.2 Merits and demerits

Prakash and Khatod in [132] compared WT to other DGs and note that the fundamental demerits of wind turbines are noise pollution, no power availability on demand because of their intermittency nature as seen in Figure 3-9.

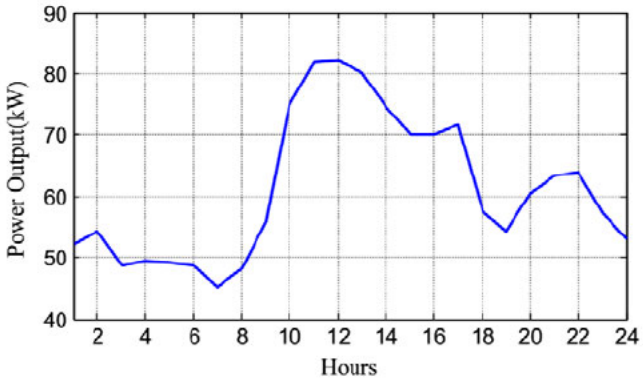

Figure 3-9: Variation of output power generated by wind turbine generator over 24 hours [110]

Additionally, their output is affected by wind speed making the power production highly dependent on wind speed as shown in Equation (3-5), they have high initial installation cost [22, 132] and cannot be used in all geographic locations.

Their main merits include less operating/generation costs, fuel free, saving land use and reduced environmental impact.

3.4.3 Power equation and modelling

The power extracted by wind turbines is

$$P_W = \frac{1}{2} c_P \rho A v_W^3 \tag{3-5}$$

where: c_P = power coefficient, ρ = air density of the wind in W/m^2, A = swept area of rotor in m^2, V_W = Average velocity of rotor blades in *m/s* or wind speed in *m/s* The power extracted is directly proportional to the square of the speed.

With respect to voltage control, Rami in [133] notes that in fixed speed WT configurations, voltage control is not possible as the reactive power in this model cannot be regulated [133]. It has made use of FACTS or static capacitors to compensate for that deficiency

3.5 Storage devices

An energy storage system (ESS) is defined as the group of equipment that allows the storage and conversion of several forms of energy into electricity that can later be used by the grid [134]. Paliwal et al. note that ESS can bridge the power gap between them and the loads by supplying power during periods of unavailability, as well as storing the excess power during high periods of wind and/or sun [110]. One of the benefits of ESS to power systems is their versatile ability to act as load or as generator, with additional increased advantages when they are connected to the grid through power electronic inverters. As classified in Figure 3-10, storage technologies are based on various principles including but not limited to electrical, mechanical and chemical.

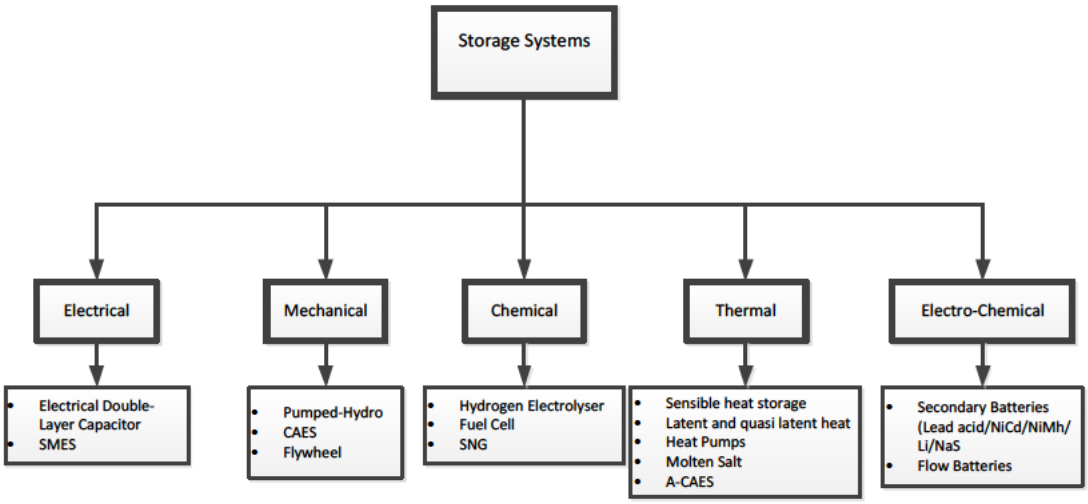

Figure 3-10: Classification of various storage technologies

With regard to the management of active networks, some applications of ESS include:

3.5.1 Bulk storage

Bulk storage can be used for

- *Load shaving*: acting as a generator, to discharge energy into the distribution network during load peak hours and/or relieve congestion in lines.
- *Enabling DG integration*: ESS can act as loads to store extra energy from DGs simultaneously increasing the network capacity to accommodate more power from DGs, especially when the DG is based on RES of a non-dispatchable and intermittent nature.
- *Provide ancillary services and power quality*: by combining charging and discharging benefits with the use of power electronic interfaces, ESS can be used to support distribution networks in a fast and reliable manner [135] and provide services including frequency regulation, spinning reserve, RE shaping services, voltage support, emergency support and intentional islanding [134].

3.5.2 Distributed Storage

Localized smaller storage units or otherwise referred to as a Distributed Energy Storage System (DESS) can be installed at the end of a feeder next to micro wind or PV, or as backup for critical loads [134].

3.5.3 Mobile storage unites

ESS can be used as vehicle-o-grid (V2G) technology to cater for a high deployment of plug-in hybrid electric vehicles (PHEV) and electric vehicles [136].

3.6 Micro turbines

Micro turbines are made up of a small turbine combined with a small generator fuelled by natural gas and which capacity can range from a ew kilowatts to megawatts [137]. Compared to conventional combustion turbines, they rotate at a higher speed, have lower pressure and their small sizes allow that they can fit a small area. They also have high efficiency, low noise, low gas emission and low installation and maintenance costs [137, 138]. Due to the the high rotating speed, micro turbines generate high frequency power (1,5 kHz – 4 kHz) [138], thus requiring AC-DC-AC converters to interface them to the grid or to operate them in parallel with other types of DG sources [137]. Micro turbines are classified as dispatchable as they operate on natural gas and do not cause intermittent generation problems.

3.7 Reciprocating internal combustion engines (RICE)

RICE use one or more pistons to convert pressure into rotating motion. It is one of the least expensive DG technologies commonly used. They are interfaced using a synchronous generator for ratings higher than 300 kW or an induction generator for lower ratings and they can be connected directly to the grid with no need for power electronic interfacing [139].

3.8 Fuel cells

A fuel cell is an electrochemical device that converts chemical energy to electrical energy and thermal energy without combustion [140]. Fuel cells utilise a convenient means of hydrogen and oxygen reaction to produce electricity and water. The principle is essentially based on the inverse of the electrolysis process[121]. Skerrett in [141] notes that the first fuel cell was built in 1839 by Sir William Grove [141], but their high cost never allow them to expand until NASA started using them on space flights to provide power and water [121].

3.9 Summary

This chapter presented the historical development of distributed generation technologies, with a particular focus on PV and Wind technologies. Their merits and demerits were highlighted

their impacts on voltage stability mentioned as well as the existing techniques to mitigate these impacts.

CHAPTER 4: DG AND VOLTAGE STABILITY ISSUES

Introduction

Distribution systems have moved from being passive systems to active networks as the level of penetration of distributed generation keeps on increasing. The stable operation of the whole grid is threatened by voltage rise issues with a permanent need for voltage control. This chapter presents a review of various methods and technologies that are used to achieve voltage control in active distribution networks. A section is dedicated to traditional means of controlling voltage while the rest of the sections deal with the impacts associated with the integration of distributed generation, together with some active distribution networks enabling technologies.

4.1 Active distribution networks

The integration of DGs of various kinds, including battery energy storage systems (BESS), into power system networks is very attractive for power utility companies, customers and societies given that they can help improve power quality and power supply flexibility and reliability; maintain system stability; optimize the distribution system; provide spinning reserves; and reduce transmission and distribution costs [142].However, large-scale integration of DG has changed the electrical distribution network from being traditionally passive to presently active network, leading to technical difficulties with essentially voltage variation as the dominant effect and power flows and voltages being determined by both the generation and the loads [3]. With this come serious challenges for operations and planning, especially with respect to voltage and currents, two key parameters that could change tremendously [134].

An active distribution network (ADN) is defined as a distribution network with systems in place to control a combination of DER comprising of DGs and Storages, including control and communication technologies that allow efficient and reliable large-scale integration of low and medium voltage networks such that distribution network operators (DNOs) can manage and accommodate this new distribution network [134, 143, 144].

4.2 Impact of DG on distribution networks

Vovos et al. in [145] mention that the proliferation of DG on electric networks results in impacts such as voltage variation, degraded protection, altered transient stability, bi-directional power flow and increased fault levels [145]. Voltage magnitude at the proximity of DG may exceed the statutory limits during maximum power output from DG and minimum power demand from

the network. Here, the network experiences the largest reverse power flow and large voltage change, which affects the network safety and stability [3].

This energy conversion mechanism can potentially deteriorate the power quality of the grid, especially as the number of grid-tied solar farms increases [146].

As such, Distribution System Operators (DNOs) will need to change their old "business as usual" passive approach to one that adopts an integration of control and communication technologies together with emerging distribution network technologies as a means of accommodating new generation in an optimal and economical manner [134].

4.2.1 Voltage level and power flows

Considering a distribution network representing a DG network as seen from Figure 4-1, voltage drop on the distribution line may be represented by Equation (4-1) as follows:

$$\Delta V = V_S - V_L = \frac{RP_L + XQ_L}{V_L} \tag{4-1}$$

where, P_L and Q_L are respectively the real and reactive power output from the DG , R and X respectively the resistance and reactance of the distribution line, and, V_S and V_L are bus voltages.

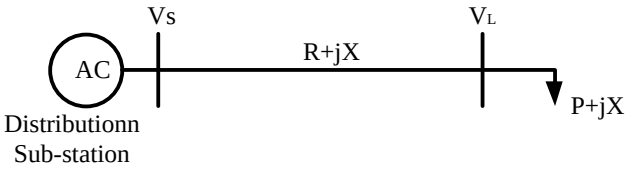

Figure 4-1: Two-nodes distribution system

In HV and MV transmission lines, the resistance R is negligible compared to X , the term RP_L in Equation 4.1 becomes also negligible compared to XQ_L, making $\Delta V \approx f(Q)$ meaning that the voltage drop is critically affected by any injection of Q. Real and reactive powers can reasonably be decoupled in this case. Fast decoupled load flow techniques and several other analytical techniques are based on the decoupling of real and reactive power. On the other hand, the resistance R at the LV distribution network is relatively higher, up to three times compared to the reactance X , making the ratio X/R relatively low. It follows that the terms RP_L and XQ_L of Equation 4.1 are both to be considered, leading to the voltage becoming dependant on

both real and reactive power: $\Delta V \approx f(P,Q)$. There is a strong coupling between the two power quantities leading to the control of frequency and voltage no longer being considered separately as they respectively depend on P and Q. Any significant amount of power injected by DG will result in a voltage rise/drop on the distribution network, especially in a weak distribution feeder with high impedance [3]. Other factors upon which voltage rise/drop would depend include DGs size and location, as well as the method used for voltage regulation [3]. Hidalgo et al. in [134] suggest that when a DG resource is to be connected to a distribution feeder, distribution network operators shall consider the following worst case scenarios: (1) No DG and maximum load; (2) Maximum DG generation and maximum load; and (3) Maximum generation and minimum load.

Below are some techniques used to mitigate the impact of DG on the voltage profile.

4.2.1.1 On-load tap changers (OLTCs)

D'Adamo et al.'s results of the global survey on planning and operation of ADNs in 2009 indicate that the coordination of voltage regulation for MV feeders with DG was accomplished with adjustable settings of the tape changer of MV/LV transformers DG [143]. OLTC is the most common and effective voltage control technique used on the distribution network to maintain a stable secondary voltage by selecting the appropriate tap position in shifting phase angle and adjusting voltage magnitude. OLTCs are used with an automatic voltage controller (AVC) relay associated to a line drop compensator (LDC) that continuously monitors the output voltage from the transformer. To avoid unnecessary OLTC operation during transient voltage fluctuation, an intentional time delay, normally within 30 to 60 seconds, is always implemented. The coordination of outputs between DGs and OLTCs is paramount in the performance of this method and as noted by Dai and Baghzouz in [147], this coordination is necessary in order to allow higher DG penetration into grids. Figure 4-2 below shows the position of the OLTC in a radial distribution network feeder with DG connected at the load bus.

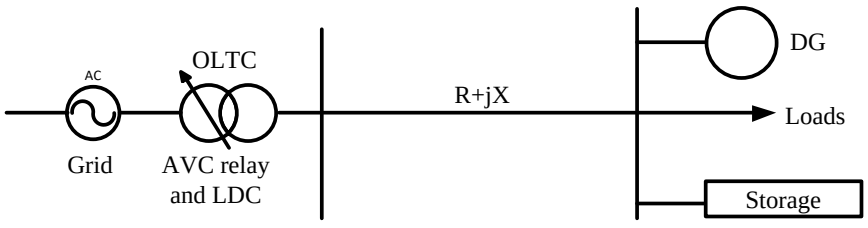

Figure 4-2: Radial Distribution Network feeder connected to DG and using OLTC as voltage control technique [3]

This method was implemented by Kim and Kim in [148] through an algorithm that allows the insertion of DGs on multiple feeders using LDC ,but without changing the OLTC position which advantage is to minimize variation and prevent frequent operation of the OLTC while however restricting DG power integration. Furthermore, the implementation of the OLTCs/AVC/LDCs had proven to be effective in the same regard, as well as allowing the maximum size of DG connection without disrupting voltage profile [149].

4.2.1.2 Power curtailment

When load demand decreases, the intermittent renewable generation peaks and the system will experience excess generation and bus voltages may exceed the grid operational limits. One of the practical solutions is to reduce the renewable source power output to a manageable level for the grid capacity. This operation is termed 'power curtailment'. With respect to DG, power is becoming more widespread, expanding across countries and penetrations increase. Power curtailments can result in operators or utilities commanding wind and solar generators to reduce output, with the aim of minimizing transmission congestion or otherwise managing the system or achieving the optimal mix of resources [150]. Power curtailment can also be performed by means of an emergency load-shedding to economically prevent voltage collapse [151], but at the detriment of adversely affecting power supply reliability.

The negative impact of the curtailment method is the loss of expected income from the Solar PV system owner.

4.2.1.3 Generator power factor control

In reference [152] Taggart and Hao suggest that the power factor at the PCC is critical for maintaining the power quality and stability of the overall system.

From Equation 4.1, the ratio P/Q is maintained constant. Thus any fluctuation in P causes a variation of voltage V . Vovos et al. in [145] stated that if Q can be compensated for the voltage variation generated by P by adjusting in the opposite direction, then the voltage variation can be maintained within statutory limits. For voltage rise situations, a more leading power factor is required at which the DG is to be connected.

To maintain the power quality of solar farms, the common-point power factor of multiple solar photovoltaic (PV) inverters needs to be maintained inside of the utility requirement range. One

solution is to utilize the communications capabilities of protective relays, meters and Solar PV inverters to integrate an active control system [152].

Taggart and Hao in [152] also demonstrates that only one controller is sufficient for multiple inverters, making the active control scheme simple and cost-effective. Finally, it examines the communications and data collection limitations, while analysing the benefits of using multiple controllers instead of a single controller when the number of inverters increases.

The solution models the power factor control problem as a closed-loop feedback system utilizing existing components of Solar PV generation sites. It demonstrates how a PI controller can be useful in maintaining the desired reference power factor for multiple inverters in a simple and cost-effective manner.

The setting of PFC at the point of common coupling (PCC) of multiple Solar PV inverters can fluctuate depending on the power quality and harmonic distortions injected by the inverters.

4.2.1.4 Battery energy storage system (BESS)

Enabling PV penetration into electrical grids presents several benefits for power system networks but require a balance of supply and demand that cannot be achieved oneself due to intermittency of the solar energy source. Because of the flexibility to control their real power output, batteries are suggested as a suitable and cost effective solution to mitigate adverse effects of intermittency and shape the fluctuation of the system's output into relatively constant power. BESS can be used to adequately smooth the output of the Solar PV-BESS sub-system for over voltage reduction and peak load shaving during high PV generation/low consumption or high demand/low solar PV generation time as illustrated in Figure 4-3, in lieu of power curtailment or reactive power injection. The quasi variable and frequently uncertain Solar Systems output resulting from intermittency and weather dependency, calls for a need to use BESS both in off-grid or in grid-tied applications.

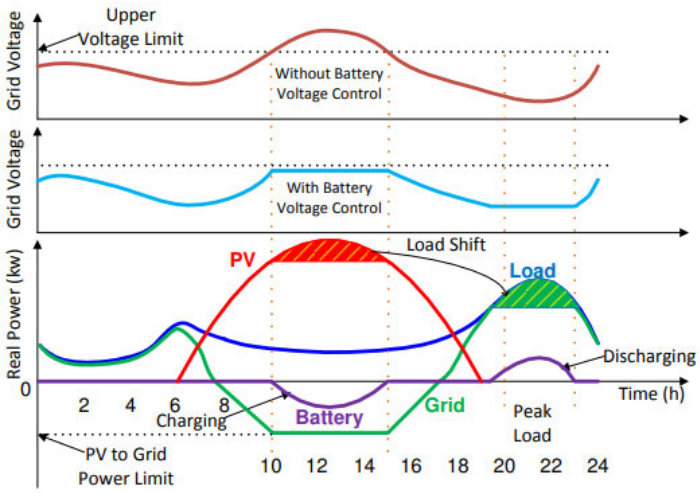

Figure 4-3: Energy management system of hybrid PV penetrated grid [153]

Although there are clear benefits of using energy storage as an enabler of solar systems penetration, it is important to consider the potential role of energy storage in relation to the needs of the electric power system as a whole [154]. In [128, 155] the authors present the challenges inherent to integrating solar energy into power systems and developed a variety of real-time control modes of operation for BESS in grid-tied solar applications. Yang in [153] proposed a method for BESS design optimization and sizing strategy considering voltage regulation, peak shaving and annual cost for distributed PV systems. To alleviate possible adverse effects for increased penetration and maximizing economic benefits smart grid developers and power systems planners are required to broaden the understanding of BESS applications.

4.2.1.5 Network configuration

Distribution network re-configuration refers to the situation when, under the condition that all the constraints to ensure the safe operation of the power grid are satisfied – such as requirements for voltage drop, line heat capacity, etc. – power supply and lines are chosen by changing the opening and closing states of each segment switch and interconnection switches, aimed at eventually forming a radial network through this choice. This is so that it may make a particular index of the distribution network, such as the line losses, voltage capacity, load balancing and so on, achieve the optimal state [115].

4.3 Optimal DG siting and sizing

4.3.1 Calculation of boundaries

Begovic et al. in [128] suggest the use of Monte Carlo Simulations to determine boundaries and found that the knowledge of total penetration of small PV systems is sufficient to calculate the effects of DG on feeders. The methodology used is to consider DG devices as parasitic sources and to impose a set of strict rules designed to limit the effects that those systems may have on the distribution feeder.

4.3.2 Review on the optimal allocation of DG

Sing and Sharma in [119] note various advantages of optimal DG planning as follows:

(i) active and reactive power losses reduction;
(ii) reduce power system oscillations;
(iii) enhance power system stability with respect to voltage, rotor angle and frequency stability;
(iv) enhance power system reliability, security, loadability and available power transfer capacity;
(v) reduce power conjunction of line; and
(vi) increase the band of operation of the system or flexible operation.

4.4 Grid requirements for photovoltaic systems

Grid requirements for Solar PV technologies are contained in standards that had historically developed and are reviewed and amended from time to time. The content of the standards differ according to countries and regions. The IEEE Std 1547™ 201, titled "*IEEE Standard for Interoperability of Distributed Energy Resources with Associated Electric Power Systems Interfaces*" a review of the 2003 version is the current international document in use. It focuses on the technical specifications for, and testing of, the interconnection and interoperability between utility electric power systems (EPSs) and distributed energy resources, and provides requirements relevant to the performance, operation, testing, safety considerations, and maintenance of the interconnection (DERs) [156].

The document includes general requirements, response to abnormal conditions, power quality, islanding, and test specifications and requirements for the design, production, installation,

evaluation, commissioning, and periodic tests. Notwithstanding specific regulations for countries, these requirements are universally needed for interconnection of DER including, synchronous and induction machines, or power inverters/converters [156]. The current version was amended in 2014, in response to the need to make changes in the 2003 version to subclauses related to voltage regulation, voltage response to Area EPS abnormal conditions, and frequency response to Area EPS abnormal conditions. Following are additional documents in the series of the 2014 reviews [156]:

- IEEE Std 1547™ [B17] that provides conformance test procedures for equipment interconnecting distributed energy resources (DER) with electric power systems (EPS).
- IEEE Std 1547™ [B18] which is the application guide for IEEE Std 1547™ .
- IEEE Std 1547™ [B19] that provides guidance for monitoring, information exchange, and control of DER interconnected with EPS.
- IEEE Std 1547™ [B20] provides guidance for the design, operation and integration of distributed resource island systems with EPS.
- IEEE Std 1547™ [B21] is a recommended practice for interconnecting DER with electric distribution secondary networks.
- IEEE Std 1547™ [B22] provides guidance for conducting distribution impact studies for DER with electric distribution secondary networks.

4.5 Summary

This chapter addressed the voltage stability issues in the context of DG. The impacts of DG on distribution networks was discussed and available existing mitigation solutions mentioned. A particular attention was given to the BESS as one of the effective ways of dealing of the intermittency of the energy source.

CHAPTER 5: NETWORK SYSTEMS MODELLING

Introduction

To analyse and demonstrate the voltage control and stability of a multi-machine power system with increasing penetration of RES, it is essential to describe and discuss different system models and components in order to understand their behaviour and impact on the overall system and predict the response to system disturbances. The components of the system at both transmission and distribution levels include generators, transformers, transmission lines, loads and the DG system to be integrated into the grid system. Models of voltage regulator equipment, other additional components such as the inverter and other sub-components of the DG system including DG power output enhancing devices are also discussed in this chapter. The models of the other components of the system such as the protection, telecommunications and metering systems are not included in this chapter as they are deemed to have mild or negligible effects on the global system voltage.

This chapter covers discussions on the system network modelling and the justification for the choice of components. Parameter settings for the techniques applied and the methodologies used are also presented in this chapter.

5.1 Simulation tool selection

5.1.1 Reasons for simulation

Real power systems are complex with respect to both the planning and the operation. Except from observations and interpretations of unpredicted events such as faults or contingencies (loss of a generator or a transmission line) occurring in an operating network, live testing for performance analysis is usually not performed, mostly because of their destructive nature. Simulation tools that are becoming smarter have been in use and have played the important role of providing design planners and engineers with a better understanding of power system operation. In this kind of simulation, all data (network topology, active and reactive power injections, controlled buses specified voltage, etc.) are prepared by the user and then the problem is submitted to the solution calculation. Even today, power flow programs are used to analyse future operating scenarios of the system. Requirements are quite different when dealing with power system real-time operations (or control).

5.1.2 The simulation tool

The study uses *DigSILENT™ PowerFactory™* versions 17 and 19 as the simulation tool for the networks models and case studies. *DigSILENT™* is an integrated graphical single-line interface including drawing functions, editing capabilities and all relevant static and dynamic calculation features for the analysis of the transmission, distribution and industrial electric power systems [157]. The tool is very useful for power system project planning and power system operation optimisation.

The seminal advantage of *DigSILENT™ PowerFactory™* over other similar software tools is the use of a single database comprising the required data for all equipment within a power system (line data, generator data, protection data, harmonic data, controller data) to easily execute all power simulation functions such as load flow analysis, short-circuit calculation, harmonic analysis, protection coordination, stability analysis and modal analysis within a single executable program environment. Other benefits drawn from the general *PowerFactory* program design concept are the functional integration, vertical integration, the database integration and the customisation functions of the tool. In fact, different program applications can be executed sequentially without re-setting the program, enabling additional software modules or engines, or reading and converting external data files. “Generation”, “Transmission”, “Distribution” and Industrial analysis can all be completed within *PowerFactory* though a comprehensive list of simulation functions that include [157] :

- Load Flow Analysis allowing meshed and mixed 1-2, and 3-phase AC and/or DC network,
- Low Voltage Network Analysis,
- Short-Circuit Analysis,
- Contingency Analysis,
- Protection Analysis,
- Reliability Analysis,
- Power Quality and Harmonic Analysis,
- Quasi-Dynamic Simulation, to perform several load flow calculations in a period of time,
- RMS Simulation executing time-domain simulation for stability analysis,
- EMT Simulation dealing with time-domain simulation of electromagnetic transients (EMT) for stability,

- Optimal Power Flow.

For almost two decades, the *PowerFactory™* software tool had been used with satisfactory performance for researchers and industrial experts in power systems analysis. With respect to this research work, the software tool is used by means of case studies for steady state as well as dynamic analysis precisely through load flow analysis, quasi-dynamic simulation, RMS and EMT simulations and contingency analysis. *PowerFactory™* also allowed the modelling of DG and other components, most of which have built-in readily available and flexible models that can be easily selected, set and controlled from the user-friendly graphical window interface of the program.

Prior to simulations of the test system models with or without DGs, several assumptions aimed to simplify some complexities and obtain accurate results are required to be made.

For the purpose of this work, the following assumptions were considered:

- The demand for load shall not exceed the installed capacity with the additional DG at the required penetration level.
- In the exception of the swing bus, all other buses in the test networks are potential candidates for the location of DG installation.
- An assumed load profile will be considered in static analysis for voltage profile and power losses determination as the accuracy of the load profile is not of utmost importance.
- PV are intermittent DG sources, implying that their planning is subject to the availability of their resources. It is assumed that for the purpose of this study, a lack of generating capacity during low or zero PV output, BESS are used to enable provision for adequate power.

5.2 Test system network models

The hypothetical power systems networks to be simulated in this study using *DigSILENT™ PowerFactory™* are the IEEE-9 Bus model and the New England IEEE 39-Bus system represented using the single line diagrams respectively provided in Figures 5-1 and 5-2 [158].

5.2.1 IEEE 9-Bus network: model description

DigSILENT™ PowerFactory™ [159] notes that the IEEE-9 Bus model was first introduced in the book *Power System control and Stability* by Anderson and Fouad [35]. This IEEE standard system model is now one of the test systems used to analyse the role of DG integration into grid power systems with regard to voltage stability and power quality enhancement. The system represents a small transmission system which consists of nine buses (nodes), three synchronous machines representing conventional generators supplying the network, three two-winding transformers, six lines and three loads [159]. The base kV levels are respectively 13.8 kV, 18,45 kV, 16,5 kV at generator buses and 230 kV at the remaining buses. Each generator is represented as a voltage source with its source impedance set arbitrarily as one Ohm. The part at which loads are connected represents the sub-transmission network. The network will be subjected to slight modifications wherever suitable for the purpose of this study by adding buses at which DG systems are integrated into the network. Details contained in this section are part of the author's publication in Loji et al. [15].

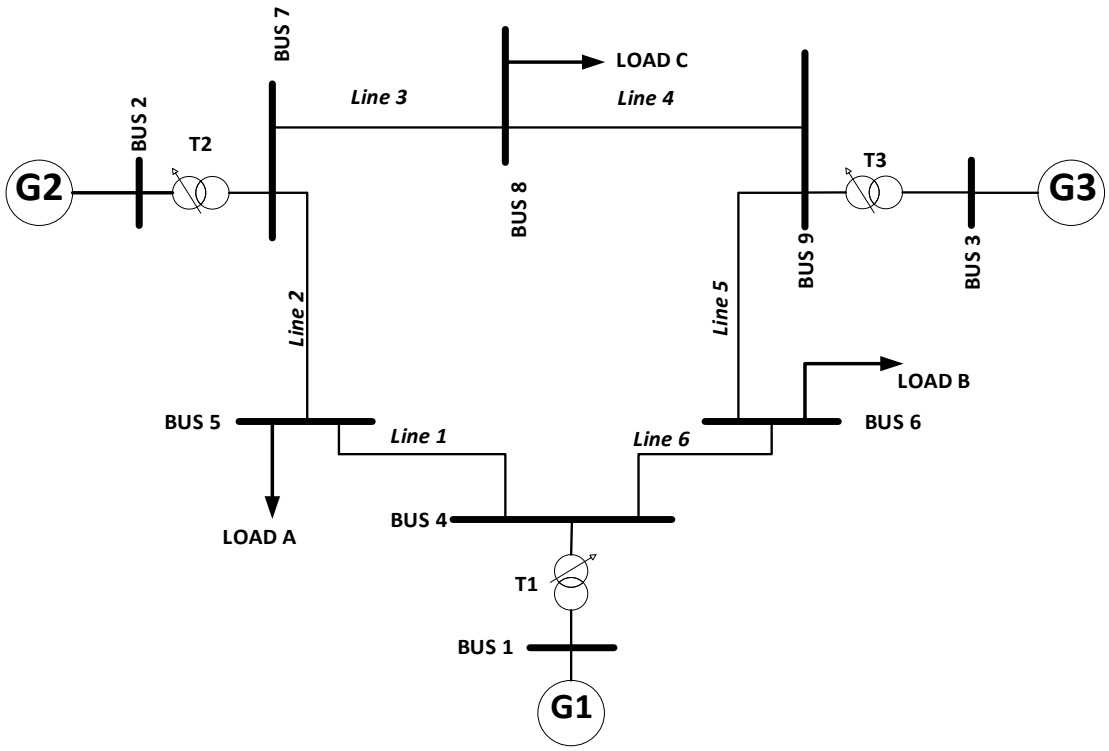

Figure 5-1: Single-line diagram of the IEEE 9-Bus system network

5.2.2 System model parameters

The following tables, Tables 5-1, 5-2, 5-3 and 5-4 respectively provide the per unitized terminal conditions of each source with a 100 MVA base of the transmission line and of the load characteristics.

5.2.2.1 Generator model characteristics and settings

Generator characteristics for the IEEE 9-Bus system are provided in Table 5-1 below:

Table 5-1: Generator characteristics of IEEE 9-Bus System

Bus	V[123]	δ[14]	P[p.u]	Q[p.u]
1	17,1600	0,0000	0,7163	0,2791
2	18,4500	9,3507	1,6300	0,0490
3	14,1450	5,1420	0,8500	-0,1145

Generator settings in *DigSILENT™ PowerFactory™* are given below in Table 5-2. Generator 1 (G1) is set up as the reference machine, while the other generators are configured to control the active power injections and the voltage magnitudes at respectively connected buses 2 and 3.

Table 5-2: Generator model settings in DigSILENT PowerFactory 2017

Parameters	Generator 1 (G1)	Generator 2 (G2)	Generator 3 (G3)
Set up	Reference Machine	To control P and V magnitude	To control P and V magnitude
Local controller mode	"constant V" at 1,04 p.u at Bus 1	"constant Q"	"constant Q"
Generation adequacy	Based on the nominal power which is 247,5 MW at nominal voltage of 16,5 kV with power factor = 1	Stochastic: based on the nominal power which is 163,2 MW	Based on the nominal power which is 108,8 MW at nominal voltage 13,8 kV
Load flow parameters	P = 71,6 MW and Q = 27 MVAr	P = 163,2 MW and Q = 6,7 MVAr	P = 85 MW and Q = -10,9 MVAr
Plant category	Hydro power plant	Steam plant	Steam plant

For RMS simulation, *DigSILENT™ PowerFactory™* makes available three models of synchronous generators, namely a standard model, a classical model and an asynchronous starting of a synchronous machine model [159].

For the purpose of this study, the standard model was considered for all the generators. This model represents a field winding in the *d-axis* and a damper winding in the *d-* and *q-axis*.

5.2.2.2 Transmission line model

In the *DigSILENT™ PowerFactory™ 2017* model, the transmission lines are modelled using the Bergeron model and Table 5-3 provides the per unitised line data on a $S_b = 100$ MVA system base at nominal voltage $U_n = 230\text{kV}$. However, since for the *PowerFactory* model input data are required in Ω/km and $\mu F/km$ respectively, line parameters are re-calculated for the network model at the nominal voltage using Equations (5-1), (5-2) and (5-3).

$$R[\Omega] = r[p.u.].\frac{U_n^2[kV^2]}{S_b[MVA]} \tag{5-1}$$

$$X[\Omega] = x[p.u.].\frac{U_n^2[kV^2]}{S_b[MVA]} \tag{5-2}$$

$$B[\mu S] = b[p.u.].\frac{S_b[MVA]}{U_n^2[kV^2]}.10^6 \tag{5-3}$$

Table 5-3: Transmission line characteristics of the IEEE 9-Bus System

Line				
From Bus	**To Bus**	**R[p.u/m]**	**X[p.u/m]**	**B[p.u/m]**
4	**5**	0,0100	0,0680	0,1760
4	**6**	0,0170	0,0920	0,1580
5	**7**	0,0320	0,1610	0,3060
6	**9**	0,0390	0,1738	0,3580
7	**8**	0,0085	0,0576	0,1490
8	**9**	0,0119	0,1008	0,2090

The lines are assumed to be overhead. The length of each line and the rated current have been set to respectively one km and one kA [159].

5.2.2.3 Load model

For the purpose of this study, loads are considered as PQ loads, meaning that they are modelled to have constant active and reactive power demand and are assumed to be voltage-dependent under normal conditions and not voltage-dependent only during load flow calculation by disabling the load option “Consider Voltage Dependency of Loads” under the load flow calculation command in the *DigSILENT™ PowerFactory™* tool. Initial load data given in per units of P and Q are listed in Table 5-4.

Table 5-4: Per unit load demand of the IEEE 9-Bus system

Load	Bus	P[MW]	Q[MVAr]
Load A	5	1,25	0,50
Load B	6	0,90	0,30
Load C	8	1,00	0,35

It shall be noted that as the accuracy of the load profile is not of utmost importance, an assumed load profile will be considered.

5.3 DG system modelling

Solar PV-based DG was considered in this study and for a successful implementation and integration to the grid, models are to be developed. An ideal control mechanism shall aim to maximise generated active power and enhance grid stability without interfering and altering system power quality.

5.3.1 PV array model

The photovoltaic system element that is used in *DigSILENT*™ - *PowerFactory*™ has been modelled as an array of PV panels that can be connected to the grid via a single inverter. For modelling purposes, the PV system can be seen as a DC source behind some inverters as shown in Figure 5-2, although a static generator model can also be used.

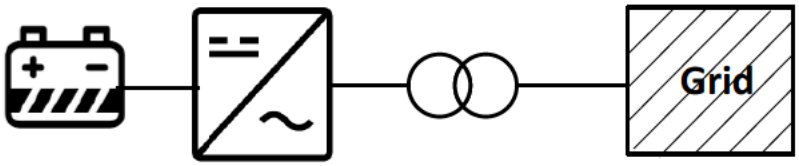

Figure 5-2: PV model representation

The PV output current I, which was represented in Chapter 3 by an exponential function in Equation 3-3, is derived from the physics of the P-N junction and is also dependent of several other parameters such as the cell short circuit current, solar insolation, the number and the configuration of connected PV cells. [160]. The much more detailed representation of the output current is provided in Equation (5-4) below:

$$I_{PV} = I_{SCA}(G) - N_p x I_0 [e^{\frac{(V_A + I_{PV} R_S) q}{n N_S k T}} - 1] \tag{5-4}$$

where I_{PV} is the array current [A], I_{SCA} is the total short circuit current of the array, V_A is the array voltage [V], I_0 is the reverse saturation of the diode, R_S is the array series' resistance, G is the solar insulation, V_0 is the open circuit voltage, $q = 1{,}6x10^{-19}C$ is the charge of an electron, $k = 1{,}38x10^{-23}J/K$ is the Boltzmann constant , T is the cell temperature in Kelvin [K].

The user can choose the mode active power input or solar calculation where, given the data of the solar panel type, arrangement of the solar array, local time and date, irradiance and date, active power can be calculated or automatically estimated with a given set point from geometrical location, date and time. On each PV system with a single inverter, a number of panels can be entered with the option of parallel, series or series-parallel connections. Input choice of number of parallel inverters and MVA rating per single inverter can also be entered. The total MW and MVAR outputs of the PV system is determined by Equation (5-5) below:

$$MW_{(PV)} = MW_{(P)} x N_{(Inv)} \tag{5-5}$$

where $MW_{(PV)}$ is the total PV active power output, $MW_{(P)}$ is the active power rating of one panel and $N_{(Inv)}$ is the number of parallel inverters. The choice of connection type, parallel or series or a combination of both, depends on the required output power, the control strategy and the topologies of the inverter employed in the integrated PV systems. Voltage-oriented control is the most common control strategy applied to grid-connected PV systems, since it is capable of controlling the DC-link and regulates the current injected into the grid [161] .The DC-DC converter model and the inverter model are discuss in detail below.

For the purpose of this study, a manual input sets method was used in all the simulation study cases.

5.3.1.1 The maximum power point tracking (MPPT) model

MPPTs are high-frequency DC to DC converters aiming to maximize the available energy exerted from the solar arrays at any time of its operation. A DC-DC converter plays the role of a magnitude transformer of an unregulated non-ideal input DC voltage U_d into a controlled DC output voltage U_d at a desired voltage, as can be seen in Figure 5-3 which depicts the boost and buck models from *DigSILENT™ - PowerFactory™* .

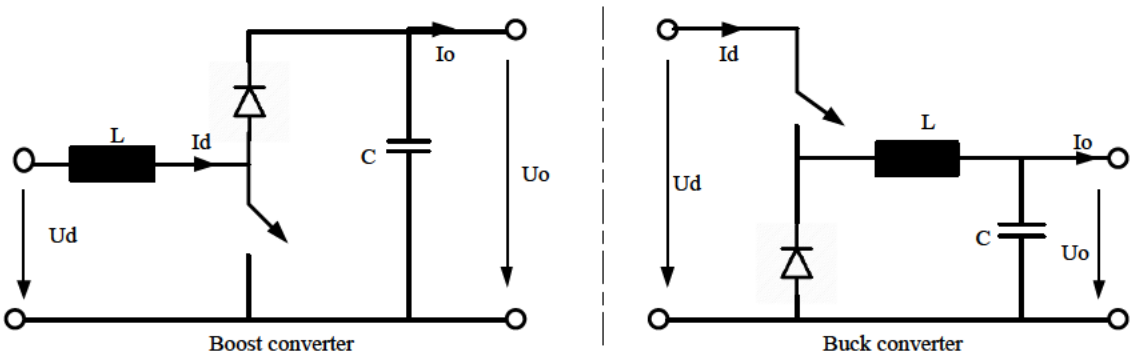

Figure 5-3: Boost and Buck DC-DC converter model [162]

Various DC-DC converter models have been developed to produce a regulated output voltage from the PV array since a single cell voltage is limited to a very low value and cells cannot, due to reliability issues, be increasingly connected in series to achieve higher voltage levels [163]. Additionally, solar cells have internal impedances that vary throughout the day depending on solar irradiance and the temperature of the cell. To overcome these issues, a converter is inserted between DC bus and PV source as illustrated in Figure 5-4 below. The converter will temporarily store the input energy and release it to the output end at different voltage. The main design criterion of the MPPT model is to adequately and correctly feed the AC module or the battery at the required voltage and current for optimal power delivery and high efficiency operation.

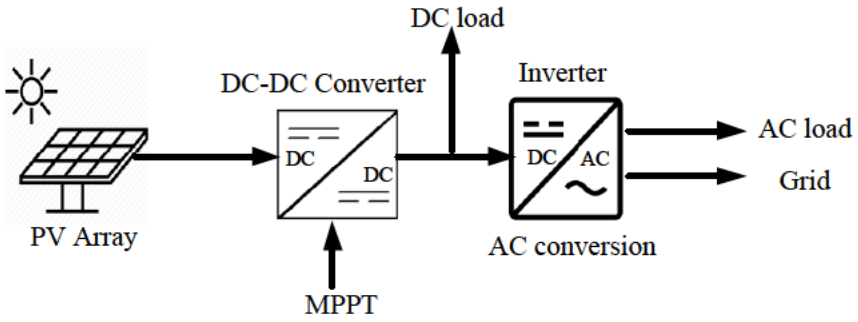

Figure 5-4: Position of the DC-DC converter and the Inverter in the mini-grid[164]

The DC-DC converter model is built in the solar PV generator model *DigSILENT™ PowerFactory™*. For load flow or RMS calculations, the basic model is a boost or buck converter with no losses and is controlled using pulse width modulation (PWM). The basic data page of the DC-DC converter is shown on Figure 5-5 below where `the parameter $AlphaU_2/U_1$ is the ratio between the secondary voltage U_2 and the primary side voltage U_1 as given in Equation (5-6):

$$\alpha = \frac{U_2}{U_1} = \frac{t_{on}}{T_s} \tag{5.6}$$

with $0 < \alpha < 2$ except the value 1 and $T_s = t_{on} + t_{off}$.

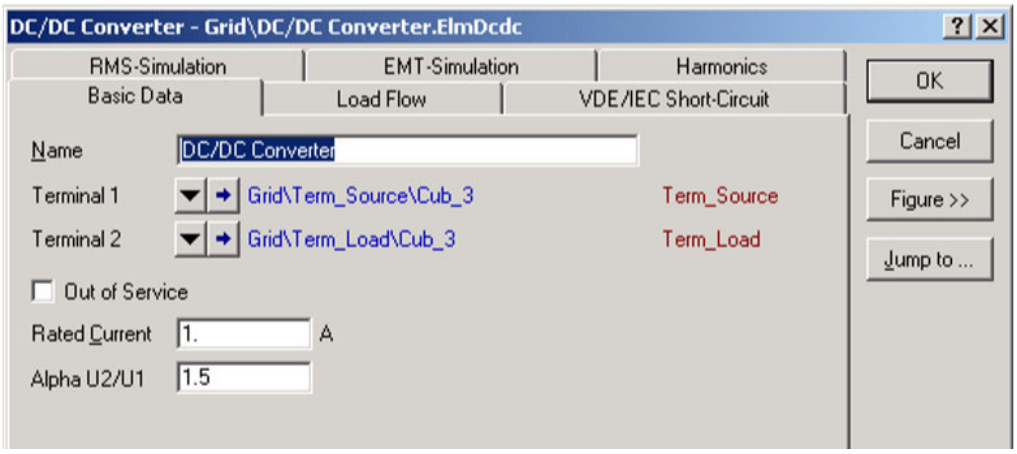

Figure 5-5: Basic data page of the DC-DC converter

The model parameters used for the IEEE 9-bus are given in Table 5-5 below:

Table 5-5: Parameters for the DC-DC converter

	Nominal S	Nominal V	Power factor	Frequency
IEEE 9-bus system	Variable ranges to be set according to cases	230 kV	1	50 Hz

5.3.1.2 Inverter model

As shown on Figure 5-4, the inverter is connected between the DC-DC converter and the grid, to convert DC power from the PV modules to local loads or to the grid through a transformer. Several inverter topologies have been developed, in particular for utilization in grid connected systems with various features enabling high efficiency. For enhanced performance of grid integrated PV systems applications, inverters form part of a power conditioning unit (PCU) which comprises the MPPT, the inverter, the controller protection interfacing and the grid interface module with or without backup batteries, as indicated in Figure 5-6. The design modelling criteria must include automatic grid synchronisation and low levels harmonic distortions [165].

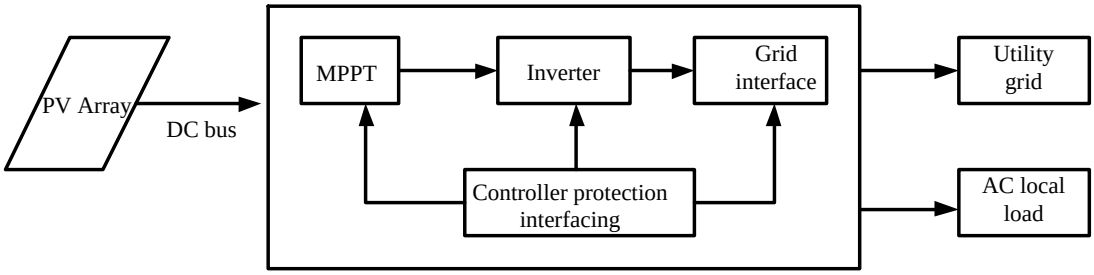

Figure 5-6 Power Conditioning Unit (PCU) without battery back-up

In addition to providing quality power, the most important characteristic requirements of the inverter are to operate over a wide range of voltages and currents, as well as to regulate output voltage and frequency to meet the point of DER connection (PoC) or point of common coupling (PCC) requirements according to IEEE Std 1547™-2018.

The PV generator model built in *DigSILENT*™ - *PowerFactory*™ has an incorporated inverter which parameters are provided in Table 5-6 below:

Table 5-6: Inverter model parameters

	Nominal S	**Nominal V**	**Power factor**	**Frequency**
IEEE 9-bus system	Variable range	230 kV	1	50 Hz

5.3.2 Grid connected PV model

DigSILENT™ - *PowerFactory*™ has an already developed and available PV system generic model (*ElmP*vsys) that includes some basic control and design features. Due to the absence of rotating machinery, the PV system generic model can be assimilated to a static generator (*ElmGenstat*), which is easy to use for even other applications such as photovoltaic generators, fuel cells, storage devices, HVDC terminal, reactive power compensators and wind generators,

The principal difference is that the PV system element provides an option to automatically estimate the active power setpoint given the geographical location, date and time, as mentioned in Section 5.3.1.

5.3.2.1 Active power calculation

For active power calculation, the option “Active Power Input” was selected with the sub-options of “Number of parallel inverters” and “Number of panels per inverter”.

5.3.2.2 Load-flow Analysis

For “Load Flow Analysis”, 5 local voltage controller can be used and are listed below: power factor control mode, voltage control, droop control Q(V) characteristic and cosphi(P) characteristic.

The first three voltage controller options are represented by the block diagram shown in Figure 5-7.

- **Power factor control**: PQ bus type option with specification of the desired P and Q power outputs at which the generator will operate.
- **Voltage control**: PV bus type with constant active power and reactive power output controlled to achieve the specified local voltage at its terminal.
- **Droop control**: DV bus type option. It has the advantage that more than one machine at one busbar could control the voltage in addition to the possibility of a single machine participation to be configured with the setting of the droop value.

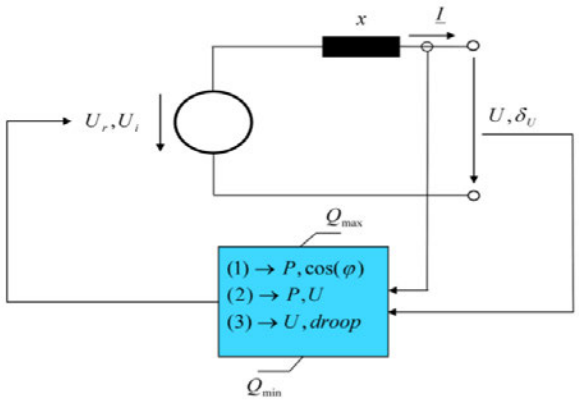

Figure 5-7: Voltage controller - options in *DigSILENT™ - PowerFactory™*

When set in the voltage control, a droop value can however be entered and the local voltage is then controlled according to Equations (5-7), (5-8) and (5-9), shown graphically in Figure 5-8 [166, 167]

$$u = u_{setpoint} - du_{droop} \tag{5-7}$$

$$du_{droop} = \frac{Q - Q_{setpoint}}{Q_{droop}} \tag{5-8}$$

$$Q_{droop} = \frac{S_{nom} x100}{droop} \tag{5-9}$$

where u is the actual voltage value at the terminal busbar, $u_{setpoint}$ is the specified voltage setpoint of the static generator, Q is the actual reactive power output of the generator, $Q_{setpoint}$ is the specified dispatch reactive power of the static generator, S_{nom} is the nominal apparent power and $droop$ is the droop value specified in percentage.

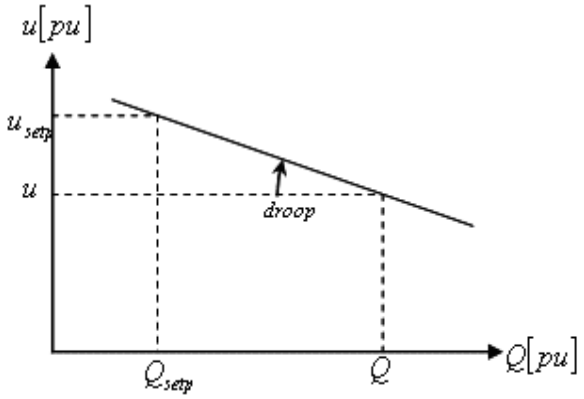

Figure 5-8: Droop voltage control[167]

- **Q(V) characteristic:** Control is achieved locally by controlling Q variable setpoint according to Figure 5-9 with U_{mim} and $U_{\max}$ corresponding to lower and upper voltage deadband limits respectively.

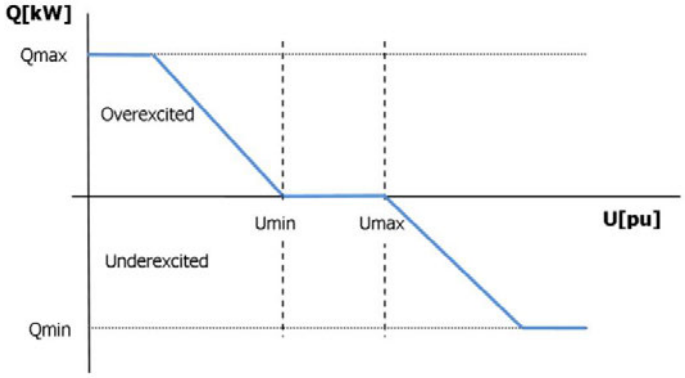

Figure 5-9: Q(V)-characteristic[166]

- **Cosphi(P) characteristic** power factor control following a specified characteristic as specified in Figure 5-10.

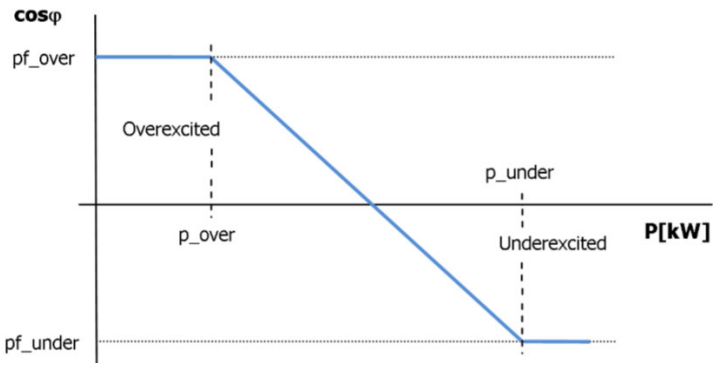

Figure 5-10: cosphi(P)-characteristic[166]

5.3.2.3 Power flow equations

Load flow in power systems analysis is performed with the aim of obtaining information regarding variables such as bus voltages magnitudes and angles, line currents, active and reactive powers through the system. In *DigSILENT™ PowerFactory™* [15], the nodal equations used to represent the analysed networks are implemented using two different formulations, namely Gauss-Siedel Load Flow equations (current equations) and the Newton-Raphson (Power equations, classical). They are derived from the single diagram in Figure 5-11 below.

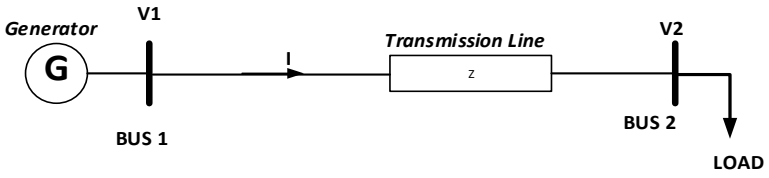

Figure 5-11: Basic single line diagram of a power system network[15]

From the first principle, the current in the transmission line is determined by:

$$\vec{I} = \frac{\vec{V}}{\vec{Z}} \text{ or } \vec{I} = \vec{Y}.\vec{V} \tag{5-10}$$

Power systems have several buses and lines forming a network. Applying Equation (5-10) to any bus numbers' network and assuming that all quantities are complex quantities:

$$[I] = [Y_{BUS}][V] \tag{5-11}$$

where $[I]$ and $[V]$ are *n x 1* matrixes, $[Y_{BUS}]$ called a bus admittance matrix, is an *n x n* matrix. Considering only row *k*, Equation (5-11) can be expended for row *k* as follows:

$$I_k = \sum_{i=1}^{n} Y_{ki}.V_i = \frac{S_k^*}{V_k^*} \tag{5-12}$$

Knowing that $S = V.I^*$ and, by developing and expending Equation 5-13 in two different ways, the following equations are obtained:

$$V_k = \frac{1}{Y_{kk}}\left[\frac{P_k - jQ_k}{V_k^*} - \sum_{i=1/i\neq k}^{n} Y_{ki}V_i\right] \tag{5-13}$$

which is the representation of the Gauss Siedel Load Flow equations, where P_k and Q_k are respectively active and reactive power injected at bus k.

And,

$$P_k - jQ_k = \sum_{i=1}^{n} |Y_{ki}V_iV_k| \angle(\theta_{ki} + \delta_i - \delta_k) \tag{5-14}$$

In Equation (5-14) above, the left hand side is in rectangular form, while the right hand side is in polar form. Re-writing the right hand side in rectangular form, Equation (5-14) is split into two equations representing the Newton-Raphson Load flow equations as follows:

$$P_k = \sum_{i=1}^{n} |Y_{ki}V_iV_k| Cos(\theta_{ki} + \delta_i - \delta_k) \tag{5-15}$$

$$Q_k = -\sum_{i=1}^{n} |Y_{ki}V_iV_k| Sin(\theta_{ki} + \delta_i - \delta_k) \tag{5-16}$$

The power solution in *DigSILENT™ PowerFactory™* will be governed by either of these two equations developed above.

5.4 Energy storage modelling

Energy storage will be used to assess the effectiveness of its use to mitigate the intermittency of solar-based power generation and smoothing out power fluctuations through the charging and discharging process. The model considered in this study is available in *DigSILENT™ - PowerFactory™* and modelling is achieved through two methods:

1. Method 1: as static generator, and,
2. Method 2: as a DC voltage source combined with a Pulse Width Modulator (PMW).

The BESS in the second method have a storing part, which is a rechargeable battery and a rectifier/inverter part. It should be noted that the two main challenges with battery models are

(1): to get a model that is accurate enough without being too complex and (2): to obtain parameters from manufacturers or to acquire them from own measurements [168].

In general, a battery model depicts the terminal voltage and the internal resistance. The internal resistance is a function of internal variables such as the Battery Status of Charge (SOC)- one if battery fully charged and zero if battery is empty- the age and the temperature of the battery [169].

5.5 Model of voltage and reactive power control schemes

DigSILENT™ - PowerFactory™ 2019 offers the following options for voltage and reactive power regulation:

- Automatic tap adjustment of transformers
- Automatic tap adjustment of shunts
- Consider reactive power limits
- Consider reactive power limits scaling factor.

The SVS was used as one of the FACTS devices to control voltage at its terminal or the voltage on a remote busbar to a specified set point.

Droop control can also be enabled to control voltage at local or remote busbar according to Equation (5-17):

$$u_{bus} = u_{set\ point} + \frac{Q_{meas}}{Q_{droop}} \tag{5-17}$$

where: u_{bus} is the voltage in *p.u.* at measurement point, $u_{setpoint}$ is the reference voltage in *p.u.*, Q_{meas} is the reactive power flow at Q-Measurement point $Q_{setpoint}$ is an input parameter for which the unit is MVAr/p.u.

If no Q-measurement point is selected, then Q is the reactive power output of the SVS. For the purpose of this study the SVS used was made of 10 capacitor units in parallel set in voltage control mode at 1 p.u voltage set point with a Q contribution set -1,62 MVAr per capacitor.

5.6 Summary

In this chapter, modelling of the systems under study for the purpose of assessing various DG penetration effects on voltage and power conditions have been presented. Models of network

elements and computational techniques as implemented in *DigSILENT™ - PowerFactory™ 2019* are also presented and explained. The study methodology is briefly referred to in this chapter but will be detailed in Chapter 6.

CHAPTER 6: RESEARCH CASE STUDIES

Introduction

A Power Systems Network cannot be physically built for research purposes. In order to investigate power systems network problems, modelling and simulations are very often the only alternative solution. This chapter presents case studies used in this research work as well as the corresponding simulations conducted on the network models presented in Chapter 5. The simulation methodology is presented and justified. Critical parameters such as voltage profile, system loadability and total power losses are investigated and monitored through case studies both in static and dynamic simulations, with the ultimate aim of identifying network stability conditions with reference to grid codes violations and mitigation solutions thereof.

6.1 Methodology

To conduct the simulations, the following methodology was applied:

- Build the network to set up the concerned case studies and/or scenarios in *DigSILENT*™ - *PowerFactory*™.
- Run the base case using two scenarios respectively for the initial normal conditions and a worst case scenario with load models set to extreme conditions.
- Execute load flow and record results of RMS/EMT simulations in static and transient modes respectively.
- Integrate FACT devices and thereafter PV systems under various conditions considering FACTS and PV location and sizing, integration of BESS and execute similar simulations as above. Record results for discussions.
- Conduct Quasi-Dynamic Simulations on some of the cases and record results.
- Perform comparative analysis

The justification and aims of the simulations conducted are provided below:

1. RMS and EMT simulations are both time-domain simulations dealing with steady-state studies for stability analysis and electromagnetic transients for stability respectively, while Quasi-Dynamic Simulations allow one to perform several load flow calculations in a period of time.

2. The aim of the steady-state or static simulations is to monitor critical parameters such as voltage profiles at bus terminals for stability assessment and steady-state power losses.
3. Dynamic transient simulations are performed to assess stability by monitoring generators' behaviours and transmission buses' voltage profile during network operation with disturbances such as faults.
4. P-V curves analysis is used for the assessment of voltage stability, system loadability or active power margin and the determination of voltage collapse point under various conditions.
5. Quasi-Dynamic mode is used to perform several load flow calculations over a period of time, precisely when investigating the contribution of BESS to voltage regulation and power system stability by offsetting intermittency.

6.2 Case 1 (Base case): Network operation with no RE integration

6.2.1 Scenario 1: Initial conditions

This base case aimed to set the reference for the analysis and comparison of future cases. The model network IEEE 9-Bus described in Figure 5-1 is built in *DigSILENT*™ - *PowerFactory*™ and simulated first in static mode to investigate voltage profile and power losses without the integration of PV systems or any other voltage support device. The network is thereafter simulated under dynamic conditions to assess the transient behaviour of the test network with reference to voltage stability. In this scenario of the base case, the analysis is done with initial normal loading and with no disturbance event set after running the classical load flows and later, a 3-phase fault is applied at Line 6-9 to investigate network's behaviour with reference to voltage stability conditions. During and after fault incidence, the following stability indicators are monitored: (1) the generator bus terminal voltages, (2) the rotor angles, (3) the generators' speeds and (4) the terminal voltages at the transmission lines buses (Bus 4, 7 and 9) and at the load buses (Bus, 5, 6, and 8). 7 and 8 are monitored during and after the fault incidence. P-V curves are also extracted for loadability assessment and load margin determination. The results of this scenario are recorded for further comparison analysis and discussions.

6.2.2 Scenario 2: Worst-case without DG integration

In order to assess and evaluate the supportive or adverse effects of FACTS devices and/or RE on the network stability under various conditions, a worst-case scenario is created and

simulated. Without RE integration, the network system is stressed by gradually increasing the total loading to create conditions that bring the test system close to stability limit. The three loads are increased by applying scaling factors functionality in *DigSILENT*™ - *PowerFactory*™ in increments of ten percent (10 %). The methodological approach of stressing the power system when assessing stability by increasing progressively the load and perform load flow calculation at each step was suggested and validated amongst others by the authors in references [170-172] respectively as a possible method of evaluating active/reactive power capabilities and power systems loadability. Results of the load flow calculations indicate voltage magnitudes at all the buses and using sensitivity analysis, the weakest buses of the network are determined. These weakest buses are then used as critical buses for the integration of FACTS devices and RE sources, with the aim of comparing their respective impacts on the network with regard to system voltage stability and power losses. Simulations similar to scenario 1 of this base case are performed and P-V curves are also plotted for stability analysis to the determination of real power margins. Results are recorded for further discussions.

6.3 Case 2: Effects on voltage support and on system stability using voltage control schemes

This case study aims to assess the impact of the installation of FACTS devices with the objectives of assessing the significance of active power enhancement for future comparison with the impact of PV-based power sources. With an SVS integrated at Bus 5 and the voltage profile, system stability and power losses are monitored and assessed both through steady state analysis and transient analysis. The Active power margin of the system is also assessed using a P-V curve analysis in static approach. Results of this case are discussed and compared to the results of the base case scenarios and Case 3 below.

6.4 Case 3: Effects of the DG integration on voltage and system stability

In this case, under the same initial settings as in Scenario 2 of the base case above, the SVS is replaced with a PV system at Bus 5. The aim is to investigate the extent to which voltage compensation and support can be achieved by injecting P at the distribution end or at load sides. The PV system is set to bring about the total power demand caused by the increase in load demand. As in the previous case, the voltage profile, the system stability and the power losses are monitored and assessed with a fault applied at Line 6-9. Loadability of the system is also assessed using P-V curve analysis. The results of this case are analysed, discussed and compared to the base case and Case 2 above.

6.5 Case 4: Impacts of DG siting on voltage and system stability

6.5.1 Scenario 1: Concentrated penetration

This case aims to investigate Solar PV location on voltage and system stability and loadability. A single concentrated unit is used in this first scenario, where the same Solar PV capacity as in Case 3 is considered, with the change of the PCC location while keeping the fault at a fixed location. The PV system is moved from the critical Bus 5 to all the other buses respectively and load flows are run after each position to assess the voltage profile, system loadability and critical voltage collapse point through RMS/EMT simulations and PV curves analysis respectively. Furthermore, in order to assess stability conditions, the results for the transient dynamic behaviour are recorded for each Solar PV location, analysed with the aim to experimentally determine the optimal location of the DG.

6.5.2 Scenario 2: Scattered PV penetration

In this second scenario, the static and dynamic stability are assessed when the Solar PV capacity is dispersed at the best identified locations from scenario 1 and the results are compared to the best of the results of scenario 1 of this current case.

6.6 Case 5: Effects of solar PV sizing on voltage and system stability

This case assesses the impact of the increased penetration of RE on the voltage stability under defined operating constraints. This case study aims to experimentally determine the optimal level of PV that could be integrated into the test network without voltage codes violation or jeopardising system stability conditions. The optimal location bus, as determined from Case 4, is used as the fixed location for placement of the PV systems of different capacities. The capacity of the PV system in gradually increased in 10 % increments from no-PV to 150 % penetration based on Equation 6-1:

$$\%PV_{PENETRATION} = \frac{TOTAL_{PV\_GENERATION}[MW]}{TOTAL_{NETWORK\_GENERATION}[MW]} \quad 6.1$$

Load flows are run after each increment and the voltage profile at Bus 4, the system loadability and the critical voltage collapse point are monitored through RMS/EMT simulations and the extraction of P-V curves respectively. With the three-phase fault at the same location, line 6-9, dynamic transient behaviour during fault is also investigated and results are compared and discussed.

6.7 Case 6: Effect of the integration of the energy storage system

This case aims to investigate the supportive or adverse impact of the integration of BESS on voltage regulation and power system stability conditions with reference to grid codes violations and mitigation solutions thereof by offsetting the intermittency of the PV energy. For this case, the IEEE 9-Bus test system is modified to include time characteristics loads and a 24-Hour load profile was assigned to the three loads based on typical residential, commercial and industrial load profiles in order to obtain a 24-Hour system load curve, shown in Figure 6-1. Similar assessments for power systems as in the previous cases are performed and in addition, Quasi-Simulation is performed to assess system performance through total losses determination over 24 hours specifically with and without BESS.

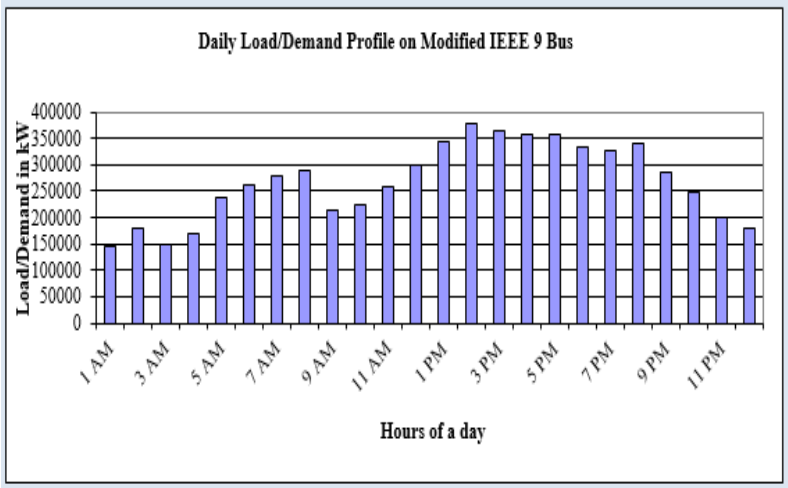

Figure 6-1: Daily load demand for the modified IEEE 9-Bus

6.8 Summary

In this chapter, six study cases and subsequent scenarios whose results are discussed in Chapter Seven were presented and explained. The aims and the purposes were provided to support and to substantiate each study case, together with the related simulation methodology.

CHAPTER 7: RESULTS: ANALYSIS AND DISCUSSION

The results and discussions of the seven case studies mentioned in chapter six are presented in this chapter. For the first five cases, both static and dynamic transient RMS simulations are run under various conditions and the results are discussed with emphasis on system voltage stability and power losses. The last case study results cover the investigation on the BESS incorporation, acting as loads to store the extra energy from intermittent DG sources to achieve voltage control and regulation in Solar PV penetrated networks.

7.1 Case 1: Network operation without RE integration

7.1.1 Scenario 1: Initial normal conditions

7.1.1.1 Voltage profile assessment using steady-state analysis

With all initial settings as presented in Chapter 5, a load flow is successfully run on the test model using the *DigSILENT*™ - *PowerFactory*™ with balance and a symmetrical three-phase system to extract the results of the calculation of active and reactive power flow, and the bus voltages. Figure 7-1 and Figure 7-2 depict the voltage magnitudes and voltage deviations at all buses.

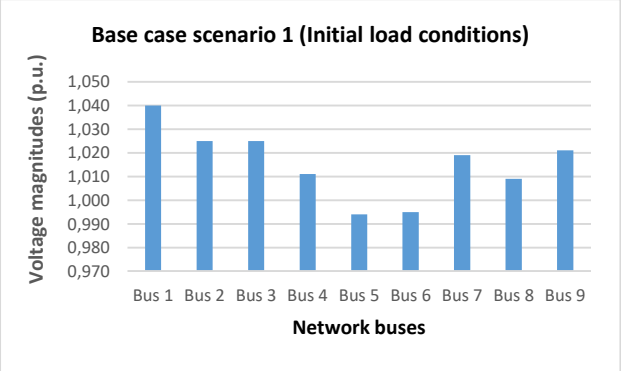

Figure 7-1: Voltage profile for the base case scenario 1 (Initial conditions and without PV integration)

It can be seen that since the generator at bus 1 was selected as the slack generator, the voltage at this bus is constant at setting voltage 1,040 p.u. The lowest voltage in the network is 0,984 p.u. at Bus 5, but the deviations are within the code margins.

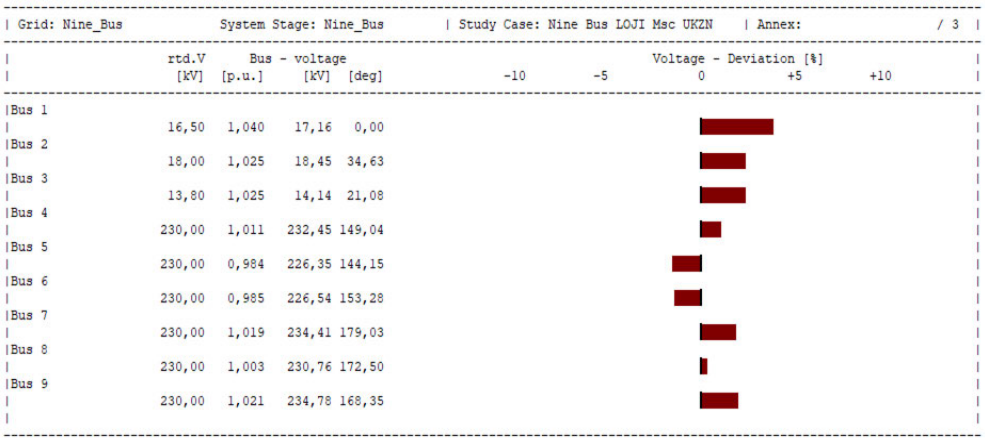

Figure 7-2: Bus voltages deviations for base case scenario 1 (initial conditions)

7.1.1.2 System stability assessment using P-V curves

The assessment of the system stability is performed through an assessment of the system loadability using P-V curves analysis. The aim is to show the maximum loadability point for considered cases, the critical voltage collapse point or the point of voltage collapse and the calculation of the MW distance to the critical point for comparative analysis. The P-V curves extracted from this scenario are displayed in Figure 7-3 and they show that the system network will reach the critical voltage point of 0,60 p.u. if the power demand increases to a maximum power of 1153,12 MW. This corroborates the analytical concept of voltage stability and the convergence of the system voltage equation towards the point of voltage collapse, as mentioned in Section 2.5 of this dissertation.

The maximum loadability point is the point where maximum P transfer can be achieved without any of the bus voltages getting to fall below the minimum required standard voltage code of 0,95 p.u. For this base case, the maximum loadability point is reached at 547,56 MW. This point is the base case operating point and will be used as reference for discussions or further investigations on this research work. The Megawatt (MW) distance to critical point, also termed loading margin, is an essential criterion for PSOs. The MW distance is estimated using the difference between the maximum loading power demand to reach voltage collapse and the power at the maximum loadability point. For this base case, the loading margin is $1153{,}12MW - 547{,}56MW = 605{,}56MW$.

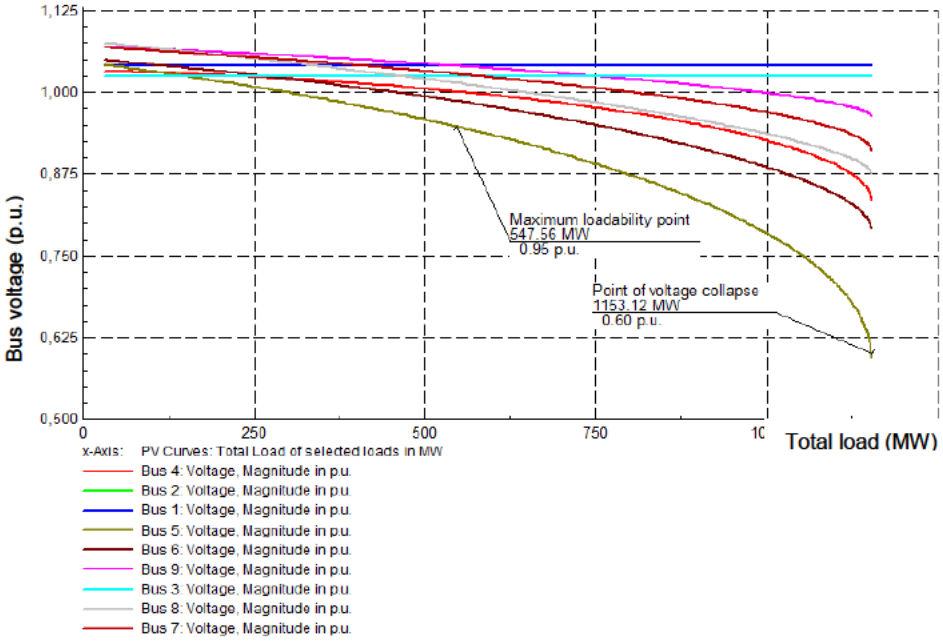

Figure 7-3: Assessment of network loadability using P-V curves for the Base Case Scenario 1 (initial conditions)

7.1.1.3 Dynamic transient stability analysis

For the purpose of transient stability analysis, a three-phase balanced fault event is applied to the network at a 50 % distance of Line 6 for a duration of 100 milliseconds and simulations run for 12 seconds. The critical fault clearing time (CFCT) was first determined by gradually increasing the duration time of the fault and monitoring the simulation results of the rotor angles, the generators' speeds and the terminal voltages of the generators. The CFCT is the fault time duration that, if exceeded, the system will be unable to return to pre-fault operating conditions or the maximum time. For this current study, the CFCT was found to be 113 milliseconds.

The transient behaviour is performed by observing the results of the rotor angle of generators G2 and G3 with respect to reference generator G1, the speeds of the three generators and the voltage profile at the generators' terminals displayed in Figure 7-4, as well as the voltage profile of the transmission lines and load buses displayed in Figure 7-5. From Figure 7-4 (a), a large uptick is observed in the relative rotor angles deviations of generators G2 and G3 with respect to the reference generator G1, followed by moderate oscillations that are damping over time after the fault has been cleared to settle at 20,44 degrees' angle difference after around 10 seconds. The system regains stability by reaching a new steady-state operating point, with the

rotor angle difference settling at +/- 5 degrees more from pre-fault conditions. The speeds of the three generators are shown in Figure 7-4 (b) describing a graph of identical shape showing a slight decrease during fault, followed by an acceptable increase of speed up to just below 1,08 p.u after fault clearing.

The generators' terminal voltages as shown in Figure 7-4 (c) dip down to 0,61 p.u. for the duration of the fault, but sharply increase after the fault is cleared to stabilise with a mild

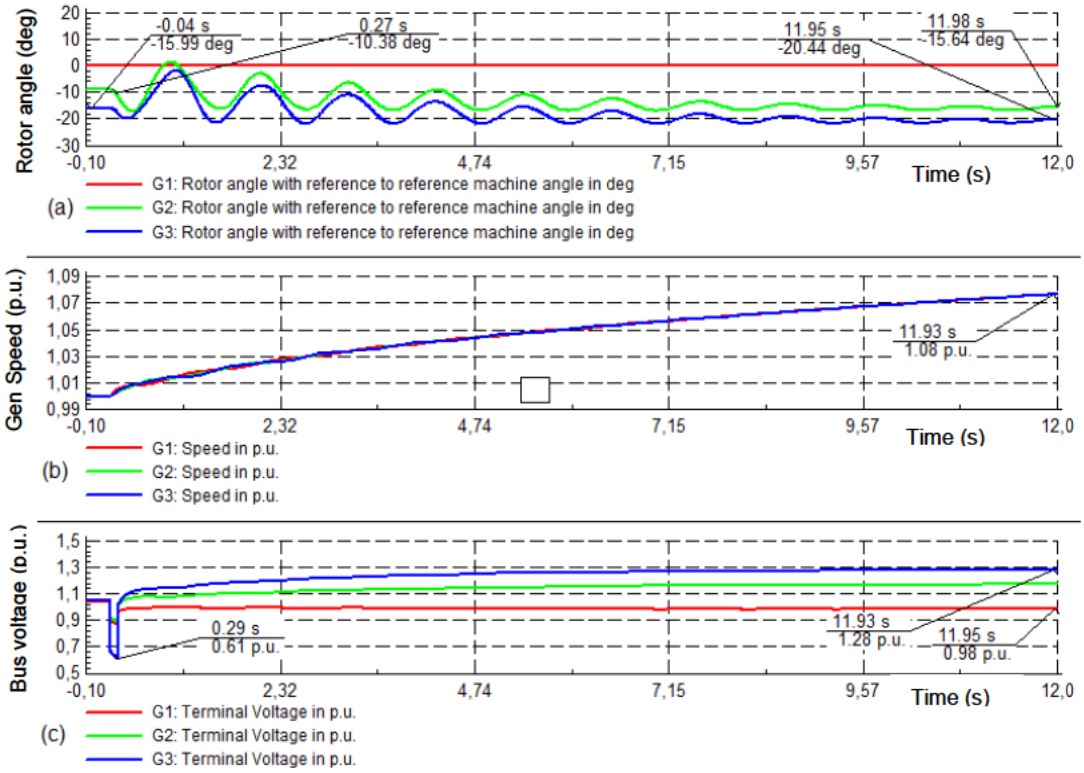

Figure 7-4: (a) Rotor angle with respect to reference machine, (b) Generator speeds and (c) Generator terminal voltages for the Base Case scenario 1 (Initial conditions)

fluctuation and settle back near to their initial pre-fault values at around 5 seconds into the simulation fluctuation and settle back near to their initial pre-fault values at around 5 seconds into the simulation

The voltage profiles of the transmission lines and load buses are illustrated in Figure 7-5. At the time the fault is applied to Line 6-9, voltages at all buses dip down for the duration of the fault to a lowest 0,26 p.u at the fault bus, Bus 6, and sharply increase after the fault has been cleared to progressively converge to a new equilibrium operating point, evidencing that the system regains stability and will not plunge into instability as a result of the disturbance.

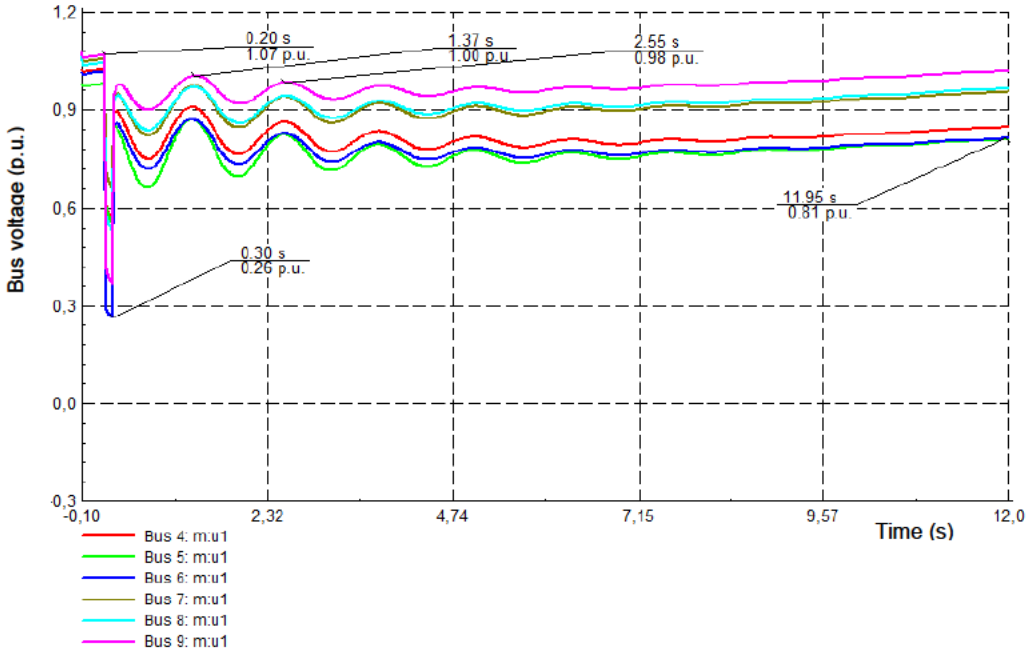

Figure 7-5: Voltage profile at the transmission line and load buses for the Base Case scenario 1 (Initial conditions)

7.1.2 Scenario 2: Extreme conditions (worst case without PV integration)

7.1.2.1 Voltage profile assessment using steady-state analysis

The results of the simulations in static mode indicate that Bus 5 is the weakest bus with a bus voltage beyond the standard code to 0,938 p.u. as shown in Figure 7-6 and Figure 7-7.

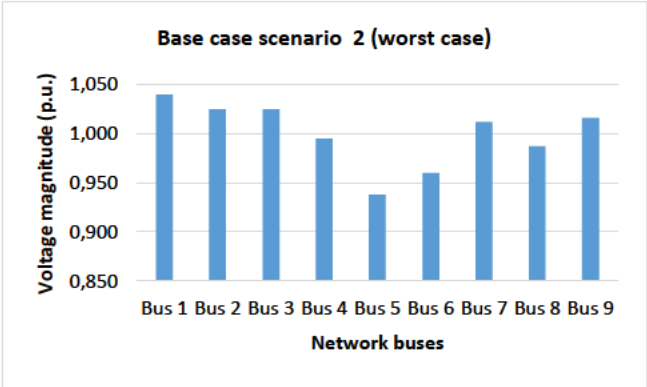

Figure 7-6: Bus voltages for Base Case scenario 2 (Worst-case scenario with no FACTS devices or Solar PV units)

This extreme condition was obtained after running the load flow at scaling factor 1,45, meaning a 45 % load increase.

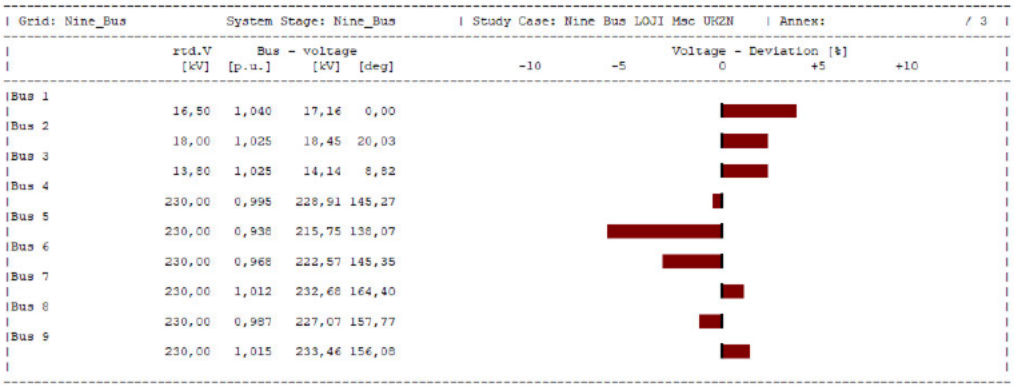

Grid: Nine_Bus	System Stage: Nine_Bus	Study Case: Nine Bus LOJI Mac UKZN	Annex: / 3

	rtd.V [kV]	Bus - voltage [p.u.]	[kV]	[deg]	Voltage - Deviation [%] -10 -5 0 +5 +10
Bus 1	16,50	1,040	17,16	0,00	
Bus 2	18,00	1,025	18,45	20,03	
Bus 3	13,80	1,025	14,14	8,82	
Bus 4	230,00	0,995	228,91	145,27	
Bus 5	230,00	0,938	215,75	138,07	
Bus 6	230,00	0,968	222,57	145,35	
Bus 7	230,00	1,012	232,68	164,40	
Bus 8	230,00	0,987	227,07	157,77	
Bus 9	230,00	1,015	233,46	156,08	

Figure 7-7: Bus voltages deviations for the Base Case scenario 2 (Extreme conditions with no FACTS and no Solar PV integrated)

Figure 7-8 illustrate the change in the voltage magnitudes from scenario 1 to scenario 2.

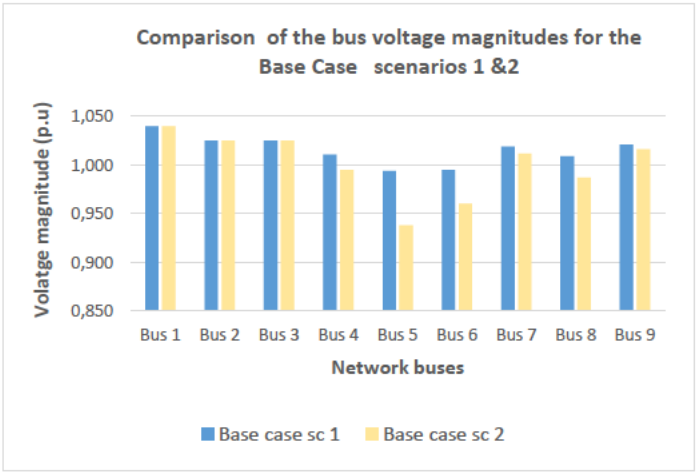

Figure 7-8: Comparison of voltage profiles for scenarios 1 and 2 of the Base Case

7.1.2.2 Voltage stability assessment using P-V curves

Figure 7-9 depicts the P-V curves for the worst-case scenario and it can be observed that the maximum loadability point has decreased from 547,56 MW to 515,31 MW, representing 6,23 %, while the point of voltage collapse moved down from 1153,12 MW to 875,04 MW. This decrease corresponds to a reduction of 40,59 % in the loading margin or the maximum power transfer to reach the critical voltage point from 605,56 MW in base case scenario 1 to 359,73 MW in this base case scenario.

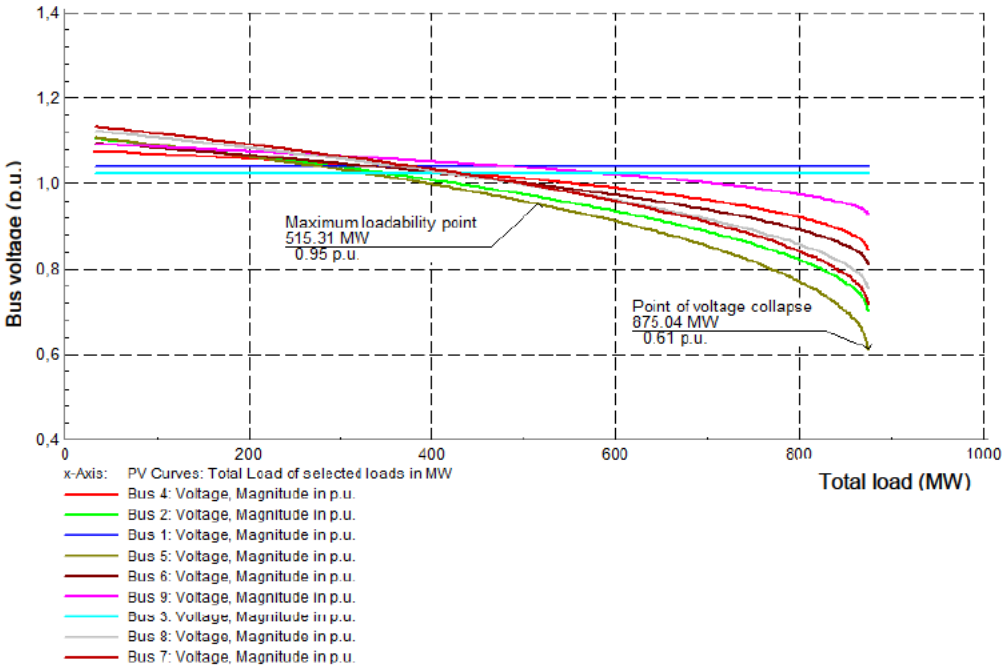

Figure 7-9: Loadability assessment of the Worst Case scenario of Case 1

7.1.2.3 Dynamic transient stability

The same nature of the fault as in the previous case is applied at 50 % distance of Line 6-9. Figures 7-10 (a), (b) and (c) show the results for the system's transient behaviour following the fault event and in comparison with base case scenario 1, the system tumbles into instability as the analysis below indicates. From Figure 7-10 (a), it is observed that G2 and G3's rotor angles oscillate around the reference generator rotor angle at a higher frequency between -176 degrees and +177 degrees. Transient stability is deteriorated as the oscillations are not followed by damping. The results of the speeds of the generators are recorded in Figure 7-10 (b). It is evidenced that the system loses stability as G1 falls out of synchronism and decelerates to stand still at around 11 seconds post-fault, while simultaneously G2 and G3 are accelerating abnormally in an unsuccessful attempt to respond to load demand. The instability condition described above is corroborated by the generators' terminal voltages as depicted in Figure 7-10 (c), which experience each intense oscillation with the slack generator voltage falling below 0,26 p.u after 11 seconds through the simulation.

The transmission lines and load buses voltage profile assessment results are presented in Figure 7-11. It is observed that all voltages are intensively fluctuating post-fault to confirm network instability status. It can be predicted that the system voltage settles at a new steady state operating point if no deliberate voltage support action is implemented.

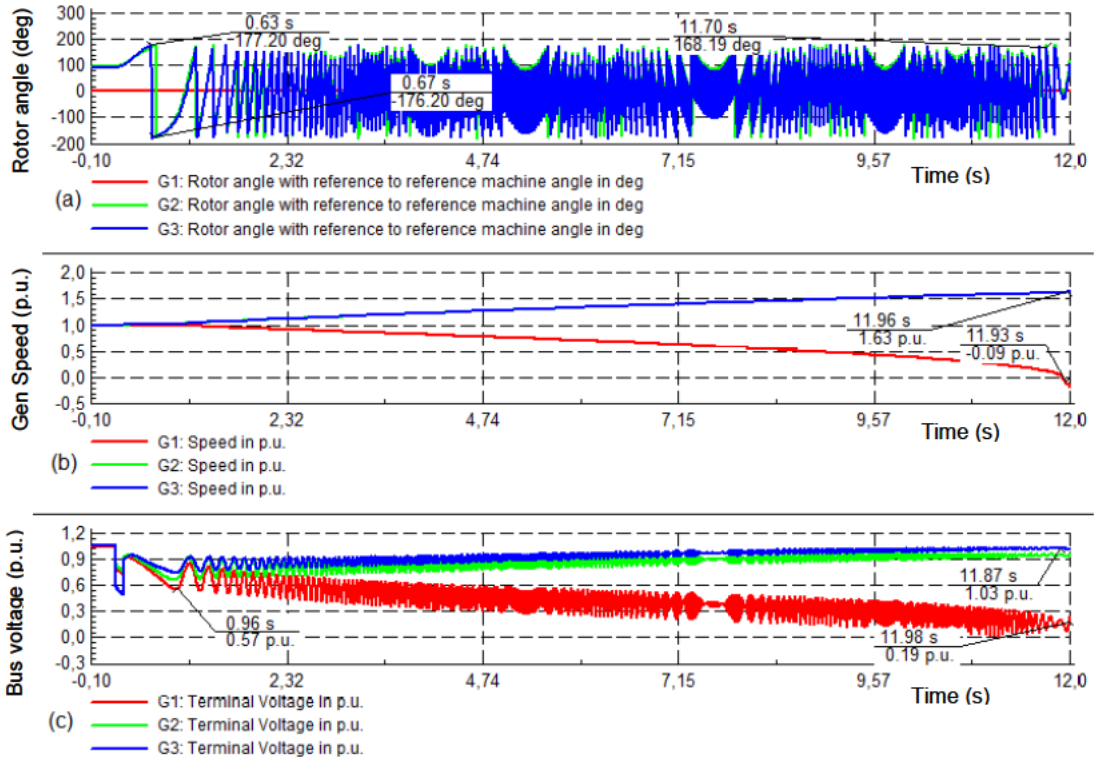

Figure 7-10: (a) Rotor angles (b) Generator speeds and (c) Generator terminal voltages for the Base Case scenario 2 (Worst conditions)

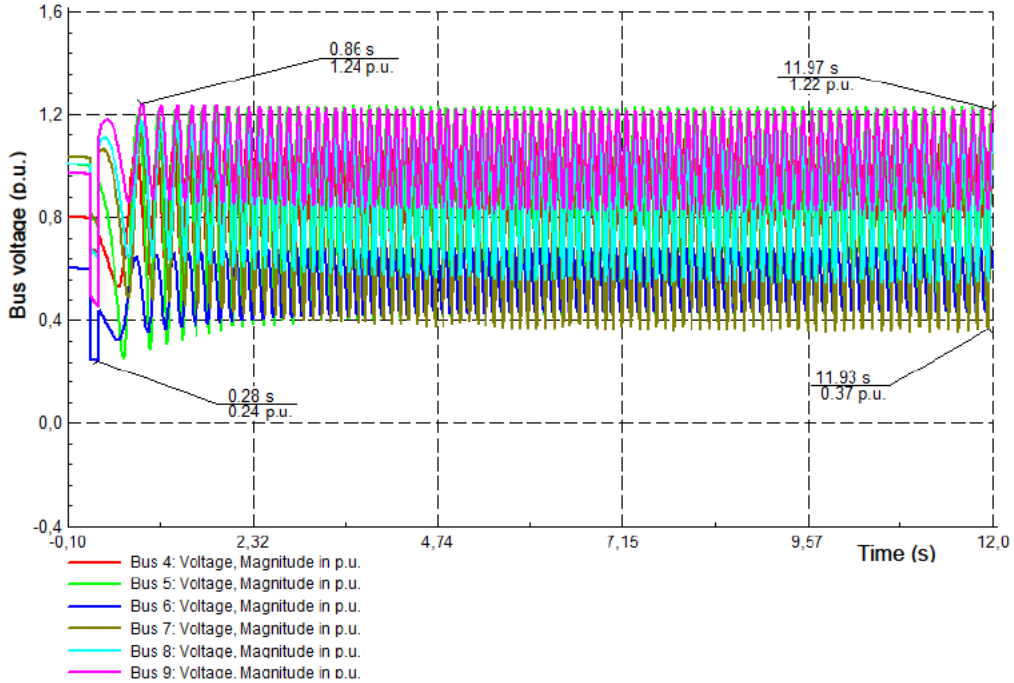

Figure 7-11: Voltage profile for the transmission lines and load buses for Base Case scenario 2 (Extreme conditions)

7.2 Case 2: Impact of voltage control schemes

7.2.1 Impact of the SVS on static voltage stability

With Scenario 2 worst-case settings, the SVS reactive power compensation device is integrated at bus 5 and the results of the static steady-state analysis show the system voltage support as depicted on Figure 7-12 and Figure 7-13. The performance of the network with no disturbance is assessed. The voltages at all the buses in comparison to Figure 7-7 fall back within code margins, meaning between 0,95 p.u. and 1,05 p.u., with particularly the voltages at Bus 5 and Bus 6 reaching 1,00 p.u. from 0,938 p.u. and 0,968 p.u. respectively, as was presented in Figure 7-7.

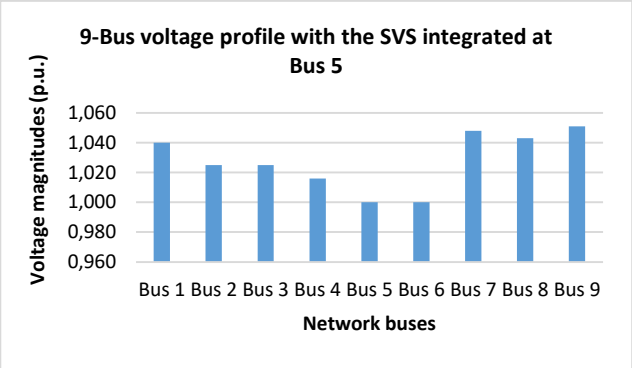

Figure 7-12: Voltage profile of network buses for the impact SVS integration at Bus 5

	rtd.V [kV]	Bus - voltage [p.u.]	[kV]	[deg]	Voltage - Deviation [%] −10 −5 0 +5 +10
Bus 1					
	16,50	1,040	17,16	0,00	
Bus 2					
	18,45	1,025	18,91	22,42	
Bus 3					
	14,14	1,025	14,49	18,08	
Bus 4					
	230,00	1,016	233,74	3,12	
Bus 5					
	230,00	1,000	230,00	4,94	
Bus 6					
	230,00	1,000	230,00	6,79	
Bus 7					
	230,00	1,048	241,15	17,12	
Bus 8					
	230,00	1,043	239,86	16,26	
Bus 9					
	230,00	1,051	241,82	15,50	

Figure 7-13: Voltage deviations effected by the integration of the SVS at Bus 5

Figure 7-14 shows the improvement of the bus voltages that is experienced after the integration of the SVS at Bus 5 in comparison to the Base Case scenarios 1 and 2 as seen in Figures 7-2 and 7-7. From a 45 % network load demand increase both in MWs and MVARs, in order to create the worst condition in Base Case scenario 2, a corresponding 5,97 % in voltage deterioration at Bus 5 was recorded. The SVS was set to compensate for the MVARs load

demand increase and a corresponding 6,18 % voltage improvement was recorded. It is noted that there is a better improvement as the voltage goes slightly above the voltage at Bus 5 in Base Case scenario 1 from 0,994 p.u. to 0,996 p.u.

Furthermore, there is no over-voltage at any of the buses after the integration of the SVS. This notice, anticipatively, preludes the discussions between the results of Case 2 and the results of the upcoming Case 3 on particularly the impact of PV source penetration on voltage in the system.

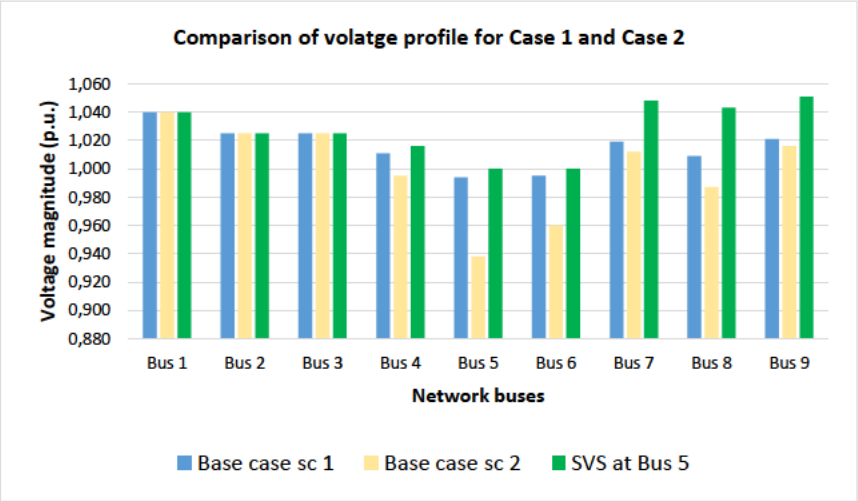

Figure 7-14: Voltage profile enhancement effects after SVS integration at Bus 5 in comparison to initial conditions and worst conditions

7.2.2 Effects of Q compensation on system loadability and stability

The assessment of the system loadability using P-V curves is illustrated in Figure 7-15. In comparison to the Worst-Case scenario, it can be seen that the system operating point or maximum loadability point has improved from 515,31 MW in Figure 7-8 to 547,46 MW in Figure 7-15. This new operating point corresponds to the operating point that was identified in the Base Case scenario 1 as displayed in Figure 7-3. On the other hand, the point of voltage collapse after the integration of the SVS is slightly improved compared to the Base Case scenario 1 from 1153,12 MW in Figure 7-3 to 1314,40 MW in Figure 7-15 below, corresponding to an increase of 17,48 % in loading margin from 605,56 MW to 766,84 MW in this case.

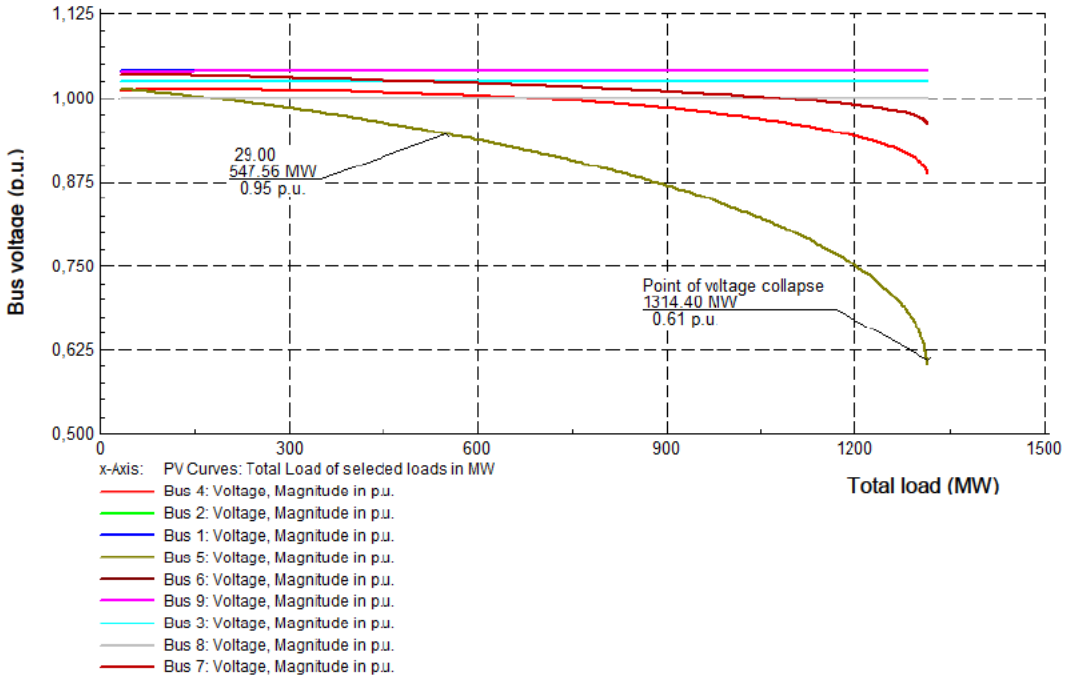

Figure 7-15: System's P-V curves after the integration of the SVS

7.2.3 Dynamic transient stability as effected by the integration of reactive power compensation schemes

The results of the dynamic transient stability analysis are given in Figure 7-16 and Figure 7-17 below after a fault of the same nature as in the previous cases and under the same conditions as applied at a 50 % distance of Line 6. From 7-16 (a), it can be observed that the rotor angles of G2 and G3 fluctuate moderately and damp over time after the fault has been cleared to settle at between a 15 and 20 degrees' angle difference after 10 seconds. The system indeed regains stability by converging toward a new stability point.

The generators' speeds are displayed in Figure 7-16 (b) and it can be noticed that there is a linear increase in the pattern similar to that observed during the simulation of the base case scenario 1 in Figure 7-4 (b), settling at 1,071 p.u. 10 seconds after fault clearing.

From Figure 7-16 (c), it can be recorded that the terminal voltages of the generators are quasi-constant, after dipping down to the lowest 0,62 p.u. at Bus 6 with no noticeable fluctuation from the time the fault is cleared. The system rapidly regains stability, settling at a new operating point. The transmission lines buses and load buses voltages profiles are shown in Figure 7-17.

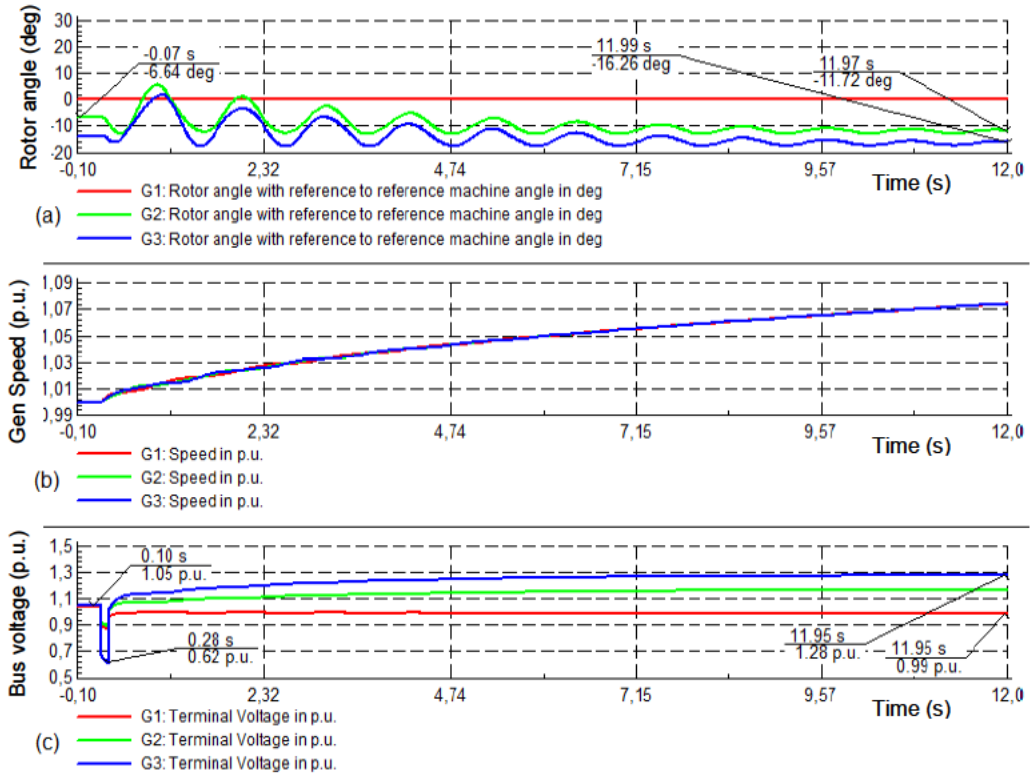

Figure 7-16:(a) Generators' rotor angle (b) Generators' speeds and (c) Generators' terminal voltages for Case 2 (Integration of SVS at Bus 5)

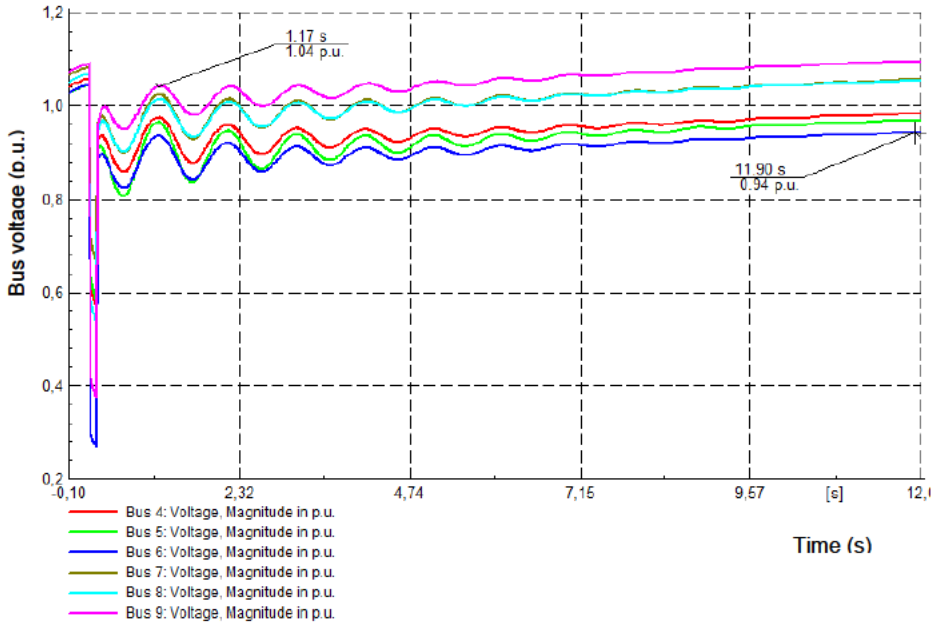

Figure 7-17: Transmission and load buses' voltage profile resulting from the effect of SVS integration

After the disturbance is removed, the voltage which dipped down to a lower 0,29 p.u. settles smoothly into a new steady state operating point, with voltage tendency to increase towards

pre-fault values. This behaviour shall be attributed to Q support from the SVS enhancing voltage stability. It is also evidenced that the stability voltage recovery time and the convergence toward a new operating point are faster with voltage support than the recovery of the base case scenario 1 as observed in the results shown in Figure 7-4.

7.3 Case 3: Effects of Solar PV grid integration without reactive power controller

In this section, the effect Solar PV on the network are investigated and results presented. Firstly, the case consists of replacing the SVS at Bus 5 from Case 3 with a 40 MW solar PV system to compensate for the total P demand caused by 45 % load increase, investigating the impact of PV placement and comparing the corresponding effects to both the Base Case and Case 2. It is projected that voltages will revert to the results of base case scenario 1. Secondly, two series of simulation scenarios are run to investigate the effects of Solar PV siting and sizing on voltage and system stability.

7.3.1 Impact of DG placement in the absence of faults

7.3.1.1 Impact on the voltage stability

This investigation aims to evaluate the extent at which Solar PV system can improve the voltage system stability when compared to the effect of the SVS at the same network location. Figures 7-18 and 7-19 respectively show the voltage profile and the voltage deviations as effected by Solar PV integration at Bus 5.

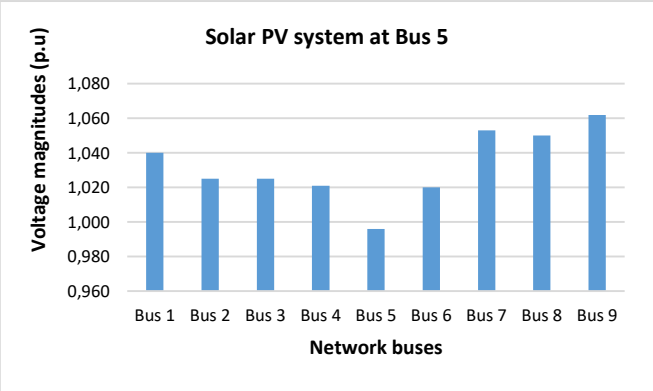

Figure 7-18:Voltage profile as effected by PV system integration at Bus 5

It can be observed that the voltage profile at Bus 5 is improved from 0,936 p.u. to 0,996 p.u.

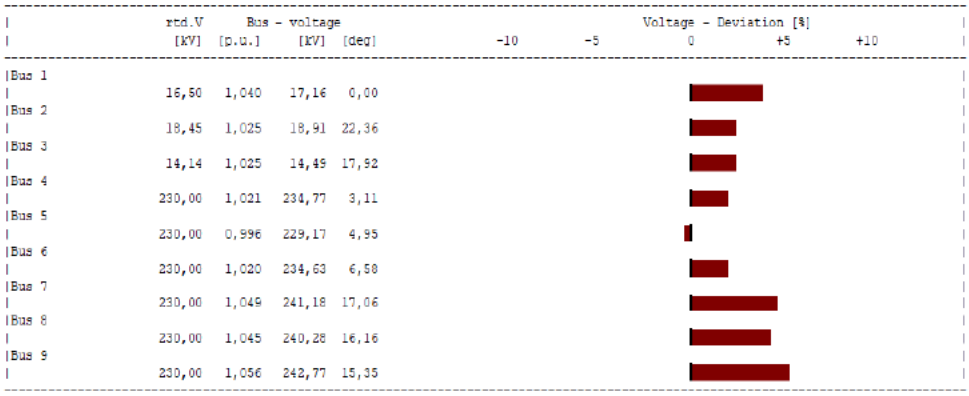

	rtd.V [kV]	Bus - voltage [p.u.]	[kV]	[deg]	Voltage - Deviation [%] -10	-5	0	+5	+10
Bus 1	16,50	1,040	17,16	0,00					
Bus 2	18,45	1,025	18,91	22,36					
Bus 3	14,14	1,025	14,49	17,92					
Bus 4	230,00	1,021	234,77	3,11					
Bus 5	230,00	0,996	229,17	4,95					
Bus 6	230,00	1,020	234,63	6,58					
Bus 7	230,00	1,049	241,18	17,06					
Bus 8	230,00	1,045	240,28	16,16					
Bus 9	230,00	1,056	242,77	15,35					

Figure 7-19: Network volatge deviations after the integration of Solar PV at Bus 5

Figure 7-20 presents a comparison between the voltage profile resulting from Base Case scenarios 1 and 2, from Case 2 and from Case 3. It can be ascertained that the improvement brought by Solar PV integration at Bus 5 is slightly below the improvement effected by the SVS integration at the same location in Case 2.

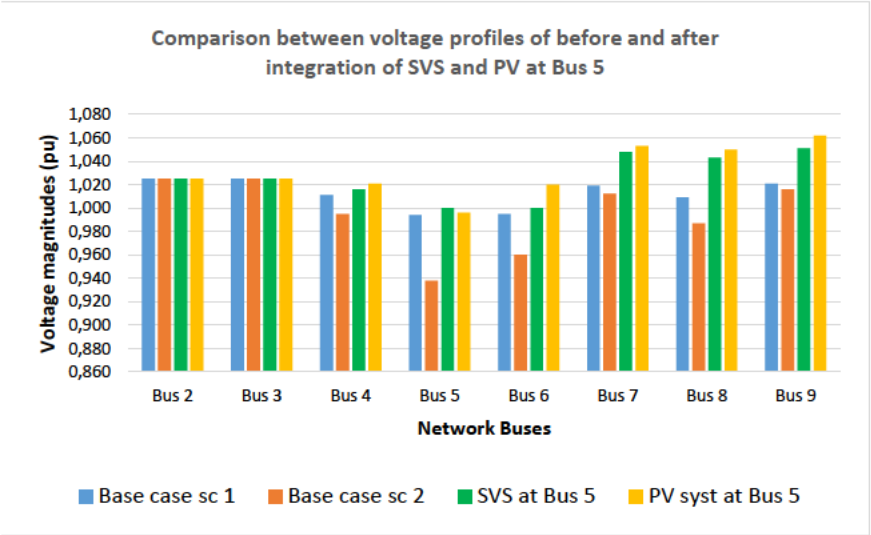

Figure 7-20: Voltage profile comparison before and after the integration of SVS and PV at critical Bus 5

Due to the fact that voltage-sensitive loads are connected to load buses, it is imperative to observe the voltage profiles at buses 5, 6 and 8 as the improvement shall remain within the acceptable limits of ± 5 %. It is verified that this condition is fulfilled as the voltages at the loads buses are 0,996 p.u., 1,020 p.u. and 1,045 p.u. at respectively Bus 5, Bus 6 and Bus 8. The transmission line Bus 9 records a mild overvoltage of 1,056 p.u. compared to 1,051 recorded after the integration of the SVS.

7.3.1.2 Impact on system loadability

The system loadability results for the case are presented in Figure 7-21.

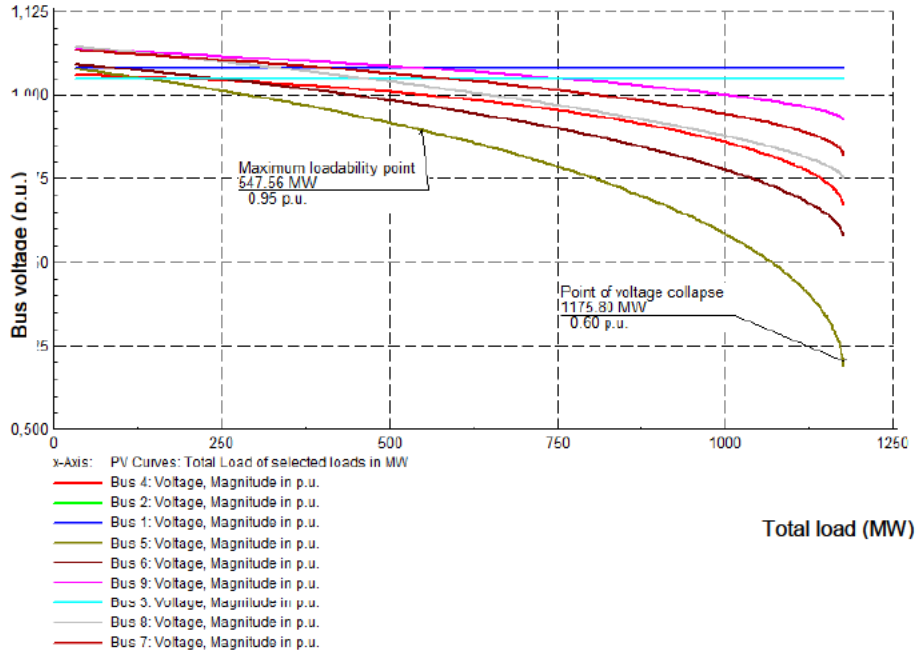

Figure 7-21: Effect of the integration of Solar PV at Bus 5 on system loadability (Case 3)

The P-V curves analysis without and with integration of SVS and the Solar PV systems are displayed in Figure 7-22 and it is evidenced that the integration of SVS at Bus 5 presents better system loadability improvement compared to the integration of PV at the same location. Although the point of voltage collapse is improved with the integration of PV compared to Case 1, from 1153,12 MW to 1175,8 MW, this improvement remains slightly below the one effected by the integration of the SVS at the same location. Furthermore, the results show that the distance to voltage collapse decreases from 766,84 MW with the SVS to 628,24 MW when SVS is replaced with Solar PV, corresponding to 18,07 % of the loading margin with the SVS at Bus 5, as presented in Figure 7-23.

With regard to the maximum loadability point, no further improvement was observed as its value remained constant at 547,56 MW for the initial conditions case, as well as for both the SVS and Solar PV integrations at Bus 5.

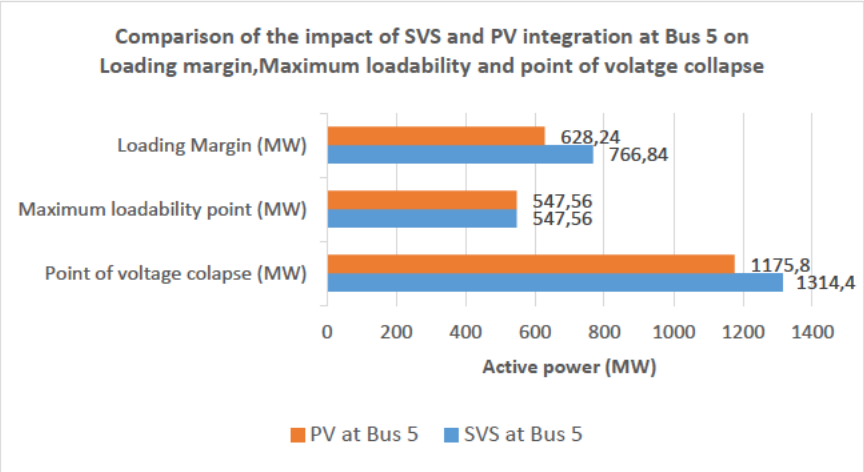

Figure 7-22: Better impact of SVS integration over Solar PV integration on loading margin and point of voltage collapse

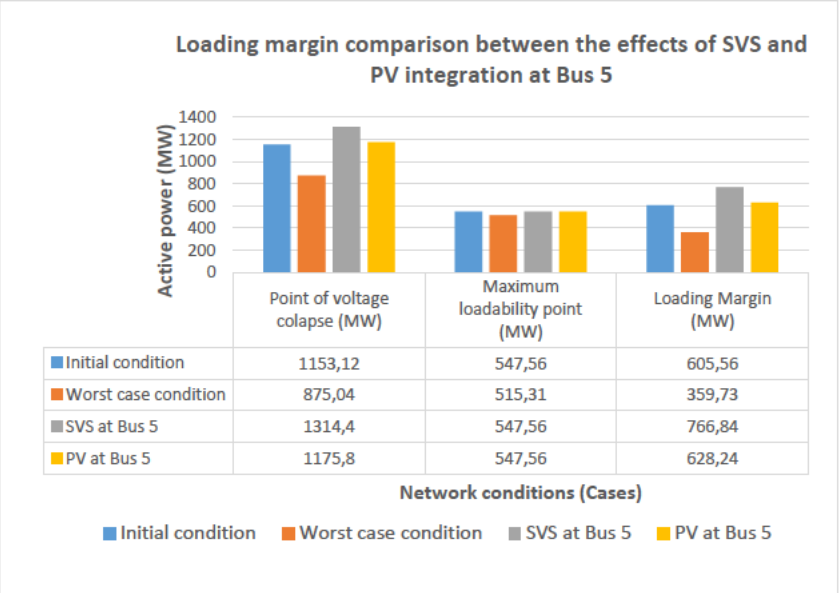

Figure 7-23: Comparison of PV and SVS integration on system loadability before and after the integration to the network (Base Case, Case 2 and Case 3)

7.3.2 Impact of DG integration under fault conditions

Transient stability results are presented in Figure 7-24. It is evidenced that the system conserves its rigidity after the fault was applied and removed, consequently converging into a new steady state of dynamic stability. From the comparative analysis of the results in Figures 7-16 (a) and 7-24 (a), it is observed a deviation of the rotor angle from their values prior fault as compared to their final values, These values are larger at G2 when Solar PV is integrated into the grid as compared to the SVS placement at the same location

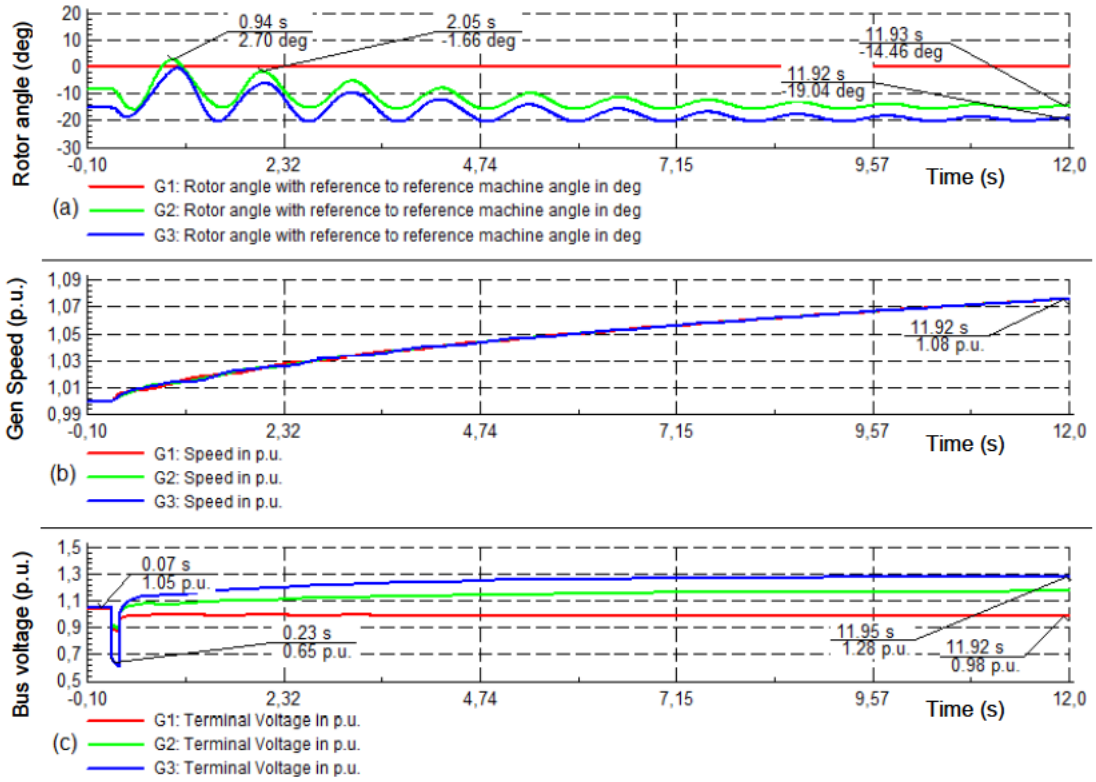

Figure 7-24: (a) Generators rotor angle (b) Generators' speeds and (c) Generators' terminal voltages for Case 3 (Integration of Solar PV at Bus 5

This can be attributed to the appearance of network weak-grid areas caused by the fact that the considered PCC, Bus 5, at which a generating unit with no rotational mass was added, is electrically closer to the generator G2. Figure 7-25 shows the differences in generators G2 and G3's rotor behaviours pre and post-fault. The trajectory of the generators' speed is similar for both the integration of the SVS and the integration the Solar PV, as is displayed in Figure 7-24 (b).

The generators' terminal voltages are depicted in Figure 7-24 (c) and it is observed that there is no substantial difference with the terminal voltage behaviour observed in Figure 7-16 (c) under the integration of the SVS, except the fact that the voltage recovery toward pre-fault values is slightly faster with SVS placed at Bus 5 than with Solar PV integrated at the same location

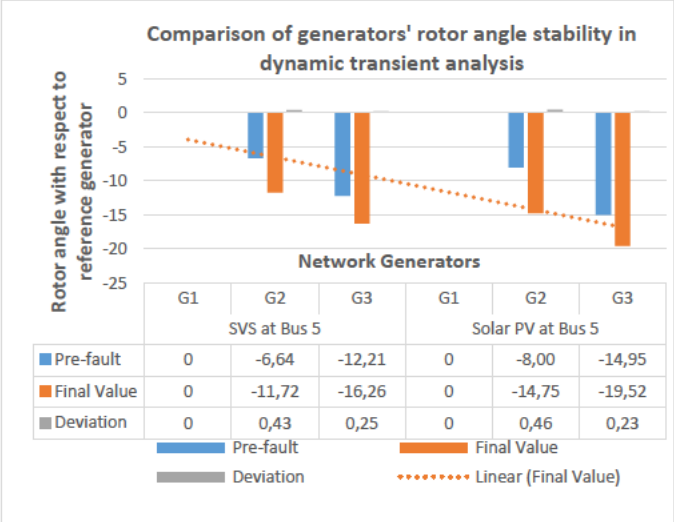

Figure 7-25: Comparison between the SVS and Solar PV integration on the generators peak rotor angle deviation

The transmission and load buses' voltage profiles are shown in Figure 7-26. It is noticed that the results of the generators' voltage behaviours, the transmission and load buses' voltages also suffer damped oscillations to settle accordingly after the fault has been removed.

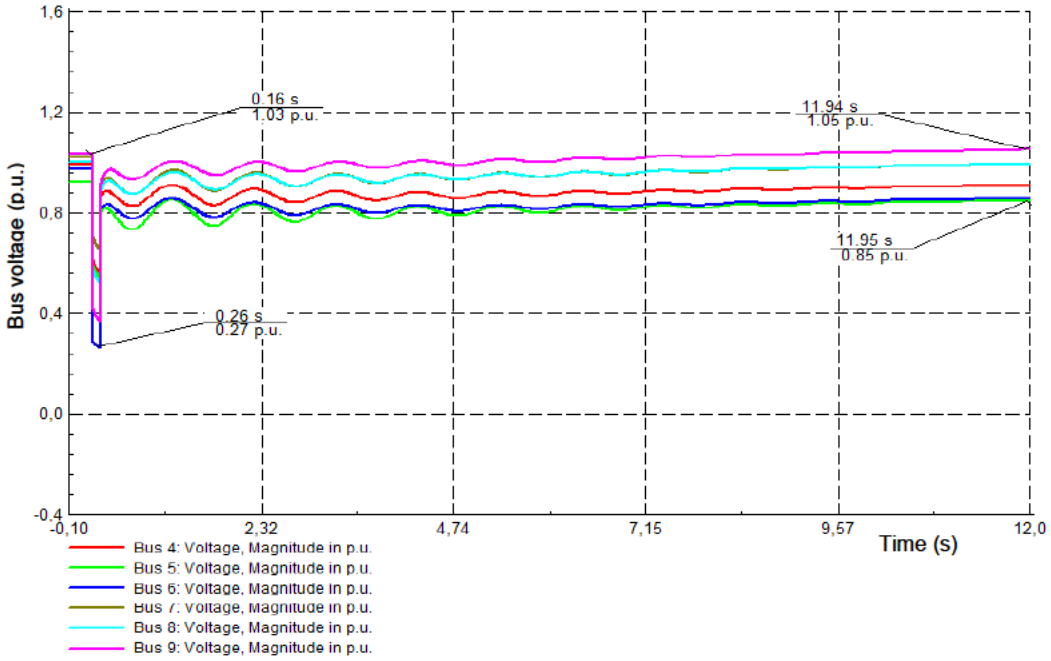

Figure 7-26: Transient behaviour of the transmission and load buses voltages after the integration of Solar PV at Bus 5

7.4 Case 4: DG siting impact

The total MW generated for the system is 197,45 MW. Based on equation 6-1, this amount is used to calculate the suitable percentage of the Solar PV penetration that will apply to various scenarios of this study case.

A 20 MVA capacity Solar PV system, representing 10 % PV penetration, is considered for the assessment of PV siting impact on voltage, system loadability and transient stability. The Solar system is first placed at the critical bus (Bus 5) and thereafter successively placed at all the other remaining PCC, except at the reference bus. The results of the selected parameters for each scenario are recorded and discussed.

7.4.1 Scenario 1: Single Solar PV unit concentrated at various locations

7.4.1.1 PV location effects in the absence of fault

In the absence of fault, the voltage profile is assessed by critical bus voltage monitoring for various locations. The simulation results of this case study are summarised in Table 7-1 and are graphically displayed in Figures 7-27 and 7-28.

Table 7-1: Results for voltage profile and system loadability as functions of the Solar PV location

Integration point (PCC)	Voltage at Bus 5 [p.u.]	% Voltage improvement	Maximum loadability point [MW]	Point of voltage collapse [MW]	Loading Margin [MW]
PV @Bus 5	0,975	4,0%	612,08	1145,81	563,73
PV @Bus 7	0,962	2,7%	547,56	1138,25	590,69
PV @Bus 6	0,955	2,0%	517,41	1136,74	619,33
PV @Bus 3	0,954	1,9%	483,05	1134,49	651,44
PV @Bus 9	0,954	1,9%	514,11	1134,47	620,36
PV @Bus 4	0,953	1,8%	529,31	1134,35	605,04
PV @Bus 2	0,952	1,7%	483,12	1134,98	651,86
PV @Bus 8	0,951	1,6%	483,05	1132,46	649,41

The voltage magnitude at Bus 5 changes depending on the Solar PV system integration point. The critical bus most improved voltage magnitude of 4,0 is achieved when Bus 5 itself serves as the PCC. This can be substantiated by two evident reasons: (1) Solar PV has no considerable Q exchange capabilities and (2) the relatively long electrical distance between Q injection point (PCC) and the location where Q is actually needed, meaning the critical bus.

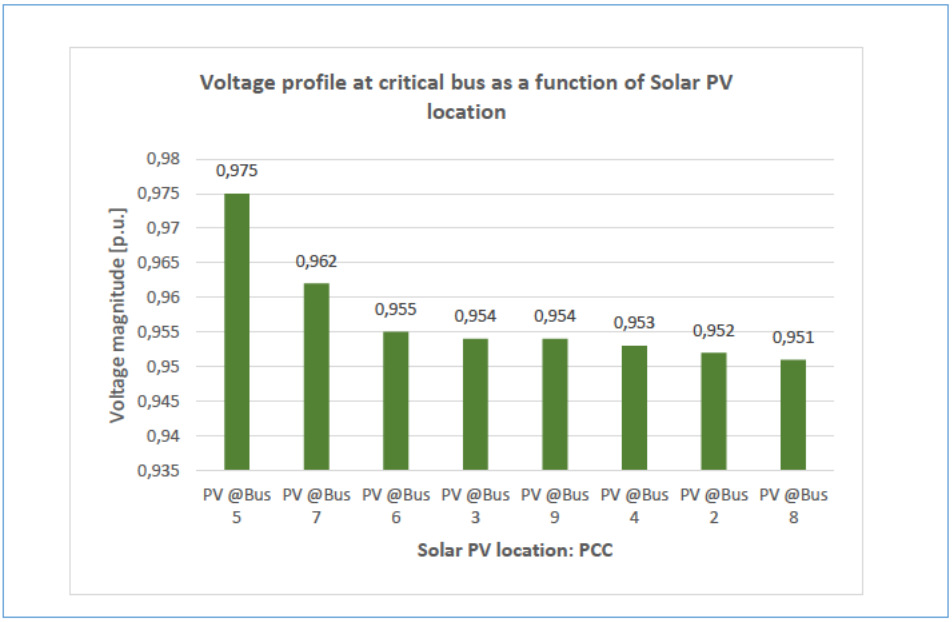

Figure 7-27: Critical bus's voltage to illustrate Solar PV siting impact on voltage profile

7.4.1.2 Impact of Solar PV location on system loadability

The results pertaining to the assessment of PV location's impact on loadability are consolidated in Table 7-1 and visualised through the graph in Figure 7-28.

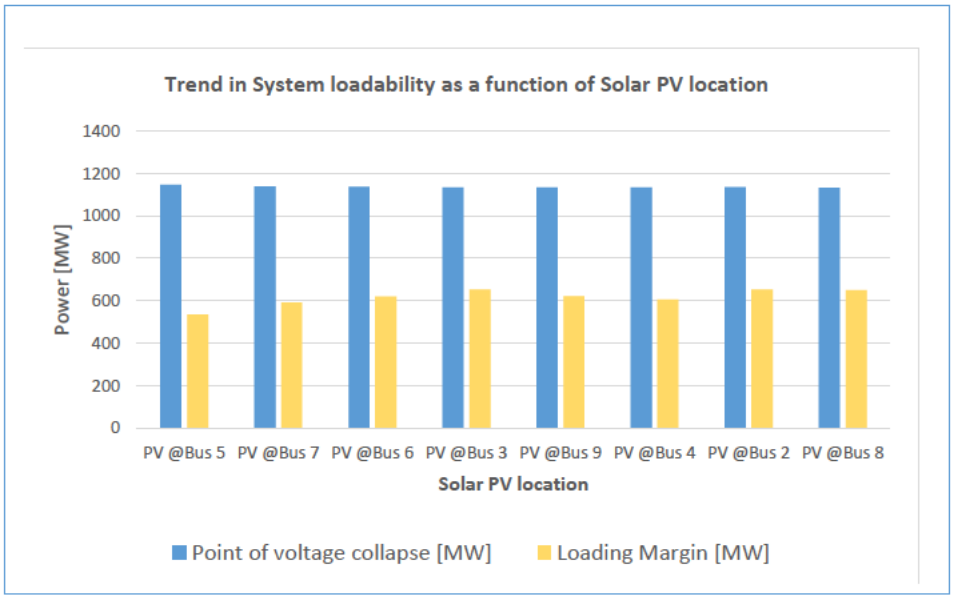

Figure 7-28 : Impact of Solar PV siting on system loadability

It is noticed that both the critical voltage point and the loading margin have not changed significantly with the change of the Solar integrated-grid PCC. From the displayed graphs in Figure 7-29, the critical voltage point and the loading margin are represented by almost straight horizontal lines, meaning with negligible gradient. The translation of this observation into the network actual technical behaviour is that Solar PV siting has no weighty impact on loadability. This confirms that except for insignificant differences in power losses, the total power balance

in the network is maintained regardless of the DG power injection point or location if the DG is the same nature and of the same capacity.

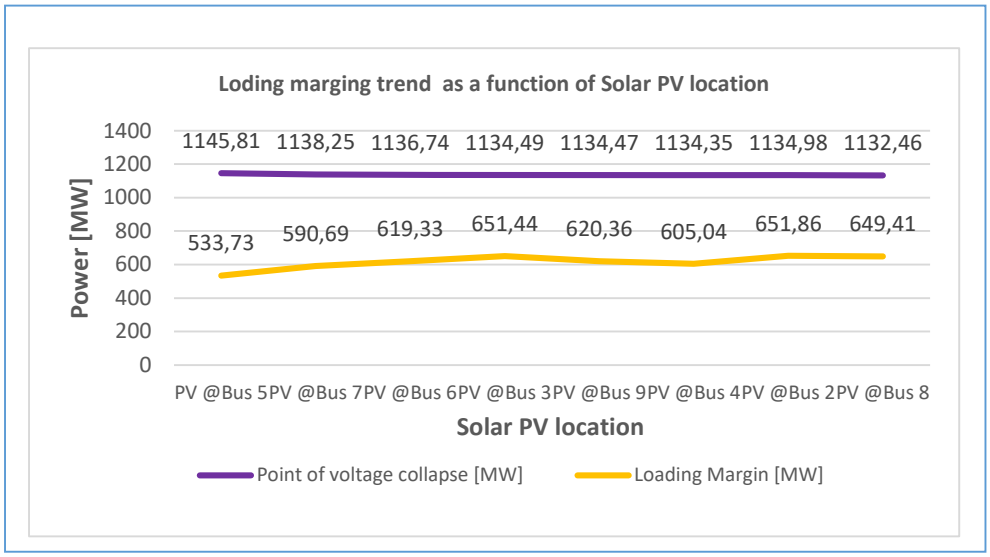

Figure 7-29: Illustration of the insignificant impact of the Solar PV siting in multi-machine network

7.4.1.3 Solar PV location impact during faults

The same system of 22 MVA capacity is integrated for the investigation of Solar PV siting on dynamic stability under fault conditions. From the initial position at Bus 5, the Solar PV system is successively placed at all the other PCCs except at reference Bus 1, while the fault location is kept unchanged at line 5 mid-distance. For a total simulation time of 12sec, a fault is applied at $t = 200ms$ for a duration of $100ms$ and then removed to monitor generators' rotor angle, speeds and terminal voltages. The system remains transiently stable when the Solar PV system is connected to buses 2, 4 and 8 and falls into instability when connected to buses 3, 5, 6, 7 and 9. Figures 7-30 and 7-31 illustrate the two behaviours representing the two cases. It can be seen that stability conditions depend on many parameters, including but not limited to the electrical distance between fault location and the Solar PV integration point.

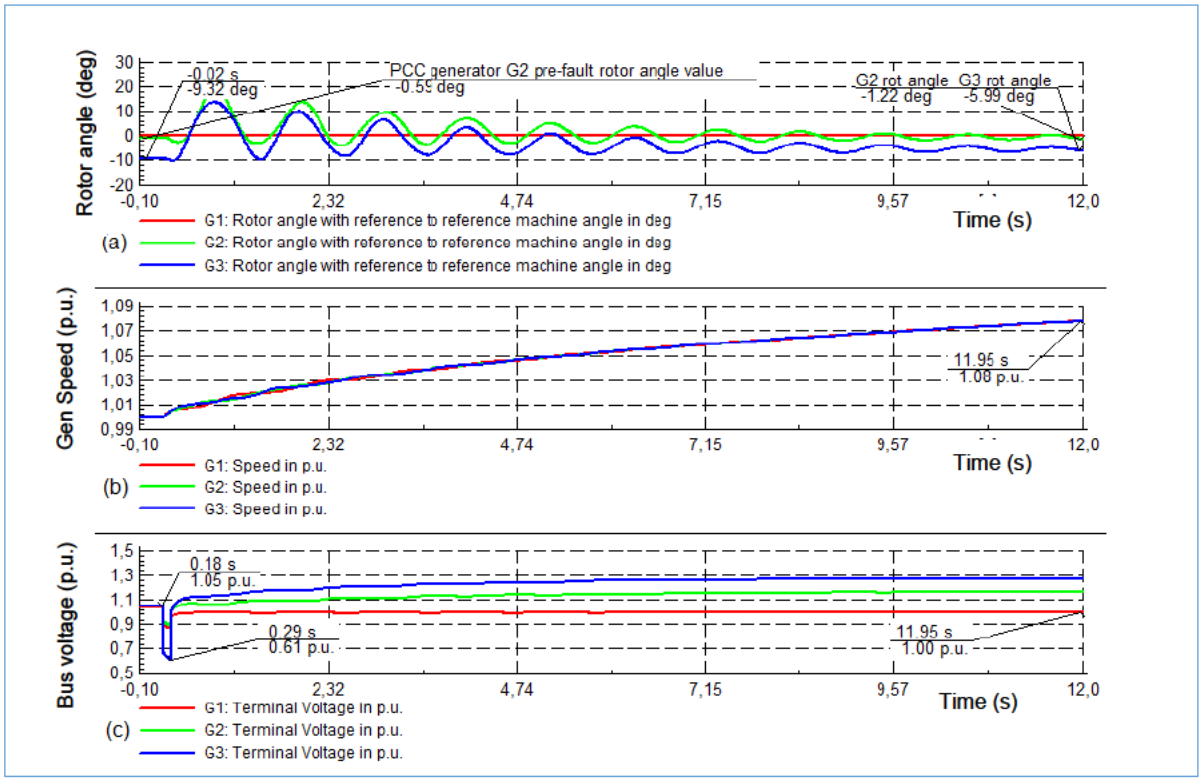

Figure 7-30: **Stable transient stability behaviour with the Solar PV at Bus 2. (a) Rotor angle of the generators (b) Generators' speeds and (c) Generators' terminal voltages**

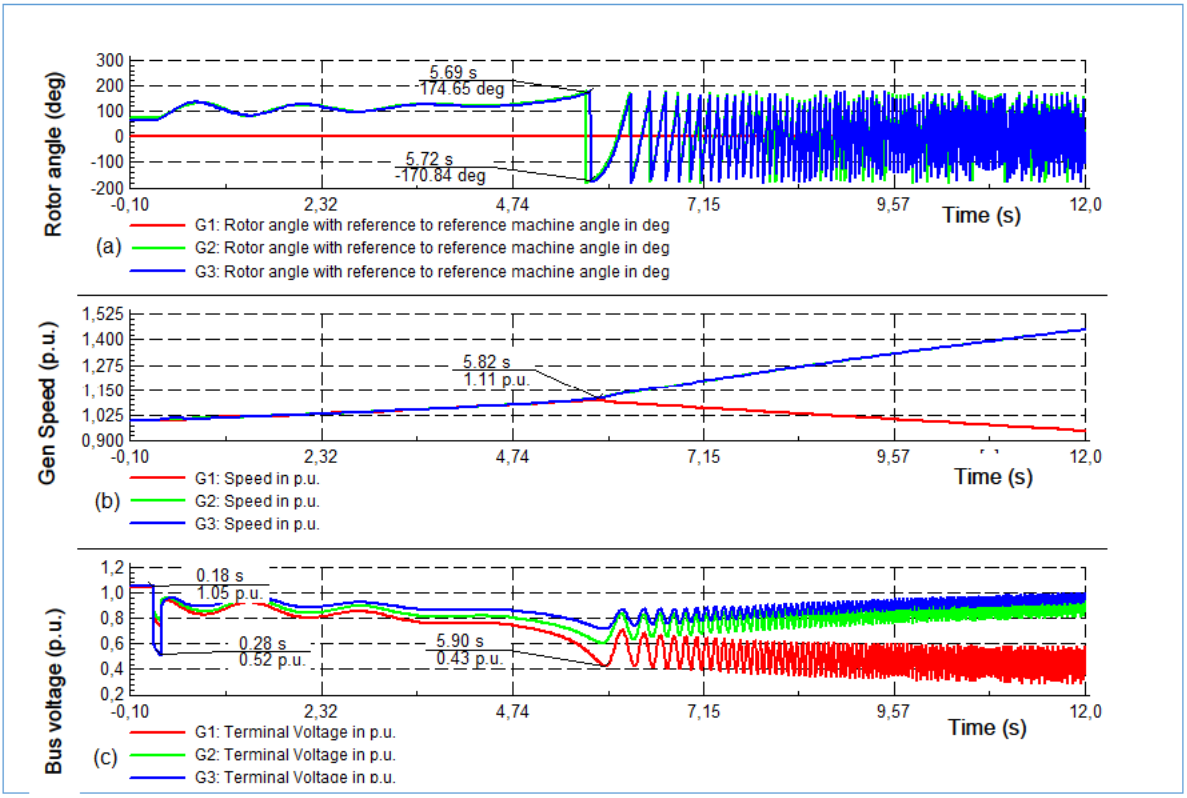

Figure 7-31: **Unstable transient stability behaviour with the Solar PV at Bus 6. (a) Rotor angle of the generators (b) Generators' speeds and (c) Generators' terminal voltages**

7.4.2 Optimal location of the Solar PV

Amongst a number of many heuristic optimization techniques, the generic algorithm (GA) is one of the best, accurate and most popular way of determining the optimal siting of Solar PV system, especially when dealing with large dimension systems. For networks with a minimal quantity of power systems elements like the one under study, the experimental or manual method is used. To experimentally determine the best location for this study, it was required to have a simultaneous focus into:

(1) The need to improve the voltage level and keeping it within standard margins,
(2) The need to improve the system loadability while maintaining minimum losses and
(3) The requirement of dynamic transient stability.

Considering the stability requirement as the sine qua non condition, the voltage level was used as a deciding criterion for the optimal location. For more than one location with the same voltage magnitude, the loading margin over the total power losses will determine the decision. In light of the above and from Table 7-2 results, it is ascertained that Bus 4 is the best compromise of 3 requirements listed above and can be nominated as the optimal PCC for integration of Solar systems with the best improved voltage magnitude 0,953 p.u. compared to buses 2 and 8. Bus 4 will be used in the next scenario for solar PV sizing impact investigation on stability.

Table 7-2: Summary of results for the optimal location of the Solar PV system on the sub-transmission network

PCC	Voltage at Bus 5	% Voltage improvement	Maximum loadability point [MW]	Point of voltage collapse [MW]	Loading Margin [MW]	Total MW losses	Total MVAr losses	Stability condition
PV @Bus 5	0,975	4,0%	612,08	1175,81	563,73	9,61	70,15	Unstable
PV @Bus 7	0,962	2,7%	547,56	1138,25	590,69	9,85	78,78	Unstable
PV @Bus 6	0,955	2,0%	517,41	1136,74	619,33	10,65	71,13	Unstable
PV @Bus 3	0,954	1,9%	483,05	1134,49	651,44	12,75	91,45	Unstable
PV @Bus 9	0,954	1,9%	514,11	1134,47	620,36	12,8	90,28	Unstable
PV @Bus 4	0,953	1,8%	529,31	1134,35	605,04	9,91	74,49	Stable
PV @Bus 2	0,952	1,7%	483,12	1134,98	651,86	12,93	96,64	Stable
PV @Bus 8	0,951	1,6%	483,05	1132,46	649,41	12,98	71,97	Stable

7.4.3 Scenario 2: Scattered Solar PV capacity at the best identified PCCs

From Table 7-2 above, Bus 2, Bus 4 and Bus 8 were identified to be the best PCC for the study network. The 20 MVA single unit Solar PV capacity used in scenario 1 is divided into 3 units

that are placed respectively at these buses. The results are consolidated in Table 7-3 and displayed in Figures 7-32, 7-33 and 7-34, 7-35 respectively for static and dynamic analysis.

Table 7-3: Comparison between the effects of concentrated single unit at a PCC and scattered capacity at various PCCs

PCC	Critical bus voltage magnitude in p.u.	% Voltage improvement from the initial case (worst case)	Maximum loadability point in MW	Point of voltage collapse in MW	Loading Margin in MW	% Improvement of Loading margin from initial case	% decrease in active power losses	Stability condition
20 MVA Single unit PV @Bus 4	0,953	1,8%	529,31	1134,35	605,04	68,19	9,05	Stable
20 MVA capacity scattered into 3,5 MVA @Buses 2, 4 and 8	0,979	4,4%	547,08	1159,81	612,73	70,33	11,54	Stable

7.4.3.1 Impact on voltage stability and system loadability

The comparison results of same capacity single concentrated and multiple scattered units show that the latter architecture presents better improvement benefits for the network steady state voltage than the first architecture, as shown in Figure 7-32.

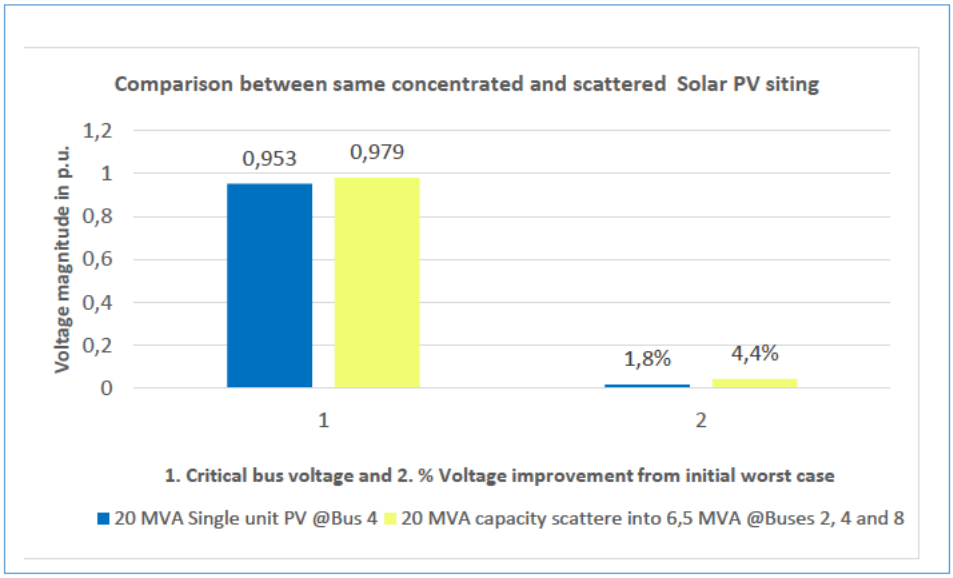

Figure 7-32: Scattered Solar PV siting architecture improved performance on static voltage stability over single concentrated units placement

The critical bus voltage has improved further from 0,953 p.u. when a single concentrated unit is placed at Bus 4 to 0,979 p.u. when the Solar PV capacity is scattered at few best candidate buses, representing 4,4 % improvement from the initial worst case voltage.

On the other hand, the point of voltage collapse has shifted to better improved loadability position moving from 1134,35 MW to 1159,81 MW which corresponds to 2,24 % when the Solar PV penetration is scattered in three smaller units compared to when a single unit was used at the best PCC (Bus 4) as presented in Table 7-3. As a result of the point of collapse shift, the megawatt distance to system collapse has also increased by 1,27 % from 605,04 MW to 612,73 MW.

7.4.3.2 Impact on transient dynamic stability

The results from Table 7-4 show indeed an improvement of the transient stability condition when the Solar PV capacity is scattered at selected locations compared to when a single Solar PV of fixed capacity is used. The improvement is evaluated through the comparison of the voltage dip through fault and the recovery time from voltage fluctuations resulting from the fault at respectively the best PCC which is Bus 4 and the critical Bus 5.

Table 7-4: Transient stability performance comparison between single Solar PV and scattered capaciity

Solar PV integration mode	Bus voltage dip during simulation		Bus voltages at the end of simulation @12 sec	
	Best PCC	Bus 5	Best PCC	Bus 5
Concentrated PV capacity @ best PCC	0,56	0,66	0,89	0,83
Scattered PV capacity @ buses 2, 4 and 8	0,58	0,67	0,91	0,89

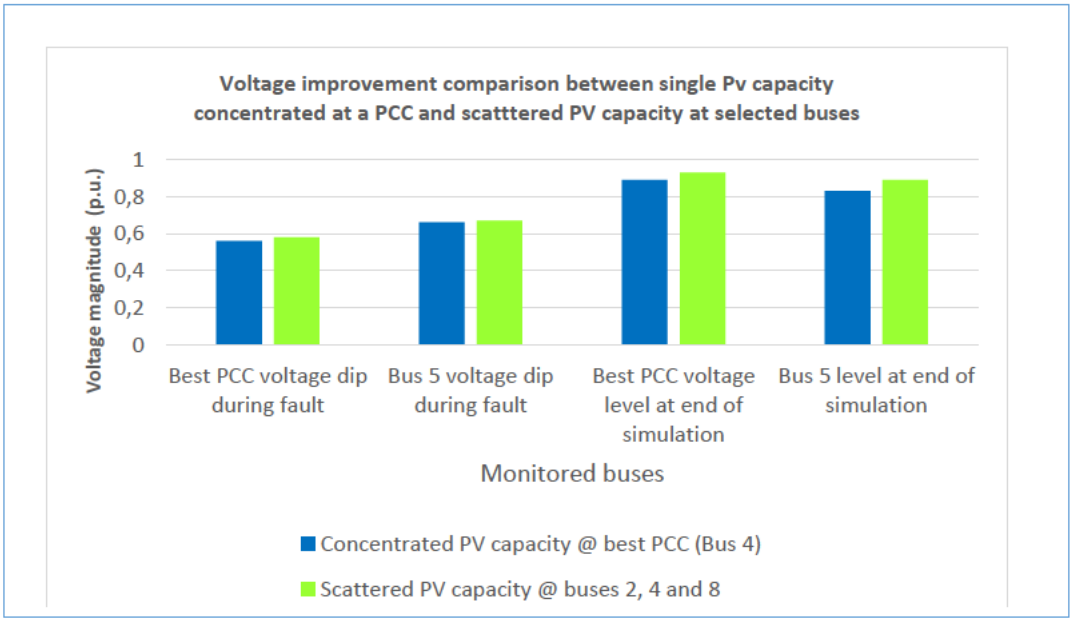

Figure 7-33: Improved dynamic stability conditions for multiple scattered Solar PV at selected buses

It can be evidenced as displayed in Figures 7-34 and 7-35, that both during fault and after the fault has been removed, the stability conditions are much more improved for both buses 4 and 5, when the solar PV capacity is scattered at buses 2, 4 and 8.

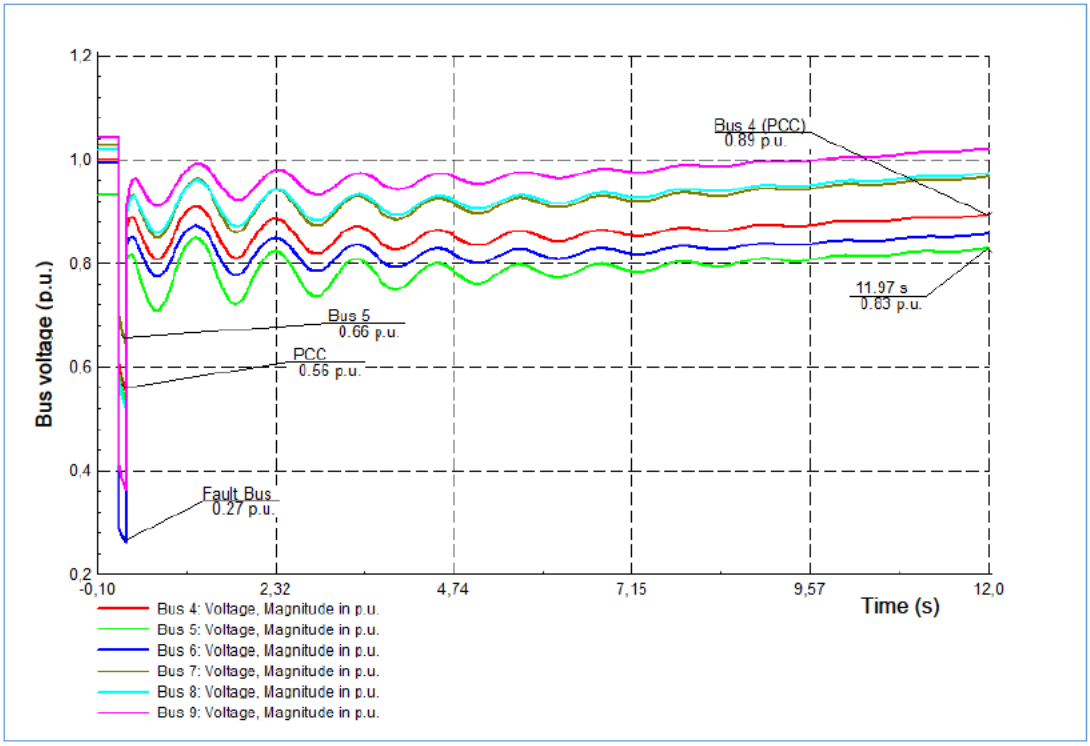

Figure 7-34: Voltage profiles at Bus 4 and Bus 5, during fault with a single Solar PV integrated at Bus 4 (Best PCC)

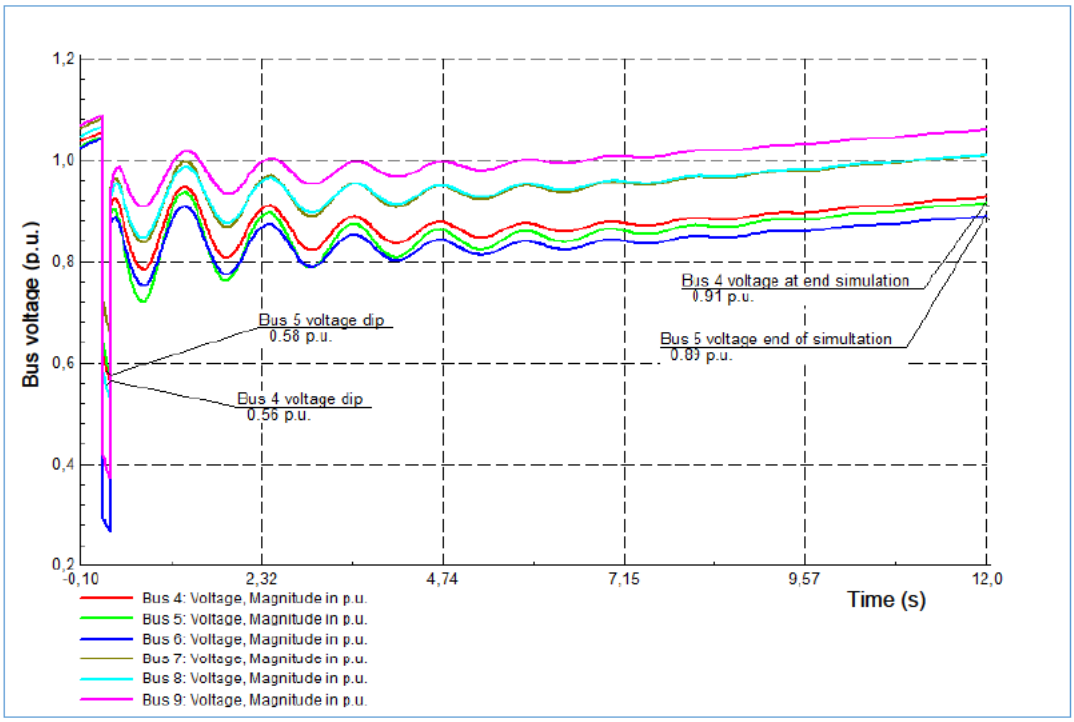

Figure 7-35: Voltage profiles at Bus 4 and Bus 5, during fault with scattered Solar PV units integrated at buses 2, 4 and 8

7.5 Case 5: Impact of Solar PV sizing

The impact of the Solar PV sizing investigation was achieved by varying the PV capacity at fixed location, Bus 4 that was identified in Case 4 as the best PCC. The case aimed to assess the impact of Solar PV capacity change on system stability through the monitoring of voltage magnitudes at the PCC and at the detected weakest bus, the point of voltage collapse, the losses and the stability condition during fault application via the rotor angle and the assessment of all buses voltage profiles behaviours. The summarized results for this scenario are consolidated in Table 7-4, and are analysed below.

Table 7-5: Summarized results for the investigation on the impact of DG sizing

% PV penetration	Voltage magnitude at PCC	V magnitude @ critical Bus 5	Voltage margin requirement	Point of voltage collapse in MW	Loading margin in MW	Total P losses	Total Q losses	Stability condition
0%	0,996	0,963	Critical bus Voltage magnitude ≥ 0,95 p,u,	1138,51	590,95	11,27	-59,31	Stable
10%	0,995	0,96		1137,62	590,06	11,28	-59,02	Stable
20%	0,994	0,958		1136,74	589,18	11,29	-58,67	Stable
30%	0,993	0,95		1136,64	589,08	11,31	-58,01	Stable
40%	0,992	0,942	Critical bus Voltage magnitude <0,95 p.u.	1135,55	587,99	11,33	-57,81	Stable
50%	0,99	0,939		1134,35	586,79	11,35	-57,3	Stable
100%	0,978	0,927		1129,44	581,88	11,59	31,27	Unstable
110%	0,97	0,925		1127,69	580,13	12,91	33,22	Unstable
140%	0,967	0,92		1125,42	577,86	12,91	38,95	No power flow convergence

7.5.1 Impact of Solar PV capacity in the absence of fault

The voltage profiles at both PCC bus and Bus 5 deteriorate with solar PV capacity increasing. From zero % PV penetration to 30 % PV grid-penetration, a corresponding bus voltage magnitude reduction of 0,963 p.u. to 0,950 p.u. or 1,35 % was recorded. Above 30 % PV penetration, the voltage at the critical bus falls below the standard required margin of 0,951 p.u. A further increase of the PV capacity results in the further deterioration of the voltage profile, despite the evidence that the system settles to a new equilibrium point for up to 90 % Solar PV penetration before falling into instability up to 140 % increase value from which the *DigSILENT*™ load flow does not converge at all. Figure 7-36 shows how the voltage profiles at Bus 4 and Bus 5 respectively change as a function of % PV penetration variation.

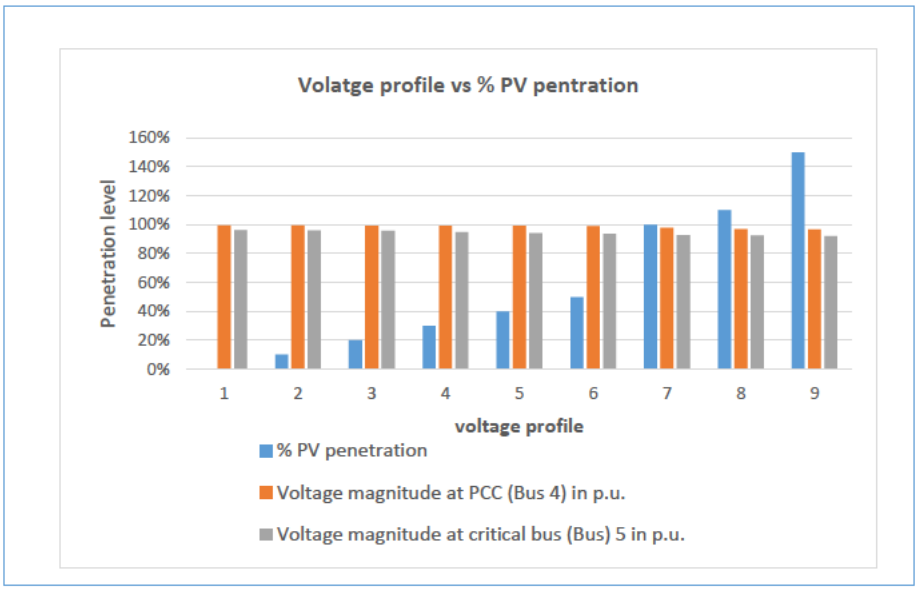

Figure 7-36: Voltage magnitude trend as impacted by increased Solar PV capacity on the sub transmission network

7.5.2 Impact of Solar PV capacity on system loadability

The results of the effect of the increased Solar PV penetration on system loadability are summarised in Table 7-5 and displayed in Figure 7-37. It is seen that both voltage collapse point and electrical power distance margin to system collapse are decreasing as the penetration level increases. For up to 150 % increase, the loading margin records a 2,21 % decrease.

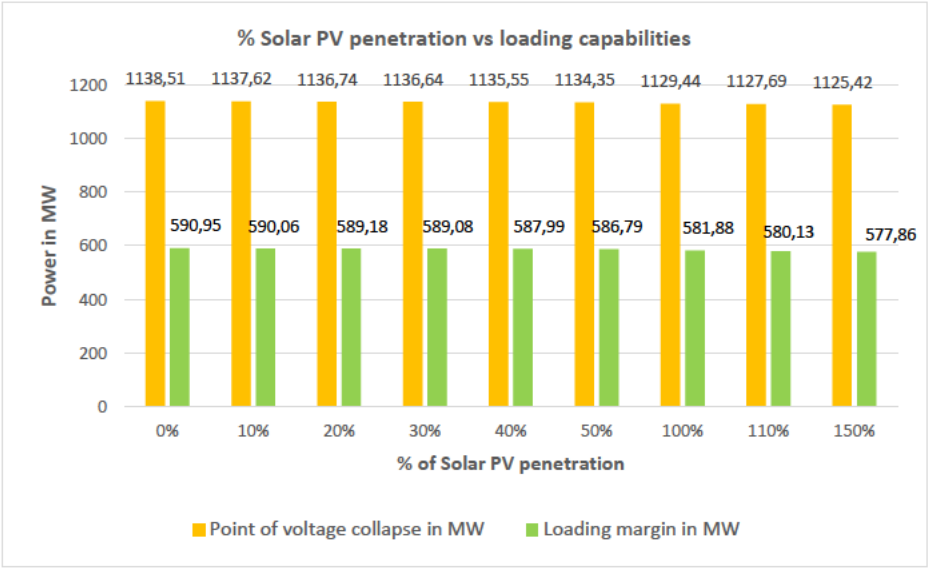

Figure 7-37: Effect of increased Solar PV penetration on the IEEE-9 Bus system loadability

7.5.3 Impact of Solar PV capacity under fault conditions

The last columns of Table 7-3 contain the stability condition outputs for different Solar PV penetration after a fault is applied and then removed. It is noticed that as the % PV penetration increases from zero to just below 100 %, the power system maintains its relative stability by moving toward a new operating point and loses stability from 100 % penetration. Figures 7-38 illustrates and describes one of the stable condition behaviour, the 30 % penetration scenario showing respectively the rotor angle, generators' speeds and generators' terminal voltages.

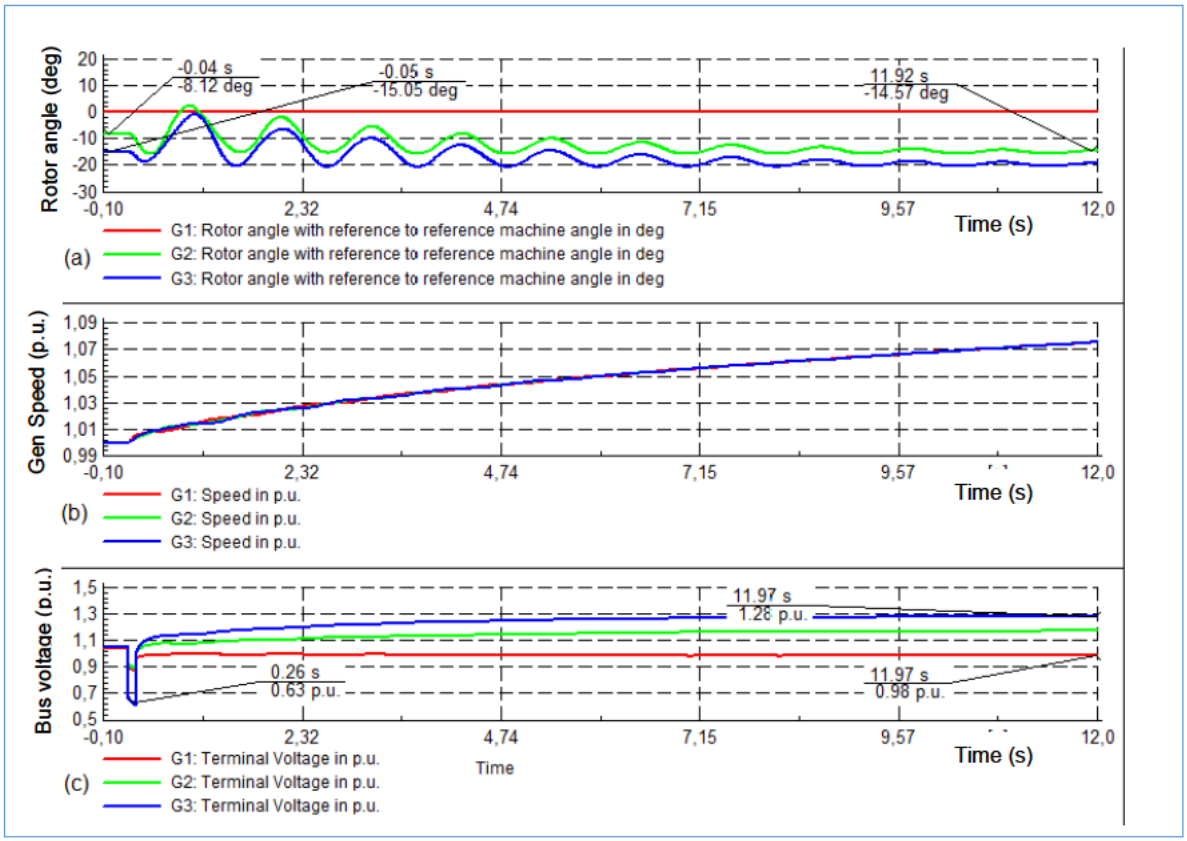

Figure 7-38: Transient stability behaviour of the network with 30 % Solar PV penetration at Bus 4. (a) Generators' rotor angles, (b) Generators' speeds and (c) Generators' terminal voltages

Figures 7-39, 7-40 and 7-41 show 3 of the unstable cases namely the 95 %, 100 % and 110 % Solar PV penetration and notice shall be given to the fact that the greater the penetration level, the smaller the starting time of intense fluctuations of rotor angles and generators' terminal voltages after the fault has been removed. With 95 % PV penetration, the system takes 10,69 seconds for the rotor angle to start fluctuating while it takes shorter times of 8,42 seconds and 7,27 seconds for 100 % and 110 % PV penetration respectively. This is the evidence that the Solar PV seconds attempts to reasonably maintain stability conditions by injecting any available MVARs to support the grid and if no external Q support is supplied, the system plunges into stability.

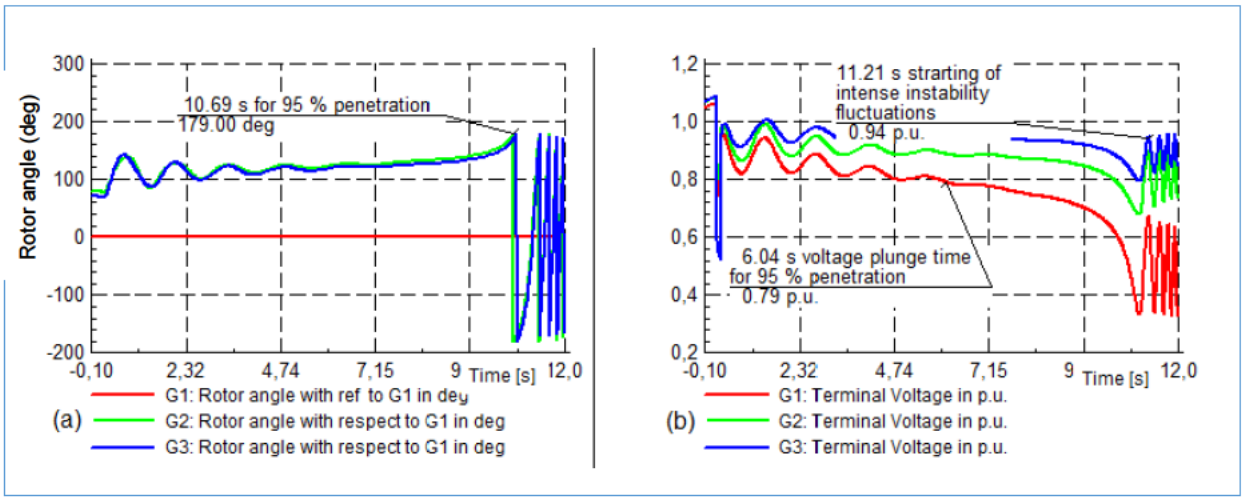

Figure 7-39: Unstable conditions illustrating 95 % PV penetration. (a) Rotor angle with respect to slack generator. (b) Generators' terminal voltages

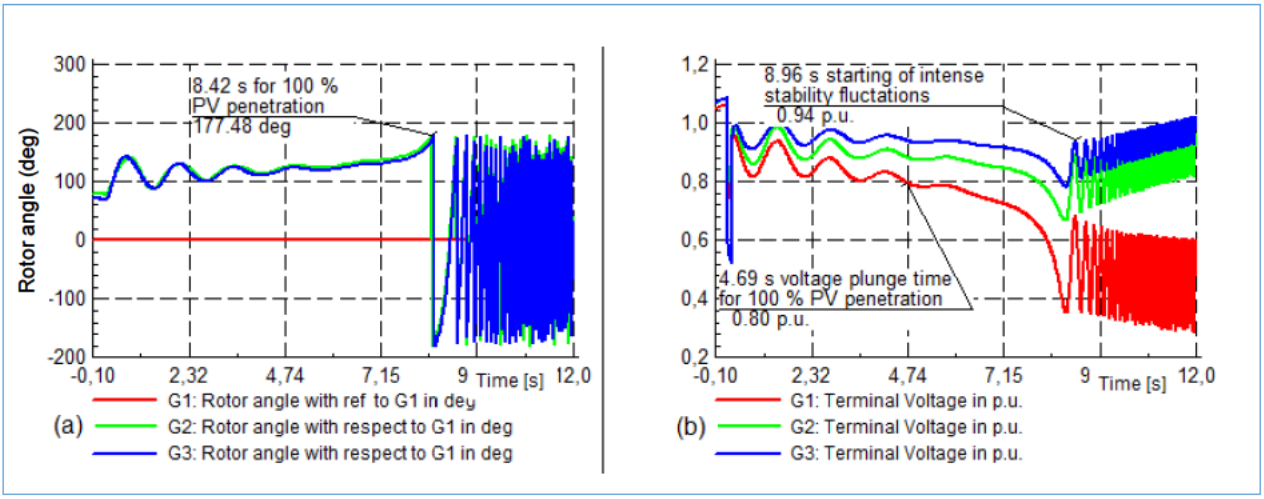

Figure 7-40: Unstable stability conditions illustrating 100 % PV penetration. (a) Rotor angles with respect to slack generator. (b) Generators' terminal voltages.

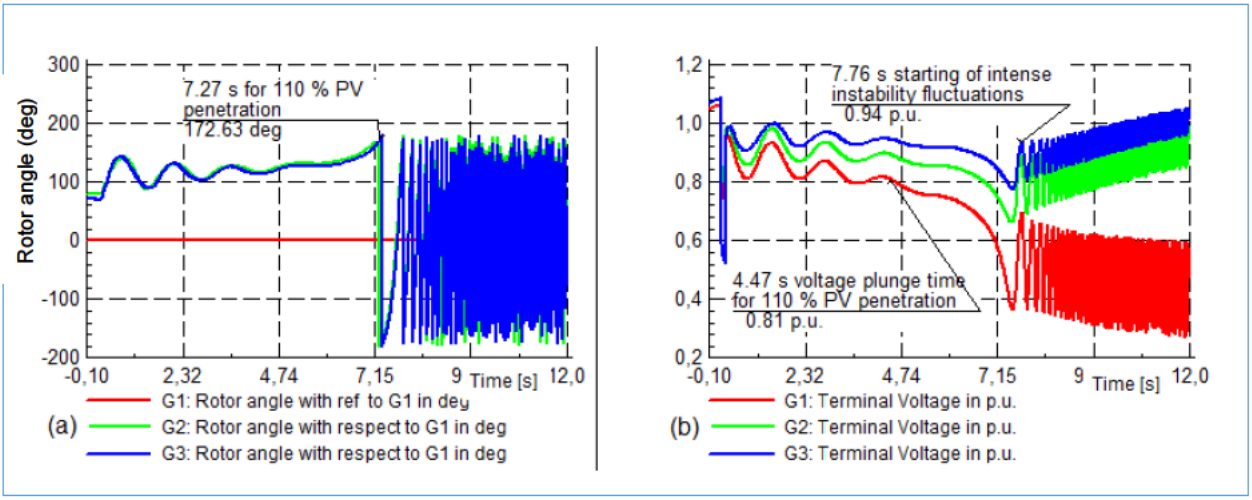

Figure 7-41: Unstable stability condition for 110 % PV penetration. (a) Rotor angles with respect to slack generator. (b) Generators' terminal voltages

It is therefore evident also that the power systems operator's (PSO) knowledge of the information about this fluctuation delay time enable them to anticipate earlier action in order to handling grid-penetration level and to predict the subsequent planning and provision of the MVARs injection that could enable a substantially higher Solar PV penetration. The use of smart and intelligent, coordination and control devices and systems is of great assistance in this regards.

7.6 Case 7: Integration of BESS

7.6.1 Losses with no battery incorporation.

In this current case, Scenario 2 of case 1 is considered as the base case. The Solar PV system is integrated at the critical Bus 5 with the aim is to investigate to what extent voltage compensation and support can be achieved by injecting P at load ends. The Solar PV system is set to bring about the total power demand due to load increase and the load characteristic is modified to include time variant load for Quasi-simulation study. Quasi-simulation is then performed to determine the total losses on the system for 24 hours and the results from Figure 7-42 show that losses are reduced from 49,9 MW in Scenario 2 to a maximum of 40,5 MW at 07:00 and a minimum loss of 32 MW at 15:00. The maximum losses in this case are however closer to Scenario 1 losses 1 with a higher gradient.

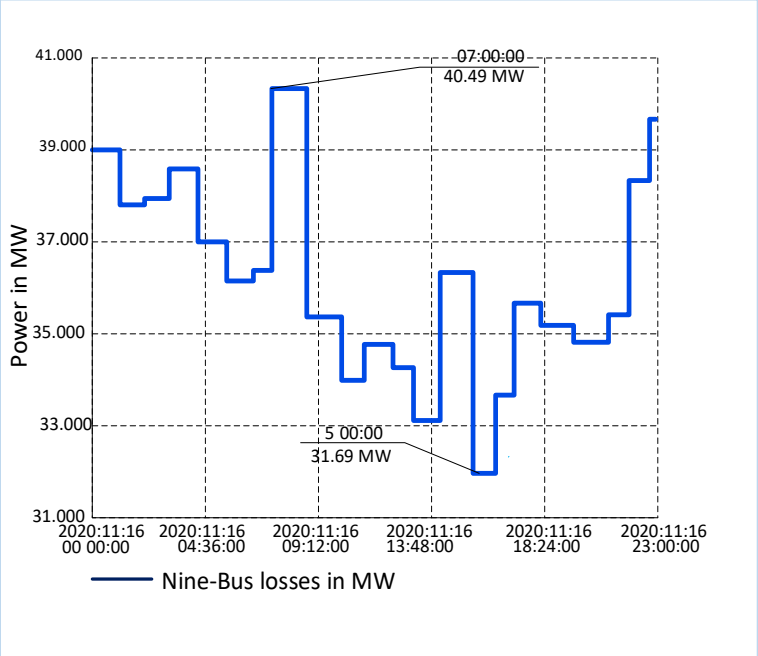

Figure 7-42: Twenty-four hour Quasi-Simulation results for the test network PV penetrated system

7.6.2 Quasi-simulation with BESS integration

The results of this case are depicted in Figure 7-43, it is evidenced that total system losses are minimal with the incorporation of BESS, as compared to all the previous cases reaching a high of 40 MW and a minimum of 38,9 MW with a very small gradient.

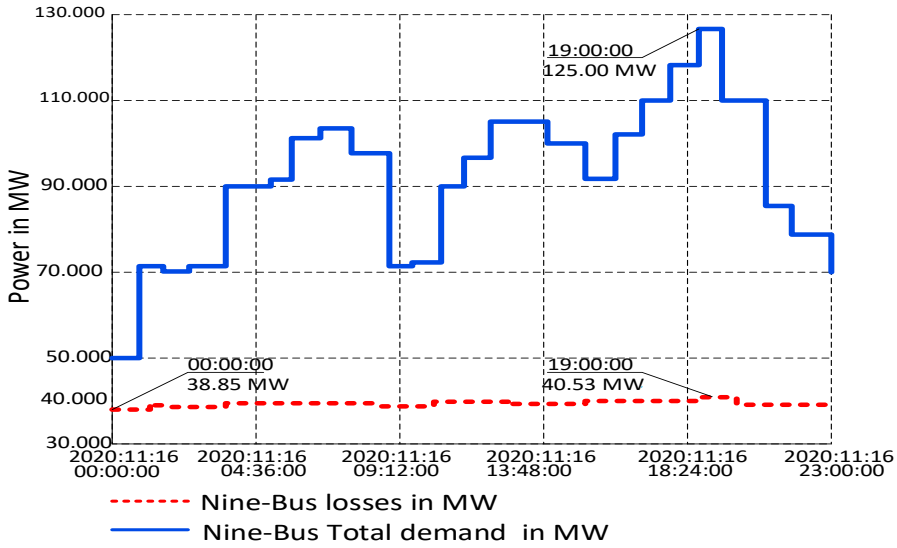

Figure 7-43: Twenty-four -hour Quasi-simulation results for the test network with PV and BESS incorporated

The simulation results evidenced the benefits of the use of BESS to reduce the total system losses indirectly improving system loadability by smoothing the system power output. The results demonstrate that the combined effect of the Solar PV-BESS system has substantial impact in reducing total power losses. This confirms the BESS's ability to act as generator, or load, respectively during high load demand/lower PV generation and lower demand//higher Solar PV generation to contribute to the voltage regulation and power system stability, offsetting effectively the intermittency of Solar PV energy sources and subsequently enabling greater RE penetration.

7.7 Summary

In this chapter, the results of the research work, based on 6 cases and which conclusions are consolidated in the next chapter were presented.

CHAPTER 8: CONCLUSION AND RECOMMENDATIONS

8.1 Conclusion

The studies conducted reveal that there are positive and negative impacts of the integration of RE inertia-less sources into a grid on voltage stability and indirectly on the system loadability and system power losses.

Firstly, the impacts on stability and system loading margins depend on the network loading status, the placement of the DG sources, the level of the DG penetration and the network fault conditions. The comparison results obtained from the integration of the Solar PV and FACTS devices under various scenarios reveal that their respective impacts and abilities to improve voltage stability differ. The results indicate that voltage stability can successfully be achieved using several approaches, including under specific conditions, the integration of Solar PV. Four different kinds of investigations on voltage and system stability were conducted throughout the study, namely the steady state analysis, the dynamic transient analysis, the loading margin and loadability and, the incorporation of BESS. The results confirm that under any operating conditions, reactive power control remains the most effective method to control voltage stability and loading capability, especially where an increasing penetration of renewable and inertia-less generating sources is planned. It was found, however, that although with no considerable reactive power generation capacity compared to the other RES, the integration of Solar PV sources at PCC show a positive impact on the network voltage profile under specifically defined conditions. This is vindicated by the fact that by manipulating reactive power exchange with the network, converter-based technologies when equipped with adequate control strategies can support the system voltage. In addition, the integration of the Solar PV near the point of power consumption contributes substantially to a decrease in transmission line currents and subsequently in transmission line voltage drops, thus impacting positively on the voltage regulation to achieve voltage profile improvement.

The results of the investigation on the dynamic stability impact of PV generation revealed that the severity of the transient stability due to the increasing penetration of Solar PV depends on the criticality of the point at which the fault occurs and the fault proximity. The penetration indeed lowers the system strength to create weak areas. Using a disturbance of the same nature and of equal severity at the same location, the Solar PV integrated system presented precarious stability conditions compared to the grid with no Solar PV or with FACTS incorporated. It was

recorded that the instability was further exacerbated by the level of penetration. This is corroborating the fact that the penetration of converter-base sources contributes to lower the short-circuit current by increasing the impedance seen from the fault point, hence posing serious voltage instability risk. The instability was observed through severe non-damped oscillations of the rotor angles, the generator terminal voltages and the transmission and load buses voltages. Using the same nature of the fault but at different locations, it was found that transient stability is worsening as the fault moves closer to the location of Solar PV system.

Improving power transfer capability is to improve transient stability. Better voltage profile and improved transient stability were achieved when the network is supported with reactive power control devices. It was evidenced that rotor angle oscillations and voltage fluctuations are moderated when the SVS is concomitantly used with the Solar PV systems. The placement of the SVS at load buses, together with the distribution of Solar PV capacity at different load buses, was the optimal combination scenario providing both the best voltage profile and the best system dynamic stability. This combination also presented the best loadability with an improvement of the operating point and the larger loading margin.

Secondly, with the incorporation of BESS, the results demonstrated that the combined effect of the Solar PV-BESS system has substantial impact on system stability as well as on the total power losses. This confirms the BESS's ability to act as generator, or load, respectively during high load demand/lower PV generation and lower demand//higher Solar PV generation to contribute to the voltage regulation and power system stability, offsetting effectively the intermittency of Solar PV energy sources and subsequently enabling greater RE penetration.

8.2 Recommendations and future work

The following recommendations pertaining to voltage control and stability analysis are made:

- DG integration will require proper planning and operation. The design should consider an accurate modelling of, amongst others, the type of grid and its strength level, the nature and profile of the load for DG optimum location and penetration level.
- To improve transient stability and provide an adequate voltage support, reactive power control philosophy and architecture should be appropriately included at selected PCC in accordance with the grid codes requirement. Attention should be given to the early detection and identification of the disturbance, the protection system and application of mitigation measures.

- Smart intelligent control systems integration associated with the protection system should be planned to essentially evaluate the operating state of the power system, fast clear eventual faults and re-adjust parameters to reasonably maintain stability.
- Future work should extend the research to other RE technologies in order to widen the understanding of voltage stability analysis in the presence of these technologies and eventually include financial constraints and benefits for each case

REFERENCE LIST

[1] G. Pepermans, J. Driesen, D. Haeseldonckx, R. Belmans, and W. D'haeseleer, "Distributed Generation: Definition, Benefits and Issues," *Energy Policy,*, vol. 33, no. 6, pp. 787-798, 2005.

[2] L. T. Berger and K. Iniewski, *Smart Grid: Applications, Communications, and Security*. New Jersey: John Wiley & Sons. , 2012.

[3] T. Xu and P. C. Taylor, "Voltage Control Techniques for Electrical Distribution Networks Including Distributed Generation," in *17th World Congress. The International Federation of Automatic Control (IFAC'08)*, Seoul, Korea, 6-11 July 2008, vol. 41, no. 2, pp. 11967-11971.

[4] M. M. Begovic, *Electrical Transmission Systems and Smart Grids: Introduction*. New York: Springer, 2012.

[5] S. Kotamarty, S. Khushalani, and N. Schulz, "Impact of Distributed Generation on Distribution Contengency Analysis," *Electric Power System Research (EPRI)*, vol. 78, pp. 1537-1545, 2008.

[6] P. Kundur, *Power System Stability and Control*. New York: McGraw-Hill, Inc., 1994.

[7] United States Department of Energy, "Final Report on the August 14, 2003 Blackout in the United States and Canada," Canada Power System Outage Task Force, 2004.

[8] REN21. "Renewable 2019 Global Status Report." https://www.ren21.net/gsr-2019/ (accessed 19/03/2020).

[9] F. S.-U. Centre/BNEF. "Global Trends in Renewable Energy Investment 2018." http://www.fs-unep-centre.org (accessed 24/06/2019).

[10] S. Henbest and M. Kimmel, "New Energy Outlook (NEO 2019) report," Bloomberg New Energy Finance (Bloomberg NEF), 2019. Accessed: 25/06/2019. [Online]. Available: https://about.bnef.com/new-energy-outlook/

[11] A. K. Kumar, M. P. Selvan, and K. Rajapandiyan, "Dynamic Grid Support Systsem for Mitigation of Impact of High Penetration Solar PV into Grid," presented at the 2017th International Conference on Power Systems (ICPS), College of Engineering Pune, India., Dec, 2017.

[12] J. Von Appen, M. Braun, T. Stetz, K. Diwold, and D. Geibel, "Time in the Sun: The Challenge of High PV Penetration in the German Electric Grid," *IEEE Power and Energy Magazine*, vol. 11, no. 2, pp. 55-64, March-April 2013.

[13] S. Banerjee, A. Mesram, and N. Kumar Swamy, "Integration of Renewable Energy Sources in Smart Grid," *International Journal of Science and Research (IJSR) Delivery*, vol. 4, no. 3, March 2015.

[14] A. G. Endegnanew, "Stability of High Voltage Hybrid AC/DC Power Systems," Ph. D Thesis, Department of Power Systems Laboratory, Swiss Federal Institute of Technology (ETH), Zurich, 2013.

[15] K. Loji, I. E. Davidson, and R. Tiako, "Voltage Profile and Power Losses Analysis on a Modified IEEE 9-Bus System with PV Penetration at the Distribution Ends," presented at the Southern African Universities Power Engineering Conference/Robotics and Mechatronics/Pattern Recognition Association of South Africa (SAUPEC/RobMech/PRASA) Bloemfontein, South Africa, January 2019.

[16] R. Marjunder, "Modelling Stability Analysis and Control of Micro-Grid," Ph.D Thesis, School of Engineering Systems, Queensland University of Technology, Queensland, 2010.

[17] J. Morel, S. Obara, and Y. Morizane, "Stability Enhancement of Power System Containing High-Penetration Intermittent Renewable Generation," *Journal of Sustainable Development of Energy, Water and Environment Systems,* vol. 3, no. 2, pp. 151-162, 2015.

[18] G. Puntsagdash, "Stability Analysis with Decentralised Control of Photovoltaic Systems," Master's Thesis, Departmenet of Electric Power Engineering, Novwegian University of Science and Technology (NTNU), Trondheim, 2017.

[19] L. Freris and D. G. Infield, *Renewable Energy in Power Systems*. New Jersey: John Wley & Sons Ltd, 2008.

[20] P. P. Barker and R. W. De Mello, "Determining the im[pact of Distributed Generation on Power Systems. Part-1. Radial Distribution Systems," in *Proceedings of IEEE PES Summer Meeting*, Seatle, USA, July 16-20, 2000, vol. 3, pp. 1645-1656.

[21] CIGRE WG 37-23, "Impact of Increasing Contribution of Dispersed Generation on Power System," Final Report. Electra, 1998.

[22] L. H. Willis and W. G. Scott, *Distributed Power Generation: Planning and Evaluation*. New York: Marcel Dekker, Inc., 2000.

[23] X. Chen, "Size Optimization of Utility-Scale Solar PV System Considering Reliability Evaluation," Master's Thesis, Department of Electrical Power Engineering, Virginia Polytechnic Institute and State University, Virginia, 2016.

[24] X. Xu, Z. Yan, M. Shahidehpour, H. Wang, and S. Chen, "Power Ssytem Voltage Stability Evaluation Considering Renewable Energy with Correlated Variability," *IEEE Transactions on Power Systems,* vol. 33, no. 3, pp. 3236-3245, 2018.

[25] G. Sharma and K. Loji, "Critical Aspects of AGC Emerging from Optimal Control to Machine Learning Techniques," *Indonesian Journal of Electrical Engineering and Informatics (IJEEI),* vol. 7, no. 1, pp. 101-114, March 2019.

[26] G. Sharma, K. Loji, and M. Kabeya, "Application of Diverse FACTS in AGC of Mulkti-area Interconnected Energy Systems," *Indonesian Journal of Electrical Engineering and Informatics (IJEEI),* vol. 7, no. 1, pp. 101-115, March 2019.

[27] I. Dobson *et al.* "Electric Power Transfer Capability: Concepts, Applications, Sensitivity and Uncertainty." Power System Engineering Center (PSERC). https://www.pserc.cornell.edu/tcc/tutorial/TCC_Tutorial.pdf (accessed 06/08/2019).

[28] J. Machowski, J. W. Bialek, and J. R. Bumby, *Power System Dynamics: Stability and Control*, 2nd ed. New Delhi: John Wiley & Sons, Ltd, 2008.

[29] R. Billinton and R. N. Allan, *Reliability Assessement of Large Electric Systems*. Boston: Kluwer Academic Publishers, 1988.

[30] A. S. Debs, *Modern Power Ssytems Control and Operation*. Massachusetts: Kluwer Academic Publishers, 1988.

[31] N. G. Hingorani and L. Gyugyi, *Understanding FACTS: Concepts and Technology of Flexible AC Transmission Systsems*. New York: IEEE Press, 2000.

[32] K. R. Padiyar, *Power System Dynamics*. Jin Xing Distripark: John Wiley & Sons (Asia) Pte Ltd, 1996.

[33] N. M. Tabatabaei, A. J. Aghbolaghi, N. Bizon, and F. Blaabjerg, *Reactive Power Control in AC Power Systems: Fundemental and Current issues*. Cham: Springer, 2017.

[34] R. Mihalic, P. Zunko, and D. Povh, "Transient Stability Control," in *Flexible AC Transmission Systems*, Y. H. Song and T. A. Johns Eds. London: Institution of Engineering and Technology, 2008, ch. 11, pp. 443-505.

[35] P. M. Anderson and A. A. Fouad, *Power System Control and Stability*, 2nd ed. Piscataway: IEEE press, Inc., 2003.

[36] L. L. Grigsby, *The Electric Power Engineering Handbook*. Florida: IEEE Press, 1998.

[37] H. Alkhatib, "Etude de la Stabilité aux Perturbations dans les Grands Réseaux Electriques: Optimisation de la Régulation par une Méthode Métaheuristique. ," PhD Génies Electriques, Génies Electriques, Université Paul Cézanne d'Aix-Marseille III, Marseille, France, 2008.

[38] P. Kundur *et al.*, "Definition and Classiffication of Power System Stability-IEEE/CIGRE Joint Task Force on Stability Terms and Definitions," *IEEE trans. Power Syst.,* vol. 19, pp. 1387-1401, 2004.

[39] L. L. Grigsby, *Power System Stability and Control*. Boca Raton: CRC Press, 2007.

[40] T. Madhuranthaka and T. G. Manohar, "A Review on Power System Voltage Stability and Optimization Techniques," *International Journal of Engineering Research ans Application (IJERA)* vol. 6, no. 11, pp. 06-14, November 2016.

[41] M. Farhoodnea, H. Zayandehroodi, M. Eslami, R. Sirjani, M. Mohammadjafari, and A. Forozia, "Power System Voltage Stability and Control-A Review," *Research Journal Applied Sciences Engineering and Technology,* vol. 4, no. 9, 2012.

[42] H. Kwatny, A. Pasrija, and L. Bahar, " Static Bifurcations in Electric Power Networks: Loss of Steady-state Stability and Voltage Collapse " *IEEE Transaction Circ. System,* vol. 33, no. 10, pp. 981-991, 1986.

[43] V. Venikov, V. Stroev, V. Idelchic, and V. Tarasov, "Estimation of Electrical Power System Steady-state Stability in Load Flow Calculations," *IEEE Transaction Power Apparatus System* vol. 94, no. 3, pp. 1034-1041, 1975.

[44] S. B. Crary, *Power System Stability* (General Electric Series). New-York: Chapman and Hall, 1945.

[45] J. B. Gupta, *A Course in Power Systems: Generation and Economic Considerations, Transmission and Distribution, Switchgear and Protection*, 11th ed. New Delhi: S. K. Kataria & Sons, 2014.

[46] S. C. Savulescu, *Real-Time Stability in Power Systems: Techniques for Early Detection of the Risk of Blackout*. New York: Energy Consulting International, Inc. , 2005.

[47] R. H. Miller and J. H. Malinowski, *Power System Operation*, 3rd ed. New York: McGraw-Hill, 1994.

[48] T. Rahman, S. Sankaran, N. Seeley, and K. Garg, "Capturing Generator Rotor Angle and Field Quantities-SDG & E Experience and Approach to Using Nontraditional Generator

Measurements," presented at the 42th Annual Western Protective Relay Conference, Spokane, Washington, 20-22 October, 2015.

[49] C. D. Vournas, P. W. Sauer, and M. A. Pai, "Relashionships between Voltage and Angle Stability of Power Systems," *International Journal of Electric Power & Energy Systems,* vol. 18, no. 8, pp. 493-500, 1996.

[50] R. Al-Abri, "Voltage Stabilyty Analysis with High Distributed Generation (DG) Penetration," Ph.D. Thesis, School of Electrical and Computer Engineering, University of Waterloo, Ontario, 2012.

[51] B. S. Abdulraheem and C. K. Gan, " Power System Frequency Stability and Control: Survey " *International Journal of Applied Engineering Research,* vol. 11, no. 8, pp. 5688-5692, 2016.

[52] U. Knight, *Power System in Emergencies: From Contingencies Planning to Crisis Management*. London, UK: John Wiley & Sons Ltd, 2001.

[53] M. Kothari, *Power System Dynamics*. IIT Delhi: Department of Electrical Engineering, , 2010.

[54] Z. Adibah, Kamaruzzaman, and A. Mohamed, "Dynamic Voltage Stability of a Distribution System with High Penetration of Grid-Connected Photovoltaic Type Solar Generator," *Journal of Electrical Systems,* vol. 12, no. 2, pp. 239-248, May 2016.

[55] A. Ameur, K. Loudiyi, and M. Aggour, "Steadt State and Dynamic Analysis of Renewable Energy Integration into the Grid using PSS/E Software," presented at the 4th International Conference on Power and Energy Systems Engineering, CPESE 2017, Berlin, Germany, 25-29 September, 2017.

[56] M. Reza, P. H. Schavemaker, J. G. Slootweg, W. L. Kling, and S. L. Van Der Sluis, "Impacts of Distributed Generation Penetration Levels on Power Systems Stability," in *IEEE PES General Meeting,* 2004, vol. 2, pp. 2150-2155.

[57] J. G. Slootweg and W. L. Kling, "Impacts of Distributed Generation on Power System Transient Stability," in *IEEE PES General Meeting,* 2002, vol. 2, pp. 862-867.

[58] Z. A. Obaid, L. S. Cipcigan, L. Abarahim, and M. T. Muhssin, "Frequency Control of Future Power Systems: Reviewing and Evaluating Challenges and New Control Methods.," *Journal of Mod. Power Syst. Clean Energy* vol. 7, no. 1, pp. 9-25, 2019.

[59] P. Daly, N. Cunniffe, and D. Flynn, "Imertia Considerations within Unit Commitment and Economic Dispatch for Systems with Non-Sysnchronous Penetration," presented at the 2015 IEEE Eindhoven Power Tech, Eindhoven, The Netherlands, 2015.

[60] P. Daly, L. Ruttledge, M. Power, and D. Flynn, "Wind Power Emulated Inertial Respone: Ancillary Service Design & System Scheduling Considerations," presented at the CIGRE Session 46, Paris, France, 2016.

[61] B. Porretta and S. Porretta, "Calculation of power systems inertia and frequency response," presented at the 2018 IEEE Texas Power and Energy Conference (TPEC), Texas, USA, 8-9 February, 2018.

[62] M. Rezkalla and M. Marinelli, "Augmenting System Inertia Through Fast Acting Reserve – A Power System Case Study with High Penetration of Wind Power," presented at the 2019 54th International Universities Power Engineering Conference (UPEC), Bucharest, Romania, 3re-6thSeptember, 2019.

[63] M. Rezkalla, M. Marinelli, M. Pertl, and K. Heussen, "Trade-off Analysis of Virtual Inertia and Fast Primary Control during Frequency Transients in a Converter Dominated Network " presented at the 2016 Innovative Smart Grid Technologies-Asia (SGT-Asia), Melbourne, VIC, Australia, 2016.

[64] M. Rezkalla, M. Pertl, and M. Marinelli, "Electric Power Systems Inertia: Requirements, Challenges and Solutions," *Electrical Engineering,* vol. 100, pp. 2677-2693, August 2018.

[65] M. Rezkalla, A. Zecchino, A. Martinenas, A. M. Prostejovsky, and M. Marinelli, "Comparison between Synthetic Inertia and Fast Frequency Containement Control based on Single Phase EVs in a Microgrid," *Applied Energy,* pp. 1-12, 2017.

[66] P. Tielens and D. Van Hertem, "The relevance of inertia in power systems," *Renewable and Sustainable Energy Reviews,* vol. 55, pp. 999-1009, 03/01 2016, doi: 10.1016/j.rser.2015.11.016.

[67] A. Ulbig, T. S. Borsche, and G. Andersson, "Impact of Low Rotational Inertia on Power System Stability and Operation," in *19th World Congress: The International Federation of Automatic Control* Cape Town, South Africa, 24-29 August 2014, vol. 47, no. 3, pp. 7290-7297.

[68] Ibraheem Nasiruddin, K. R. Niazi, and G. Sharma, "Study on Dynamic Participation of Wind Turbines in AGC of Power Systems," *Electric Power Component and Syst.,* vol. 43, no. 1, pp. 44-55, 2014.

[69] K. P. Parmar, M. S. Singh, and D. P. Kothari, "Load Frequency Control of a Realistic Power System with Multi-Source Power Generation," *Elect. Power Energy Syst,* vol. 42, pp. 426-433, 2012.

[70] G. Sharma, I. Nasiruddin, K. R. Niazi, and R. C. Bansal, "Robust Automatic Generation Control Regulators for a Two-area Power System Interconnected via AC/DC tie-lines Considering New Structures of Matrix Q " *IET-Generation and Transmission and Distribution,* vol. 10, no. 14, pp. 3570-3579, 2016.

[71] G. Sharma, I. Nasiruddin, K. R. Niazi, and R. C. Bansal, "Adaptive Fuzzy Critic Based Control Design for AGC of Power System Connected via AC/DC tie-lines," *IET-Generation and Transmission and Distribution,* vol. 11, no. 2, pp. 560-569, 2017.

[72] Ibraheem Nasiruddin, P. Kumar, and D. P. Kothari, "Recent Philosophies of Automatic Generation Control Strategies in Power Systems," *IEEE Trans. Power Syst.,* vol. 20, no. 1, pp. 346-357, 2005.

[73] CIGRE, "System Protection Schemes in Power Networks," in "CIGRE Task Force 38.02.19 Technical Report," 2000.

[74] M. R. Aghamohammadi, S. S. Hashemi, and M. S. Ghazizadeh, "A Novel Index for Online Voltage Stability Assessment Based on Correlation Characteristic of Voltage Profiles," *Iranian Journal of Electrical & Electronic Engineering* vol. 7, no. 2, pp. 131-139, June 2011.

[75] S. B. Bhaladhare, A. S. Telang, and P. P. Bedekar, "P-V, Q-V Curve - A Novel Approach for Voltage Stability Analysis," presented at the 2013th National Conference on Innovative Paradigms in Engineering & Technology (NCIPET), 2013.

[76] M. K. Jalboub, A. M. Ihbal, H. S. Rajamani, and R. A. Abd-Alhameed, "Determination of Static Voltage Stability-Margin of the Power System prior Voltage Collapse," presented at the The Eighth International Multi-Conference on Systems, Signals and Devices (SSD 2011), Sousse, Tunisia, 22-25 March, 2011.

[77] R. Kumar, A. Malik, and G. Dalakoti, "Power Flow & Voltage Stability Analysis using MATLAB," *International Research Journal of Engineering and Technology (IRJET)*, vol. 4, no. 1, pp. 93-99, January 2017.

[78] J. P. Barret and C. Barbier, "An Analysis of Phenomena of Voltage Collapse on a Transmission System," *Révue Générale de l'Electricité*, vol. 89, no. 7, pp. 3-21, 1980

[79] N. Parsai and A. Thakur, "PV Curve-Approach for Voltage Stability Analysis " *International Journal of Scientific Research Engineering & Technology (IJSRET)*, vol. 4, no. 4, pp. 373-377, April 2015.

[80] V. Ajjarapu and C. Christy, "The Continuation Power Flow: A Tool for Steady State Voltage Stability Analysis," *IEEE Transactions on Power Systems*, vol. 7, no. 1, pp. 416-423, 1992.

[81] R. J. Koessler, "Voltage InstabiIity/Collapse - An Overview," *IEE Colloquium on Voltage Collapse (Digest No: 1997/101)*, pp. 1/1-1/6, 1997, doi: 10.1049/ic:19970562.

[82] S. Chakrabarti. "Notes on Power System Voltage Stability." Department of Electrical Engineering, IIT. http://home.iitk.ac.in/~saikatc/EE632_files/VS_SC.pdf (accessed 26/04/2020).

[83] S. Thanekar, J., W. Z. Gandhare, and A. P. Vaidya, "Voltage Stability Assessment of a Transmission System - A Review," *International Journal of Elecrical Engineering & Technology (IJEET)*, vol. 3, no. 2, pp. 182-191, July 2012.

[84] C. W. Taylor, *Power System Voltage Stability*. McGraw-Hill, 1994.

[85] N. T. Hawkins, "Voltage collapse and its avoidance," in *IEE Colloquium on Voltage Collapse (Digest No: 1997/101)*, London, UK, 1997, pp. 2/1-2/6, doi: 10.1049/ic:19970563.

[86] E. Saadati and A. Mirzaei, "Voltage Stability Indices: Taxonomy, Formulation and Calculation algorithm," *International Journal of Science, Engineering and Innovative Research*, vol. 8, pp. 1-8, Feb 2016.

[87] Y. Lee and S. Han, "Real-Time Voltage Stability Assessment Method for the Korean Power System Based on Estimation of Thévenin Equivalent Impedance," *Applied Sciences*, vol. 9, no. 8, pp. 1-19, 23rd April 2019, doi: 10.3390/app9081671.

[88] C. W. Taylor. "Voltage Stability for Undergraduates." University of Minnesota Power Group Internet-Based Monthly Seminar. http://people.ece.umn.edu/groups/power/month_sem/pres_11.pdf (accessed 22/03/2019).

[89] T. Van Cutsen, "Voltage Instability: Phenomena, countermeasures and analysis methods," in *Proc IEEE*, 2000, vol. 88, pp. 208-227.

[90] K. L. Lo, T. X. Zhu, S. K. Tso, and Q. Y. Zeng, "Different aspects of voltage collapse assessment and enhancement " in *IEE Colloquium on Voltage Collapse (Digest No: 1997/101)*, London, UK, 1997, pp. 6/1-6/8, doi: 10.1049/ic:19970567.

[91] C. Reis, A. Andrade, and F. P. Maciel, "Line Stability Indices for Voltage Collapse Prediction " in *International Conference on Energy and Electric Drives*, Lisbon, Portugal, 239-243, March 2009.

[92] F. A. Athowibi and M. W. Mustafa, "Line Voltage Stability Calculations in Power Systems," presented at the IEEE International Conference on Power and Energy (PE Con2010), Kuala Lampur. Malaysia, pp. 396-401, December 2010.

[93] P. Kessel and H. Glavitsch, "Estimating Voltage Stability of a Power System " *IEEE Transactions on Power Systems,* vol. 1, no. 3, pp. 346-354, July 1986.

[94] C. Sharma and M. G. Ganness, "Determination of the Applicability of using Modal Analysis for the Prediction of Voltage Stability," presented at the IEEE Transmission and Distribution Conference, Chicago, April, 2008.

[95] Y. Tamura, H. Mori, and S. Iwamoto, "Relashionship between Voltage Instability and Multiple Load Flow Solutions in Electric Power Systems," *IEEE Transactions on Power Apparatus and Systems,* vol. 102, no. 5, pp. 1115-1125, May 1983.

[96] T. V. Custem and C. D. Vournas, *Voltage Stability of Electric Power Systems*. Kluwer Academic Publishers, 1998.

[97] B. H. Chawdhury and C. W. Taylor, "Voltage Stability Analysis: V –Q Power Flow Simulation Versus Dynamic Simulation," *IEEE Transactions on Power Ssytems,* vol. 15, no. 4, November 2000.

[98] S. Corsi and G. N. Taranto, "Voltage instability - The different Shapes of the Nose," presented at the Revitalizing Operational Reliability Symposium, 2007.

[99] T. Van Cutsen, "A Method to Compute Reactive Power Margin with Respect to Voltage Collapse " *IEEE Transaction on Power Systems,* vol. PWRS-6, pp. 145-156, 1991.

[100] B. Gao, G. K. Morison, and P. Kundur, "Voltage Stability Analysis using Modal Analysis," *IEEE Transactions on Power Systems,* vol. 7, no. 4, pp. 1529-1542, November 1992.

[101] M. A. Pai, A. Kulkarni, and P. W. Sauer, "Parallel Dynamic Simulation of Power Systems," *IEEE Symposium on Circuits and Systems,* vol. 2, pp. 1264-1267, 1990.

[102] H. Sangwook, B. Lee, S. Kin, and Y. Moon, "Development of Voltage Stability Index using Synchro-Phasor Based Data," presented at the Transmission and Distribution Conference and Exposition: Asia and Pacific, 2009.

[103] P. G. Krishna and T. G. Mahonar, "A Novel Voltage Stability Analysis of Power System," *International Journal of Elecrical and Electronics Engineering Research (IJEEER),* vol. 3, no. 3, pp. 187-200, August 2013.

[104] A. Tiwarian and V. Ajjarapu, "Event Identification and Contingency Assessment for Voltage Stability via PMU " presented at the 39th North America, North America, 2007.

[105] N. Mahmud and A. Zahedi, "Review of Control Strategies for Voltage Regulation of the Smart Distribution Network with High Penetration of Renewable Distributed Generation," *Renewable and Sustainable Energy Reviews,* vol. 64, pp. 582-595, October 2016.

[106] O. E. Oni, K. I. Mbangula, and I. E. Davidson, "Dynamic Voltage Stability Studeies Using a Modified IEEE 30-Bus System," *Transactions on Environment and Electrical Engineering* vol. 1, no. 3, 2016.

[107] V. Bhadoria, S., N. Singh, and Shrivastava, "A review on Distributed Generation Definitions and impacts on Distribution System," presented at the Conference: International Conference on Advanced Computing and Communication Technologies (ICACCT™-2013), Nov, 2013.

[108] T. Ackermann, G. Andersson, and L. Soder, "Distributed Generation: a Definition," presented at the Electric Power Systems Research 2001.

[109] A. S. N. Huda and R. Zivanovic, "Large-scale Integration of Distributed Generation into Distribution Networks: Study Objectives, review of models and Computational Tools," *Renewable and Sustainable Energy Reviews,* vol. 79, March 2017.

[110] P. Paliwal, N. P. Patidar, and R. K. Nema, "Planning of Grid Integrated Distributed Generators: A Review of Technology, Objectives and Techniques," *Renewable and Sustainable Energy Reviews,* vol. 40, pp. 557-570, 2014.

[111] M. M. Bello, "Spatial Modelling and Dynamics of Photovoltaic Generator for Renewable Energy Application," Master's Thesis, School of Electrical, Electronic and Computer Engineering, University of KwaZulu-Natal, Durban, 2006.

[112] B. Delfino, "Modeling of the Integration of Distributed Generation into the Electrical System," in *Power Engineering Society Summer Meeting*, USA, IEEE, Ed., 2002: IEEE, pp. 170-175.

[113] H. A. Gil and G. Joos, "Models for Quantifying the Economic Benefits of Distributed Generation," *IEEE Transactions on Power Systems,* vol. 23, no. 2, pp. 327-335, May 2008 2008.

[114] L. L. Lai and T. F. Chan, *Distributed Generation: Induction and Permanent Magnet Generators*. West Sussex: John Wiley & Sons Ltd., 2007.

[115] X. Meng and Z. Pian, " Direction-Coordinating Based Ant Colony Algorithm and its Application in Distribution Network Reconfiguration," in *Intelligent Coordinated Control of Complex Uncertain Systems for Power Distribution Network Reliability*: Elsevier, 2016, ch. 7, pp. 143-167.

[116] M. Yiming and K. N. Miu, "Switch Placement to Improve System Reliability for Radial Distribution," *IEEE Transaction on Power Systems,* vol. 18, no. 4, pp. 1346-1352, November 2003.

[117] M. Kennedy, "Distributed Generation: Harder than it looks," *IEEE Power Engineer Journal,* vol. 17, no. 1, pp. 8-9, February 2003.

[118] N. M.-A. Mutombo, "Development of Neuro-Fuzzy Strategies for Prediction and Management of Hybrid PV-PEMFC-Battery Systems," Doctor of Philosophy in Electrical Engineering, College of Agriculture, Engineering and Science, University of Kwazulu Natal, Durban, KwaZulu Natal 2017.

[119] B. Singh and J. Sharma, "A review on Distributed Generation Planning," *Renewable and Sustainable Energy Reviews,* vol. 76, pp. 529-544, March 2017.

[120] J. P. Dunlop, *Photovoltaic Systems,* 3rd ed. Illinois: American Technical Publishers, Inc., 2012, p. 502.

[121] R. Messenger and J. Ventre, *Photovoltaic Systems Engineering*. Boca Raton: CRC Press LLC, 2000.

[122] K. Zweibel, *Harnessing Solar Power: The Photovoltaics Challenges*. New York: Plenum Press, 1990.

[123] T. Markvart, *Solar Electricity*, 2nd ed. West Sussex: John Wiley & Sons Ltd, 2008.

[124] R. Charron and A. K. Athienitis, "Design and Optimisation of Net-Zero Energy Solar Homes," in *ASHRAE Transactions*, 2006, vol. 112, no. 2, pp. 285-295.

[125] M. W. Siti, "Optimal Energy Control of a Grid Connected Solar-Wnd based Electric Power Plant," Doctor of Philosophy, School of Engineering, College of Agriculture, Engineering and Science, University of Kwazulu Natal, Durban, South Africa, 2016.

[126] M. Farhoodnea, A. Mohamed, H. Shareef, and H. Zayandehroodi, "Power Quality Analysis of Grid-Connected Photovoltaic systems in Distribution Networks," *Electrotechniczny (Electrical Review)*, vol. *2013/2a*, pp. 208-213, 2013.

[127] Alternative Energy Tutorials. "Solar Cell I-V Characteristic." http://www.alternative-energy-tutorials.com/energy-articles/solar-cell-i-v-characteristic.html (accessed 19/04/2020).

[128] M. M. Begovic, A. Pregelj, A. Rohatgi, and D. Novosel, "Impact of Renewable Distributed Generation on Power Systems," in *34th Hawaii International Conference on System Sciences*, Hawaii, 2001: IEEE.

[129] *IEEE Recommended Practice for Utility Interface of Photovoltaic (PV) Systems*, IEEE 929-2000 Standard, 2000.

[130] K. Divya and P. N. Rao, "Models for Wind Turbine Generating Systems and ther Application in Load Flow Studies," vol. 76, no. 9, pp. 844-856, 2006.

[131] Wind Power Monthly. "Ten of the Biggest Wind." 2018. https://www.windpowermonthly.com/10-biggest-turbines (accessed 16/04/2020).

[132] P. Prakash and K. Khatod, "Optimal Sizing and Siting Techniques for Distributed Generation in Distribution Systems: A Review," *Renewable and Sustainable Energy Reviews*, vol. 57, pp. 111-130, 2016.

[133] G. Rami, "Contrôle de Tension auto Adaptif pour des Productions Decentralisées d'Energies Connectées au Réseau Electrique de Distribution," PhD, Energie Electrique, Institut National Polytechnique de Grenoble, Grenoble, France, 2006.

[134] R. Hidalgo, C. Abbey, and G. Joos, "A review of Active Distribution Networks Enabling Technologies," presented at the IEEE PES General Meeting, 2010.

[135] E. Veldman, M. Gibcscu, J. G. Slootweg, and W. L. Kling, "Technical Benefits of Distributed Storage and Load Management in Distribution Grids," in *PowerTech 2009 IEEE* Bucharest, June 28th - July 2nd 2009: IEEE, pp. 1-8.

[136] R. J. Thomas. (2009, July-Aug.) Putting an action plan in place. *Power and Energy Magazine IEEE*. 26-31.

[137] P. Fu-Sheng and H. Shyh-Jier, "Design and Operation of Power Converter for Micro-Turbine Powered Distributed Generator with Capacity Expension Capability " *IEEE Transaction Energy Conversion*, vol. 23, pp. 110-118, 2008.

[138] M. Uzunoglu, O. Onar, M. Y. El-Sharkh, N. S. Sisworahardjo, A. Rahman, and M. S. Alam, "Parrallel Operation Characteristics of PEM Fuel Cell and Microturbines Power Plants " *Journal of Power Sources*, vol. 168, pp. 569-576, 2007.

[139] R. C. Dugan and M. F. McGranaghan, *Electric Power Systems Quality*, 2nd ed. New York: McGraw-Hill, 2002.

[140] D. M. Ali, "A Simplified Dynamic Simulation Model (prototype) for a Stand-alone Polymer Electrolyte Membrane (PEM) Fuel Cell Stack," presented at the Power System Conference MEPCON, Midde-east, 2008.

[141] P. J. Skerrett, "Fuel UPD," *Popular Science*, June 1993.

[142] M. N. Marwali, J. Jung, and A. Keyhani, "Control of Distributed Generation Systems - Part II: Load Sharing Control," *IEEE Transactions on power Electronics*, vol. 19, no. 6, pp. 1551-1561, November 2004.

[143] C. D'Adamo, S. Jupe, and A. C., "Global Surveyon on Planning and O[peration of Avtive Distribution Networks - Update of CIGRE C6.11 working group activities " in *20th International Conference and Exhibition on Electricity Distribution - Part 1*, 2009, pp. 1-4.

[144] J. Tengku, H. Tengku, A. Mohamed, and H. Shareef, "A Review on Voltage Control Methods for Active Distribution Networks," *Przeglad Electrotechniczny*, 2012.

[145] P. N. Vovos, A. E. Kirprakis, A. R. Wallace, and H. G. P., "Centralised and distributed voltage control: Impact on distributed generation penetration.," *IEEE Trans. on Power Systems*, vol. 22, no. 1, pp. 476-482, February 2007.

[146] S. K. Khadem, M. Basu, and M. F. Conlon, "Power Quality in Grid Connected Renewable Energy Systems: Role of Custom Power Devices," in *Proceedings of the International Conference on Renewable Energies and Power Quality*, Granada, Spain, March 2010.

[147] C. Dai and Y. Baghzouz, "On the Voltage Profile of Distribution Feeders with Distributed Generation. ," in *Proceedings of the IEEE Power Engineering Society Summer Meeting*, 2003, pp. 456-461.

[148] T. E. Kim and J. E. Kim, "A Method for Determining the Introduction Limit of Distributed Generation in Distribution System. ," in *Proceedings of the IEEE Power Engineering Society Summer Meeting*, Vancouver, Canada, July 2001, vol. 1, pp. 451-461.

[149] F. A. Viawan, A. Sannino, and J. Daalder, "Voltage Control with On-load Tap Changers in Medium Voltage Feeders in Presence of Distributed Generation " *Electric Power System Research*, vol. 77, pp. 1314-1322, 2007.

[150] L. Bird, J. Cochran, and X. Wang, "Wind and Solar Energy Curtailment: Experience and Practices in the United States," National Renewable Energy Laboratory (NREL), March 2014

[151] S. K. Tso, T. X. Zhu, Q. Y. Zeng, and K. L. Lo, "Evaluation of Load Shedding to prevent Dynamic Volateg Stability based on Extended Fuzzy Reasoning," in *IEE Proceedings on Generation, Transmission and Distribution*, 1996, vol. 144, no. 2: IEE, pp. 81-86.

[152] D. Taggart and K. Hao, "Power Factor Control for Grid-Tied Photovoltaic Solar Farms," in *CIGRE-AORC Technical Meeting 2018 – International Conference on Global Energy Transition – Issues and Challenges*, Gangtok, India, May 24–25, 2018.

[153] Y. Yang, "Optimization of Battery Energy Storgare Systems for PV Grid Integration Based on Sizing Strategy " Doctor of Philosophy, Department of Electrical and Computer Engineering, Florida State University Libraries, Florida, 2014.

[154] P. Denholm, E. Ela, B. Kirby, and M. Milligan, "The role of energy storage with renewable electricity generation," National Renewable Energy Laboratory NREL. Tech. Rep. NREL/TP-6A2-47187, Colorado, January 2010. Accessed: 18/06/2020. [Online]. Available: https://www.nrel.gov/docs/fy10osti/47187.pdf

[155] C. A. Hill, M. C. Such, D. Chen, J. Gonzalez, and W. Mack Grady, "Battery Energy storage for enabling integration of distributed solar power generation " *IEEE Transactions on Smart Grid*, vol. 3, no. 2, June 2012.

[156] *IEEE Standard for Interconnection and Interoperability of Distributed Energy Resources with Associated Electric Power Systems Interfaces*, IEEE STANDARDS ASSOCIATION, New York, February 2018.

[157] DigSILENT *PowerFactory*, "DigSILENT *PowerFactory2017* User Manual," DigSILENT GmbH, Gomaringen, Germany, June 2017.

[158] DigSILENT *PowerFactory2017* r4652, "39 Bus New England System," Heinrich-Hertz-Str. 9, 72810 Gomaringen, Germany. www.digsilent.de, 2017.

[159] DigSILENT *PowerFactory2017* r4650, "Nine-Bus System," Heinrich-Hertz-Str. 9, 72810 Gomaringen, Germany. www.digsilent.de, 2016.

[160] T. Matlokotsi, "Power Quality Enhancement in Electricity Networks Using Grid-Connected Solar and Wind Based DGs," Master of Science Degree in Electrical Engineering, Department of Electrical Engineering University of Cape Town (UCT), Cape Town, 2017.

[161] N. Hamrouni, M. Jraidi, and A. Chérif, "New Conrol Strategy for 2-stage grid-connected photovoltaic power system," *Renewable Energy*, vol. 33, no. 10, p. 2212, 2008.

[162] DigSilent *PowerFactory*2017, "Technical Reference Documentation - DC-DC converter," Heinrich-Hertz-Str.p.72810.Gamaringen, Germany. www.digsilent.de, 2016.

[163] A. Ghosh, P. K. Saha, and G. K. Panda, "Chaos and Control of Chaos in Current Controlled Power Factor Connected AC-DC Boost Regulators," *International Journal of Modern Engineering Research*, vol. 2, no. 4, pp. 2529-2533, July-August 2012 2012.

[164] A. Ghosh and S. Sai Saran, "High-Gain DC-DC Step-up Converter with Multilevel Output Voltage," presented at the *2018 International Symposium on Devices, Circuits and Systems (ISDCS)*, Howrah, 2018.

[165] G. Rampinelli, A. Krenzinger, and F. C. Romero, "Mathematical Models for Efficiency of Inverters used in Grid Connected Photovoltaic Systems," *Renewable and Sustainable Energy Reviews*, vol. 34, pp. 578-587, 2014.

[166] DigSILENT *PowerFactory2017*, "Technical Reference Documentation - PV System," Heinrich-Hertz-Str.9.72810. Gamaringen, Germany, www.digsilent.de, 2016.

[167] DigSILENT *PowerFactory2017*, "Technical Reference Documentation - Static Generator," Heinrich-Hertyz-Str.9.72810. Gameringen. Germany. www.digsilent.de, 2016.

[168] DigSILENT *PowerFactory*, "Battery Energy Storage Systems," DigSilent, Gomaringen, Germany, 2010.

[169] N. K. Medora and A. Kusko, "Dynamic Battery Modelling of Lead-Acid Batteries using Manufacturer's data," presented at the Twenty-Seventh International Telecommunications Conference, 2005.

[170] J. S. Huang, Z. H. Jiang, and M. Negnevitsky, "Loadability of Power Systems and Optimal SVC Placement," *Electrrical Power and Energy Systems*, vol. 45, pp. 167-174, 2013.

[171] P. Mehta, P. Bhatt, and V. Pandya, "Optimal Selection of Distributed Generating untits and its Placement for Voltage Stability Enancement and Energy Loss Minimization," *Ain Shams Engineering Journal*, vol. 9, pp. 187-201, Dec 2018.

[172] M. Sulaiman, A. F. M. Nor, and N. R. Bujal, "Voltage Instability Analys on PV and QV curves for Radial-Type and Mesh-type Electrical Networks," *International Review of Electrical Engineering (I.R.E.E),* vol. 10, no. 1, pp. 109-115, January-February 2015.